Automatic Change-based Diagnosis of Structures Using Spatiotemporal Data and As-Designed Model

by

Vamsi Sai Kalasapudi

A Dissertation Presented in Partial Fulfillment
of the Requirements for the Degree
Doctor of Philosophy

Approved April 2017 by the
Graduate Supervisory Committee:

Pingbo Tang, Chair
Oswald Chong
Keith Hjelmstad

ARIZONA STATE UNIVERSITY

May 2017

ABSTRACT

Civil infrastructures undergo frequent spatial changes such as deviations between as-designed model and as-is condition, rigid body motions of the structure, and deformations of individual elements of the structure, etc. These spatial changes can occur during the design phase, the construction phase, or during the service life of a structure. Inability to accurately detect and analyze the impact of such changes may miss opportunities for early detections of pending structural integrity and stability issues. Commercial Building Information Modeling (BIM) tools could hardly track differences between as-designed and as-built conditions as they mainly focus on design changes and rely on project managers to manually update and analyze the impact of field changes on the project performance. Structural engineers collect detailed onsite data of a civil infrastructure to perform manual updates of the model for structural analysis, but such approach tends to become tedious and complicated while handling large civil infrastructures.

Previous studies started collecting detailed geometric data generated by 3D laser scanners for defect detection and geometric change analysis of structures. However, previous studies have not yet systematically examined methods for exploring the correlation between the detected geometric changes and their relation to the behaviors of the structural system. Manually checking every possible loading combination leading to the observed geometric change is tedious and sometimes error-prone. The work presented in this dissertation develops a spatial change analysis framework that utilizes spatiotemporal data collected using 3D laser scanning technology and the as-designed models of the structures to automatically detect, classify, and correlate the spatial changes

of a structure. The change detection part of the developed framework is computationally efficient and can automatically detect spatial changes between as-designed model and as-built data or between two sets of as-built data collected using 3D laser scanning technology. Then a spatial change classification algorithm automatically classifies the detected spatial changes as global (rigid body motion) and local deformations (tension, compression). Finally, a change correlation technique utilizes a qualitative shape-based reasoning approach for identifying correlated deformations of structure elements connected at joints that contradicts the joint equilibrium. Those contradicting deformations can help to eliminate improbable loading combinations therefore guiding the loading path analysis of the structure.

DEDICATION

I dedicate this dissertation to my father and my mother, Satya Murthy Kalasapudi M.A., and Padmavathi Kalasapudi M.A., whose support for higher education motivated me to reach greater boundaries and take up higher challenges. I owe a lot to my parents for their continuous support and belief in me.

ACKNOWLEDGEMENTS

This dissertation would have never been possible without the help of my committee, Dr. Pingbo Tang (Chair), Dr. Keith Hjelmstad, and Dr. Oswald Chong. I am very thankful for their continuous support and valuable inputs on my dissertation.

My deepest appreciation goes to my advisor Dr. Pingbo Tang for his motivation and persistent guidance. I am deeply indebted to him for supporting my career goals and having belief in me. I sincerely thank him for his encouragement and for helping me reach greater heights in my life. I could not have imagined having a better advisor for my Ph.D. study.

I am grateful for all my colleagues and friends at Arizona State University, especially Zia Ud Din, Hariharan, Abbas, and Cheng Zhang for their immense intellectual and emotional support. I would also like to thank Dr. Yelda Turkan from Oregon State University for guiding me in my first research project and providing valuable suggestions.

Finally, I acknowledge Firas Shalabi and Duong Van from Iowa State University, Ben Bunge from the Weitz Company and Bob Darling from the Baker Group, Jimmy Camp and Ryan Jones from Maricopa DOT for their help in providing the 3D laser scanning data, design drawings of the bridge and sharing their expertise and practical experiences.

This dissertation is based upon the work supported by National Science Foundation (NSF) under Grant No. 1443069 and Grant No. 1454654. NSF's support is gratefully acknowledged. Any opinions, findings, conclusions, or recommendations

expressed in this dissertation are those of the author and do not necessarily reflect the views of NSF or Arizonas State University.

TABLE OF CONTENTS

Page

Page

Page

LIST OF FIGURES

Figure Page

Figure Page

LIST OF TABLES

Table Page

CHAPTER 1

INTRODUCTION

Currently, American Society of Civil Engineers (ASCE) rates United States transportation infrastructure with a grade of "D" as in poor and at risk (ACSE 2013). Deterioration of infrastructure facilities such as the transportation infrastructure will affect a large number of people for a longer span of time. Government authorities allocate a large amount of federal and state resources for maintaining the transportation infrastructure to facilitate public at daily basis. Since the great recession of 2008, funding became a deficit. The Economic development research group predicts that transportation infrastructure will have funding deficit of approximately $90 billion by 2020 (ASCE 2012). Hence, there is a need for reliable structural health monitoring tools that can detect, analyze, and predict the exact condition of a civil infrastructure.

Technological advancements led to increase in acquiring detailed geometric data of an infrastructure. Several destructive and non-destructive methods can identify the geometric deterioration of a structure, determine the defects and aid in its condition assessment planning (Hobbs and Tchoketch Kebir 2007). However, such technological advancements still lack supporting tools to predict the accurate condition of an infrastructure for providing appropriate assessment results. These condition assessment methods heavily rely on experienced professionals for predicting the loading behavior of a structure and identify damaged elements. Current structural health investigation methods include finite element analysis (FEA), non-destructive testing, and periodic investigations by professional engineers that approximately predict the condition of an infrastructure (Abu-Yosef 2013; Green and Cebon 1994; Mabsout et al. 1997). The major

disadvantage of using the conventional structural health monitoring methods is the tedious process of identifying all the combinations of causes that lead to the abnormal loading behavior of a structure.

Several researchers started collecting three-dimensional (3D) imagery data for performing a detailed geometric evaluation of a structure (José and Fernández-Martin 2007; Park et al. 2007; Zogg and Ingensand 2008). 3D imagery data collection technology such as 3D laser scanners has the capacity to capture dense point cloud data of a structure with mm-level accuracy (Akinci et al. 2006; Tang et al. 2010). Such point cloud data can be used to detect differences between as-designed models and as-built conditions (Kalasapudi et al. 2014a). Previous studies focused on using point cloud data to analyze the geometric changes of a structure during its service period (Chen et al. 2010; Goor 2011). In addition, researchers identified correlations among the observed geometric changes between an as-designed model and an as-built laser scanning data for performing construction quality assessment and control (Kalasapudi et al. 2014b; Kalasapudi and Tang 2015a). Such studies indicate the potential of using detailed point cloud data to conduct change based condition diagnostic studies of a civil infrastructure. Manually identifying the geometric changes from the point cloud data and analyzing their correlation with a design model is tedious and often error-prone. In addition, associating objects from the as-designed model with points in point clouds in an efficient and reliable manner is challenging, especially when spatial changes occur (Tang et al. 2013). Hence, there is a need for the development of an automatic geometric change based condition assessment approach that is computationally efficient and can accurately predict the loading behavior of a civil infrastructure.

Automated change based assessment methods using 3D imagery data provide detailed visual analysis results for engineers to make reliable decision-making. The major advantage of using 3D imagery data is that engineers can utilize the visual interpretation of the actual as-built scenarios and the availability of robust automatic image processing algorithms. However, several previous studies majorly focused on defect detection and 3D geometric analyses (Zogg and Ingensand 2008). Such studies did not analyze the actual cause of observed geometric change and the relationship between all the observed changes of the connected elements of a structure. It important for an automated change based assessment approach to identify how the identified changes influence each other and what changes actually interact with the loading behavior of the structure. For instance, few changes occur due to changes in the material property of an element or due to changes in the boundary condition between its neighboring elements. Hence, a comprehensive spatial change based condition assessment approach need to automatically identify the geometric spatial changes, classify the observed spatial changes based on its actual cause, and correlate the observed changes to reliably identify those changes that interact with the structures loading path and simulate the as-is structural behavior.

The goal of the developed research is to provide automated tools for construction project managers and structural engineers to perform a change based condition assessment of civil infrastructure using 3D imagery data. The author developed automatic algorithms that focus on accurate change detection, geometric change classification, and change correlation to reveal the most possible loading behavior of the structure. The developed research objectives help in automating the spatial change detection, change the

classification, and change correlation process between different data sets (as-designed vs. as-built/ as-built vs. as-built). The author predicts that the developed automated spatial change-based diagnosis approach using spatiotemporal imagery data and model can serve as a better indicator of the accurate as-is condition of structure and aid in predicting abnormal behaving elements under a structure's loading conditions.

Motivation

The following paragraphs provide details about the motivating case of the developed research using a simple case study. The case study details a 3D laser scanning data based condition assessment on a Steel Water Tank using spatial change analysis approach (Kalasapudi and Tang 2015a). It details the process of data collection, data pre-processing, data analysis, and preliminary results that show the potential of using 3D laser scanning data for geometric change based condition assessment of a structure. The author structured the motivating case using a spatial change-based diagnosis study that utilizes spatial change detection, spatial change classification, and spatial change correlation for providing comprehensive condition assessment methodology of civil infrastructures. This motivating case also shows the need for automating the data analysis approach by developing an automated visual change pattern recognition using the water tank structure as a case study. Before providing the details about the potential of using 3D laser scanning data for condition assessment of the steel water tank, the author discusses the limitations of current condition assessment approaches for water tanks in the following paragraph.

Current condition assessment approaches for steel water tank include manual checking, non-destructive testing of steel, geometric data analysis using data collected

using traditional sensor technology such as total stations, etc. (Abu-Yosef 2013; Green and Cebon 1994; Mabsout et al. 1997). However, such assessment approaches have many practical limitations. The condition assessment inspectors often face accessibility limitation for performing manual checking and non-destructive testing on the upper part of the steel tank structure (Agdas et al. 2012). For instance, it is difficult and unsafe to access the roof of the steel water tank for conducting visual inspections. Traditional sensor methods such surveying using total station have several limitations that include the amount of time required to plan (sensor network planning), collect data, and interpret the findings (Deruyter 2013). Geometric survey of the water tank using a total station sensor often requires a large amount of time and intense manual data processing, which makes periodic spatial change detection impractical and sometime error prone. In addition, total station surveying data lack reliable tools that can classify the detected spatial changes as global (changes due to rigid body motion) and local (changes constrained to the structure) spatial changes. Such change classification aids engineers to resolve the mixed patterns of global and local deformations observed in the deviations between geometries of a structure.

Local changes of the structure include element level deformations such as rotation of the element, change in the shape of element, etc. Such local level deformation information is crucial to understand the loading behavior of the structure. In addition, several local changes may accumulate to form global changes (changes due to rigid body motion) of the structure or vice versa. Hence, it is extremely crucial to classify the detected spatial changes and understand its actual origin. However, detecting local deformation require detailed mm level accurate geometric data of the structure and

collecting mm level accurate data for performing spatial change classification using total station is impractical and extremely tedious. Additionally, traditional condition assessment methods majorly focused on identifying the defect of a structure but fail to examine methods for exploring the correlation between the detected defects and their relation to the behaviors of the structural system. Recognizing the correlations between the identified defect can significantly reduce the amount of resources and time spent on periodic maintenance of the structure. Practical limitations and computational complexities of traditional condition assessment methods make change interpretation unreliable and impossible to perform. Hence, several researchers started exploring a new technological advancement that can capture detailed 3D geometric data within minutes.

3D laser scanning provides detailed spatial data required for performing spatial change detection of the steel water tank. Such spatial change detection (between design model and laser scanning data or between two sets of laser scanning data) can provide information about elements that undergo changes after the construction of the water tank structure and during the structure's service life. Such spatial changes include element level deformations, rotation, and displacements, etc. that have an effect on the structural integrity of the steel water tank. 3D laser scanning data can also help in classifying the detected spatial changes into global and local changes. The detailed geometric data captures both global and local changes of the steel water tank and its relationship between the structure's neighboring environment. Understanding the interactions between the structure and its surrounding environment will aid in performing reliable spatial change classification.

Several previous studies have utilized qualitative and quantitative methods to represent and classify local and global changes of structures captured using 3D laser scanning data (Mosalam et al. 2014). Such studies show the potential of using 3D laser scanning data for accurately detecting and classifying spatial changes of steel water tank structure. In addition, the classified spatial changes can also provide the information about the loading behavior of individual elements of the structure. Several combinations of load on the structure can cause the observed spatial change and manually checking every load combination is tedious and sometimes becomes impossible for large civil infrastructures. Hence, the spatial change classification can aid in reducing the possible number of loading combinations that caused the observed spatial change. Identification of the loading behavior of individual structural elements will help in detecting the most possible loading on the structure. Periodically detecting the changes in the applied load on the steel water tank structure can identify defected elements that have anomalous loading behavior and help focus on individual structure elements rather the diagnosing the whole structure causing wastage of maintenance resources allotted to the structure. Hence, there is a need for a spatial change-based diagnosis framework that utilizes spatiotemporal 3D laser scanning data for performing an accurate and reliable structural condition assessment. The following section provides details about the use of 3D laser scan for performing a detailed geometric assessment of the steel water tank.

Overview of the test subject and the data collection procedure

The drawings of the Steel Water Tank show that the tank is a combination of a cylinder and a cone (Figure 1). The height of the cylindrical part is 9.75 meters, the height of the conical part is 1.67 meters, and the overall radius of the water tank is 21.34

meters. To investigate the feasibility of using 3D laser scanning data, the author collected eleven scans that comprise of seven exterior scans and four interior scans. The data was collected using a Faro Scene laser scanner (FARO Technologies Ltd.). In addition, the author has utilized commercially available software's to preprocess the scans and register them manually into a single global coordinate system. Figure 1(a&b) shows all four interior and seven exterior scans perfectly registered together. The major purpose of this case study is to determine the feasibility of using 3D laser scanning data to perform: (1) Spatial change detection between as-built 3D laser scanning data and as-designed model; (2) Classification and correlation of the detected spatial changes; (3) Detecting the possible loading on the water tank using the correlated spatial change patterns. The following sections will provide details about the data processing procedure for analyzing the Steel Water Tank using the change analysis approach.

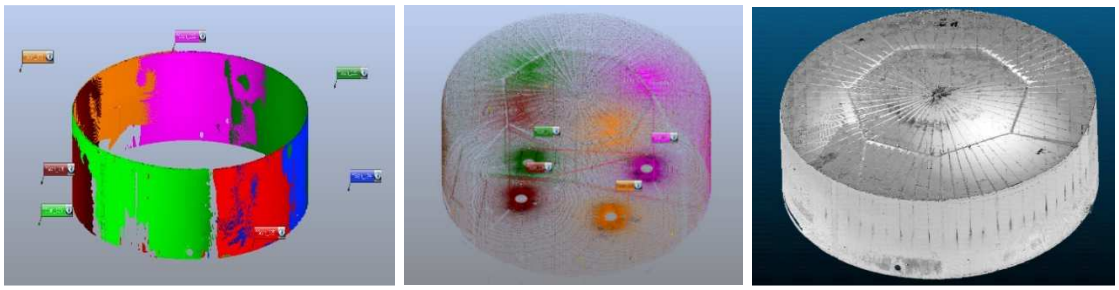

(a) (b) (c)

Figure 1. (a) Seven exterior scans (b) Four interior scans (c) Registered steel water tank data

Deformation Analysis using 3D Laser Scanning Data: Challenge of Change Detection

Deformations of the Steel Water Tank are geometric spatial changes that happen to the structure during its service period. Such deformations can occur due to change in the type of loading conditions, changes in the boundary condition or change in the environmental condition surrounding the water tank structure. Traditional deformation measurement techniques include installing strain gauges, accelerometers, or fiber optic

sensors, etc. (Guo et al. 2011; Kovačič et al. 2015). These sensors are capable of transferring quantitative information that is used to analyze displacements and deformations of a structure at several locations. For instance, to measure the deformations of the Steel Water Tank, structural engineers need to mount at least 4-5 sensors on each individual element of the structure (Caetano and Cunha 2003). Such process is expensive and requires an abundant amount of resources and time. Numerical simulation studies such as Finite Element Analysis (FEA) try to overcome the limitations of contact sensor technology. It provides the information about possible deformations of the structure using the structure's load carrying capacity. However, such technique requires accurate as-built geometric information of the structure to provide a comprehensive structural assessment. Traditional surveying tools such as Total Stations can measure the required geometric information of the structure (Fröhlich and Mettenleiter 2004). Such surveying tools require a huge amount of time and a licensed professional to operate and generate geometric data necessary for generating accurate as-built information (Erickson et al. 2013).

Currently, 3D imaging technologies have gained huge popularity in the field of visual inspection of large-scale civil infrastructure facilities (Fröhlich and Mettenleiter 2004). Several researchers started using 3D laser scanning technology to capture and analyze deformations of large-scale infrastructures (Lee and Hyo 2013; Olsen et al. 2009; Park et al. 2007). To identify the deformations of the Steel Water Tank structure, the author has utilized 3D laser scanning data to compute its deviation with an as-designed model of the tank. Such process consists of accurately registering the 3D point cloud data against the as-designed model of the water tank. The as-designed model consists of

individual elements of the water tank structure, such as a cylinder of radius 21.34 meters; a circular plane of radius 21.24 meters, etc. Comparing the point cloud data with the design model will result in identifying the geometric deviations of the water tank structure. Figure 2 show the comparison results of the 3D point cloud data with that of the as-designed model of the water tank structure.

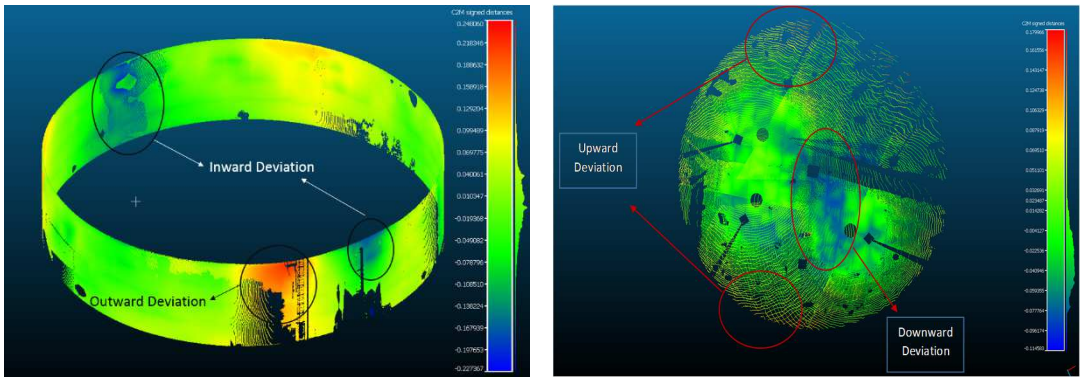

Figure 2. Deformation of the steel water tank using 3D point cloud data ("Red" indicates positive deviation; "Blue" indicates negative deviation)

This case study proves that 3D point cloud data can be a potential tool in identifying several types of deformation of a civil infrastructure at mm-level accuracy. However, manually segmenting and registering individual elements from the as-designed model with that of the corresponding elements in the as-built point cloud data is laborious and computationally expensive. This process usually takes hours to segment a point cloud data of a structure into individual elements even using a powerful processing computer. It also depends on how dense is the captured laser scanning data. Denser the point cloud data, longer the time it takes for data processing (segmentation and registration). Hence, there is a need for the development of an automated change detection approach that can reduce the amount of data processing time for identifying the changes between an as-designed model and as-built laser scanning data.

Manual comparison of 2D and 3D imagery data against as-designed models is tedious and error-prone. The majority of the previous change detection studies relied on the "nearest-neighbor searching" paradigm to associate the as-designed model with as-built data (Kim et al. 2014; Xiong et al. 2013). The nearest neighbor searching approach associates each point in a 3D laser scan data with an as-designed model object that is the "nearest neighbor." In other words, the algorithm considers that each as-built data point in the 3D laser scan data belongs to the object that is in its neighborhood, and the algorithm takes the closest object as the object that corresponds to these points. The nearest neighbor search algorithm then calculates the distances between the corresponding as-designed model objects and as-built data points, and visualize these distances using a color-coded "deviation map." Such a deviation map highlights the parts that data points are deviating away from their nearest as-designed model objects. Nevertheless, the nearest neighbor searching approach has several limitations that may lead to data-model mismatches. More specifically, nearest neighbor searching could fail to provide reliable results when associating a large number of similar and small objects packed in relatively small spaces, such as mechanical rooms of large facilities (Kalasapudi et al. 2014a; Tang et al. 2013, 2015). Figure 3 provides an example to illustrate these limitations. In this case, the ducts in as-built data are associated with the wrong ducts in the as-designed model because of the misalignment between the ducts in the as-designed model and as-built model. This observation indicates that the nearest neighbor searching algorithm failed to accurately associate ducts that were subjected to changes between the as-built and as-designed models. Such cases create a need for the development of robust and reliable change detection process to identify crucial changes

that may affect the service condition of an infrastructure. Hence, there is a need to develop an accurate, robust, and automated spatial change detection approach that can reliably detect spatial changes between an as-designed model and as-built laser scanning data.

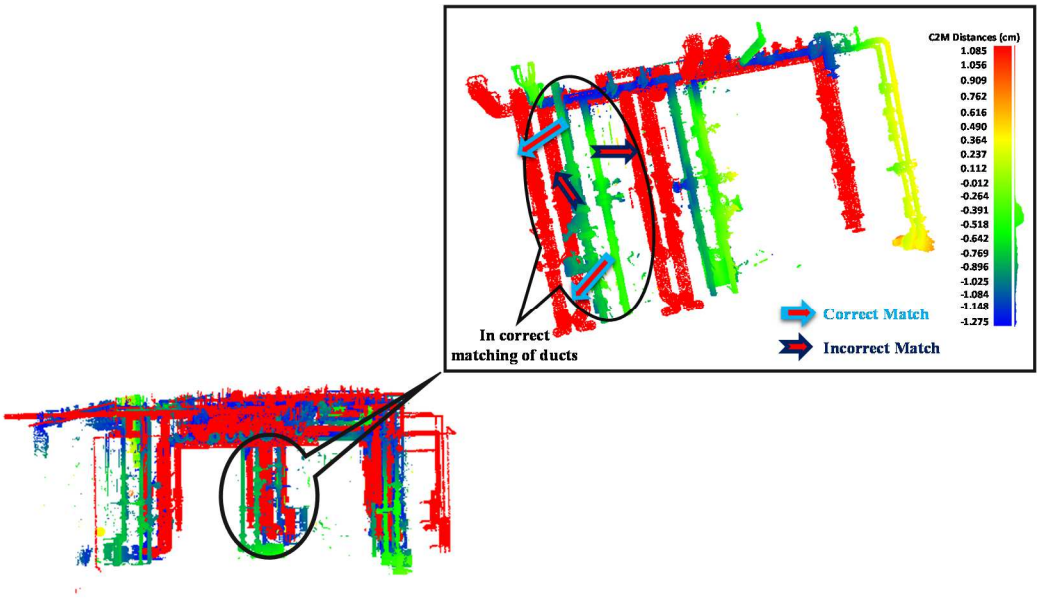

Figure 3. Matching using nearest neighbor searching (Incorrect matching results)

Resolving the Mix of Global and Local Spatial Changes: Challenge of Change Classification

Deviations between the as-designed model and the as-built laser scanning data contain both global and local spatial changes. A local change is the geometric shape deformation of an element whereas the global change is the deviation of an element from its original place. It is important to understand and classify such changes, as local and global changes often influence each other. Certain global changes cause local deformations, and few local deformation leads to global deviations. Hence, there is a need to classify changes and understand what types of changes occur together. Few examples include classification of changes based on (a) type of deformations of the

individual elements; (b) type of building material of the individual element; (c) type of environmental conditions etc. The major advantage of such change classification approach is it reduces the amount of computation required to process each and individual changes and understand their impact on the service condition of the structure. Therefore, it is necessary to develop reliable algorithms that can automatically track and classify the observed spatial changes for understanding what kind of changes often triggers the collapse of the structure. Currently, structural engineers use visual inspection methods, sensors such as accelerometers, laser interferometers, and global positioning systems (GPS) for continuous spatial change monitoring of structures (Yi et al. 2013). All these methods have several disadvantages in accurately detecting changes that aid in performing reliable bridge condition diagnostics of structures (Briaud and Diederichs 2007). Visual inspection methods for civil infrastructures are tedious and heavily rely on the experience of the structural engineer (Moore et al. 2001).

Conventional surveying tools such as Total Station or accelerometer sensors can measure the geometries of the structure and identify the spatial changes. Total station sensors require professional engineers to operate and collect sparse geometric data, which is insufficient for conducting detailed deformation measurements of the water tank (Fröhlich and Mettenleiter 2004). Such surveying tools require huge amount time and a licensed professional to operate and generate dense geometric data for generating accurate as-built information (Erickson et al. 2013). Accelerometers sensors require intense sensor network planning to mount those sensors on all the elements of the water tank structure. If the planned sensor network is incorrect, the output is inaccurate due to the resulting numerical integration errors (Park et al. 2007). The reliability of the data

collection depends on the accuracy of the planned sensor network and has accessibility limitations of mounting the sensors in unsafe parts of the structure. These sensors have the capability to detect the displacement at the mounted locations on the structure but fail to detect the relationship between all the detected displacements between interconnected elements of the structure. Three-dimensional imaging technologies, such as 3D laser scanning, complement the subjective visual inspection and conventional surveying methods (e.g., total stations and tapes) through enabling engineers to conduct more detailed and objective spatial change analysis of bridges (e.g., deformations of structures). Unfortunately, reliable spatial change analysis of bridge structures based on 3D imagery data heavily rely on inspectors' structural engineering knowledge and skills of manually analyzing spatial data patterns.

Figure 4 shows the comparison results of the 3D point cloud data with that of the individual as-designed model of the water tank structure. The comparison results show that the water tank has undergone several geometric spatial changes that include a decrease in the length of the central column, changes in the slope of the roof, deformation of the exterior surface of the tank, and deviations on the floor of the tank. Based on these observations, initially, the author assumed that a hydraulic loading might have caused the push on the exterior surface and on the floor of the water tank that may lead to such deformations. Similarly, the combined dead load of the tank and the water inside may have caused the compression of the central column, which also affected the warping of the rafters connected to it. This water tank underwent significant repair and was shutoff for certain period.

After the repair process, the author collected another set of 3D laser scanning data and compared it with the previously available data set. These investigations revealed that there is a change in the height of the exterior visible surface of the water tank identifying that the tank may have undergone foundation settlement. Hence, not all the assumptions made previously by the author may be reliable for performing the condition assessment of the water tank.

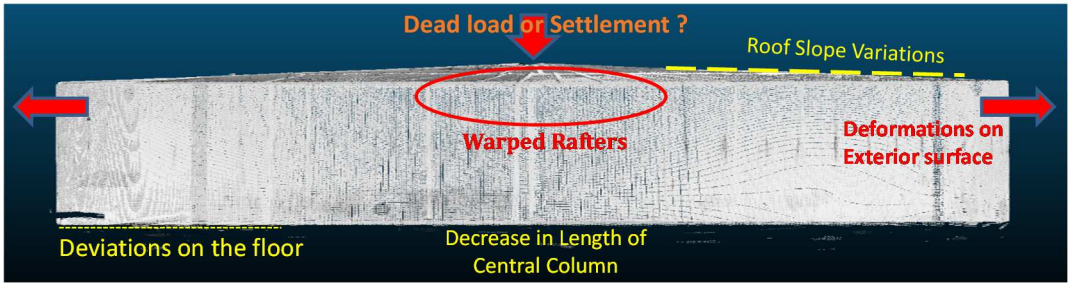

Figure 4. Spatial changes of a steel water tank

In general, settlement of the entire water tank depends on the interaction between the tank and its surroundings whereas dead/hydraulic loading is specific to the tank itself. This study by the author shows that the detected deformations of the structure can be due to a mix of both the rigid body motion (global deviation) and local deformation of the individual element. The author predicts that the comparison results between two 3D imagery data sets could be mixing global rigid body motions, and local shape changes, and usually, objects' rotations or translations cause difficulties for analyzing local shape changes. None of the existing change analysis methods can reliably resolve the mixture of global and local changes of structural elements, while engineers need the information about both the types of changes for structural condition diagnosis. Hence, it is extremely important to resolve the problem of measuring deformations that are caused due to mixed

global and local spatial changes for performing accurate and reliable condition assessment.

Identifying the Loading Behavior using the Correlated Change Patterns: Challenge of Change Correlation

Spatial changes such as deformations of individual elements cause changes in the structures loading behavior. If individual elements undergo larger deformations, they may lose their load carrying capacity. It is necessary to identify elements that have abnormal deformations. If there is a change in the structures loading behavior, it may suggest that the few elements along the direction of loading transfer have anomalous behavior. Correlated spatial changes can help in identify the loading behavior of the structure, and these identified changes help to accelerate the structural behavior simulation. Figure 5 shows the detected direction of loading transfer of the Steel Water Tank structure under hydraulic loading and gravity (dead load). The hydraulic load due to a continuous flow of water causes the exterior cylindrical surface to deform outward. Similarly, the gravity load causes axial compression in the central column, which is also transferred to the exterior cylindrical surface along the connected rafters. If the central column has undergone large deformations, it will lose the load carrying capacity and the complete loading behavior of the structure changes. In such situation, there will be excess load transferred to the exterior surface increasing its local deformation via the connected rafter. Such spatial change path connectivity analysis approach can help in identifying elements that are abnormally behaving under loading and are on the verge of its structural collapse.

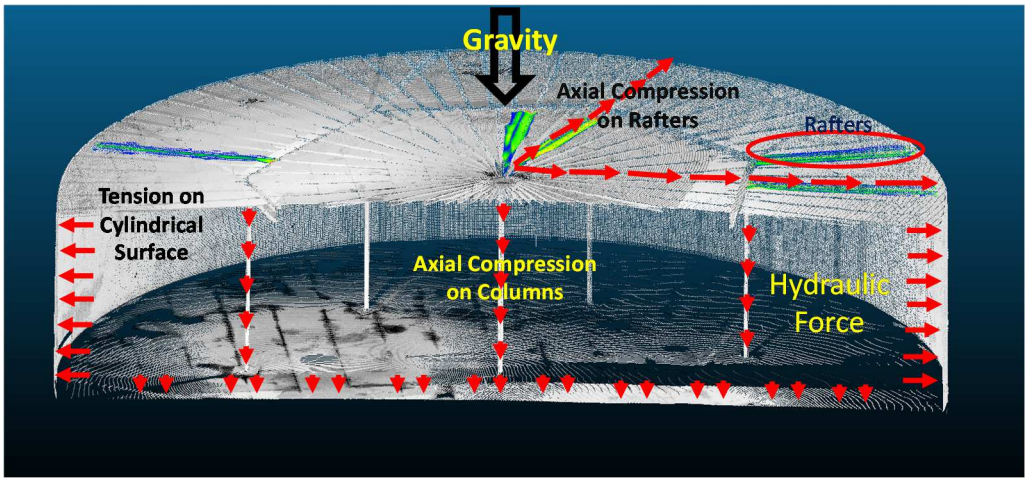

Figure 5. Direction of loading transfer of the steel water tank

An example of such approach is using the methods of joints to analyze a truss structure by identifying the internal forces of truss elements. However, the major challenge is to identify certain spatial changes that correlate with the loading behavior of the structure. Several deformations are caused due to environmental conditions, accidents, etc. that are difficult to detect. Hence, it is important to identify spatial changes that occur together and cause changes in the structure loading behavior. However, structural engineers rely on a large amount of quantitative geometric data collected using the 3D laser scanning technology to identify the spatial changes and interpret the structural behavior. Such approach is tedious and requires intense computation to significantly narrow down the number of possible loading combinations that can lead to the detected spatial change of an element. Hence, there is a need for the development of computationally efficient shape representation techniques that accurately represent the deformed shapes of the elements of the structure and aid in simulating the as-is structural behavior.

Problem Statement

Visual change patterns detected using 3D laser scanners can aid in performing reliable condition diagnostics of a civil infrastructure. Detecting spatial changes that influence the loading behavior of the structure will help in determining damaged elements. Current condition assessment studies focused on identifying the defects on an element of the structure but failed to correlate the detected defect with the loading behavior of the entire structure and its connected elements. Several studies proved the potential of using visual changes patterns to detect and analyze structural failures using 3D imaging technologies. However, these studies rely on manual change analysis techniques that are usually tedious, require constant human intervention, and are often error prone. In addition, previous studies failed to automate the change detection process to automatically detect spatial changes between an as-designed model and as-built conditions rather relied on error prone nearest neighbor searching technique for matching. Spatial changes of an object influence other connected objects and tend to propagate along the interconnected building networks. Inability to automatically detect spatial changes will result in accumulation of the effect of such spatial changes and loss in efficient construction quality control.

Classification of spatial changes such as local and global changes is crucial for conducting effective change analysis study of the structure. Such change classification will aid in understanding how spatial changes influence each other. It is important to understand how local deformations accumulate to form global changes or how global changes lead to local deformations of structural elements. Additionally, utilizing the qualitative information of the changes (e.g. direction of deformation) rather than using

quantitative information (e.g. amount of deformation) provides computationally efficient and effective change analysis study.

Automatic change classification studies can aid in determining what clusters of changes often interfere with the loading behavior of the structure. It is crucial to detect those spatial changes that cause changes in the structure's loading behavior leading to abnormal deformations of the structural elements. Hence, automated spatial change correlation study can lead to the development of spatial change accumulation approach to automatically simulate the loading behavior of the civil infrastructure.

Vision

The major goals of the developed research are:

a. Develop a computationally efficient and automated spatial change detection process between the as-designed model and as-built laser scan model generated from 3D laser scans
b. Automatically classify element level local deformations and global changes (rigid body motion) of the civil infrastructure elements and resolve the mix of the global and local spatial change analysis
c. Accelerate the structural behavior simulation using a qualitative shape-based reasoning approach that reliably represents the deformed shape of the elements of a structure.

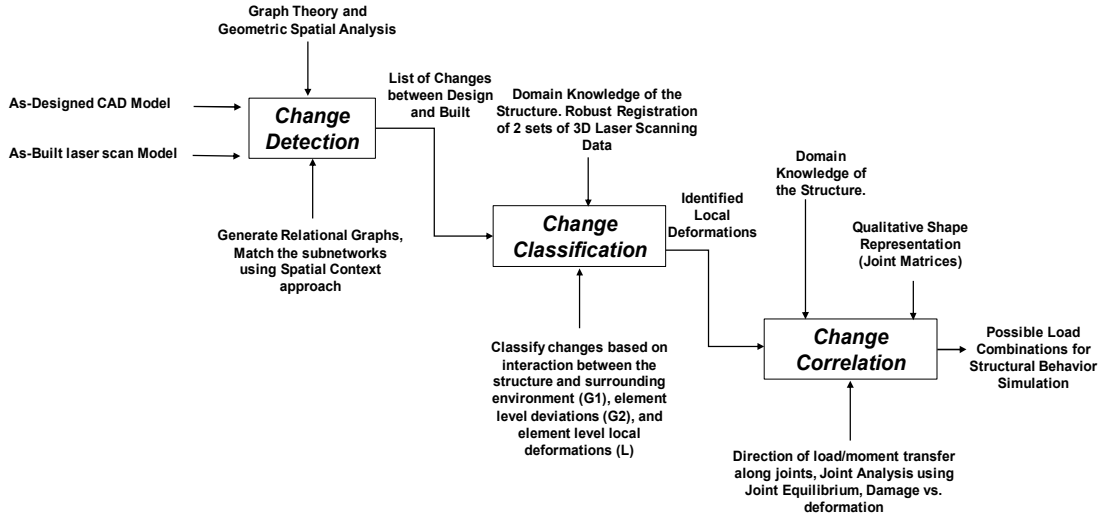

Figure 6. Vision of the automated change analysis approach

Figure 6 shows the overall flowchart of the automated change analysis approach. The approach's target is to automatically generate the loading path of a structure to detect abnormal deformation behavior of the connected structural elements. The inputs of the approach include an as-designed CAD (Computer Aided Design) model and as-built laser scan model of the inspected civil infrastructure. The as-designed model consists of the pre-construction geometric relationships between the all the structural elements. Similarly, the as-built laser scan model extracted from the 3D point cloud data of the structure provides the post construction geometric relationships between the structural elements. These inputs require data pre-processing to remove unwanted information that does not represent the geometric features of the inspected infrastructure.

The flowchart highlights the major outputs from each task that lead to the development of the loading path of the infrastructure. Given the as-designed model and the as-built laser scan model as inputs, the approach automatically detects spatial changes between them using a relational network graph generation process (Change Detection).

Using the detected spatial changes, the approach them uses a robust registration technique to automatically classify the changes between two sets of 3D laser scanning data collected at different time intervals. This approach will identify element-level local deformations and global changes (Change Classification). The qualitative representation of the classified spatial changes will aid in determining the groups of connected elements that have similar behavior under loading. Identifying patterns among those groups can aid in detecting the load transferring along the connected groups and finally help in accelerating the structural behavior simulation (Change Correlation).

Research Questions

a. To examine an automatic and computationally efficient spatial change detection algorithm to identify the spatial changes between an as-designed model and as-built data captured using 3D laser scanner
b. To enable automatic change classification of every element of a civil infrastructure and to resolve the difficulties of mixed global and local deformations
c. To explore a qualitative shape-based reasoning approach for accelerating the structural behavior simulation under loading

Research Method

Automatic spatial change-based diagnosis approach consists of three major steps. The first step consists of detecting spatial changes between an as-designed model and as-built 3D laser scanning data. The second step deals with classifying the spatial changes detected between two set of 3D laser scanning data collected at different time intervals. The last

step analyses the classified spatial changes develops a qualitative deformed shape representation technique and identifies a list of possible loading condition causing the observed spatial changes.

The research methods in the dissertation include the following tasks:

a. Spatial change detection: The author utilized the computational efficiency of the traditional nearest neighbor searching and combined with a spatial context approach to develop a robust and accurate spatial change detection framework. This framework relies on generating a relational network graph to represent each individual element of a building system and match the generated relational graph of the as-designed model with its corresponding as-built laser scanning data.
b. Spatial change classification: The author collected two sets of 3D laser scanning data of several highway bridges across China and United States. The spatial change classification method automatically classifies the observed spatial changes between the two sets of 3D laser scanning data as global deviations (rigid body motion) and element level local deformations.
c. Spatial change correlation: The author investigated several previous qualitative shape representation techniques to represent the deformed elements of a structure. The change correlation method deals with utilizing the qualitative deformed shape representation technique to eliminate the improbable loading combinations causing failure of joint equilibrium condition between the local deformations of connected structure elements at joints.

Dissertation Organization

The Introduction chapter of this dissertation provides a brief overview of the conducted research and identifies the potential of the research study using a strong motivation case. This chapter also elaborates the vision of the author based on the discussed research objectives. The overall dissertation is elaborated to provide specific research contributions that are highlighted and discussed in the research vision section. The author concludes the dissertation (Chapter 5) by summarizing the entire research study, its contributions to the literature and briefly mentions the future research directions. The three chapters discussed between the introduction and conclusion section is being prepared to submit for publication as separate journal articles. The following paragraphs describe the outline of each chapter.

Chapter 2 describes a computationally efficient spatial change detection framework for accurately detection spatial changes between an as-designed BIM model and as-built laser scanning data. This chapter presents a computationally efficient spatial-change-detection approach that reliably compares as-designed Building Information Models (BIMs) and 3D as-built models derived from laser scan data. It integrates nearest neighbor searching and relational graph based matching approaches to achieve computationally efficient change detection and management. A case study using data collected from a campus building was conducted to compare the new change detection approach proposed in this chapter against the state-of-the-art change detection techniques. The results indicate that the proposed approach is capable of making more precise data-model comparisons in a computationally efficient manner compared to existing data-model comparison techniques.

Chapter 3 details the development of spatial change classification approach using 3D laser scanning data of highway single pier bridge structures. This chapter provides a detailed systematic framework to automatically classify the detected spatial changes as global deviations (rigid body motion) and element level local deformations calculated between two 3D imagery data sets collected at different times for the same bridges. The major objective of this chapter is to detect both global and local changes of bridge elements to reveal how global and local changes of structural elements collectively lead to structural systems behaviors. The developed approach follows a hierarchical change classification process. That process starts with a robust 3D data registration algorithm that automatically aligns most of the feature points (e.g., edges and corners of objects) extracted from the two compared 3D imagery data sets and identify "outlier" features that signify global rigid body motions. The algorithm then segments point clouds into data segments of individual structural elements and conduct element-level registration to eliminate rigid body motions of structural elements and isolate local shape changes of these elements. Automatic change classification results on the laser scanning data of two single-pier bridges validated the reliability of this algorithm in resolving various global and local spatial changes of bridge elements and revealing the interactions among those changes.

Chapter 4 presents a qualitative shape-based reasoning for correlating the observed local spatial change to accelerate the structural behavior simulation. This study develops a novel qualitative shape representation technique to represent both the local and global geometric spatial changes of the structure, utilize the classified changes to

eliminate improbable loading conditions and narrow the scope of loading combination causing the observed changes.

References

Abu-Yosef, A. E. (2013). "Development of Non-Contact Passive Wireless Sensors for Detection of Corrosion in Reinforced Concrete Bridge Decks."

ACSE. (2013). "Report Card for America's Infrastructure." American Society fo Civil Engineers, (March), 1–74.

Agdas, D., Rice, J. A., Martinez, J. R., and Lasa, I. R. (2012). "Comparison of Visual Inspection and Structural-Health Monitoring As Bridge Condition Assessment Methods." Journal of Performance of Constructed Facilities, 26(4), 371–376.

Akinci, B., Boukamp, F., Gordon, C., Huber, D., Lyons, C., and Park, K. (2006). "A formalism for utilization of sensor systems and integrated project models for active construction quality control." Automation in Construction, 15(2), 124–138.

Asce. (2012). "Failure to act: the economic impact of current investment trends in water and wastewater treatment infrastructure." 61.

Briaud, L., and Diederichs, R. (2007). "Bridge Testing." Nondestructive Testing (NDT), 1–4.

Caetano, E., and Cunha, A. (2003). "Ambient Vibration Test and Finite Element Correlation of the New Hintze Ribeiro Bridge." 21st IMAC Conference & Exposition 2003, 0–6.

Chen, L., Lin, L., Cheng, H., and Lee, S. (2010). "Change Detection of Building Models." Symposium A Quarterly Journal In Modern Foreign Literatures, XXXVIII, 121–126.

Deruyter, G. (2013). "RISK ASSESSMENT: A COMPARISON BETWEEN THE USE OF LASER SCANNERS AND TOTAL STATIONS IN A SITUATION WHERE TIME IS THE CRITICAL FACTOR." 13th SGEM GeoConference on Informatics, Geoinformatics And Remote Sensing, 687–694 pp.

Erickson, M. S., Bauer, J. J., and Hayes, W. C. (2013). "The Accuracy of Photo-Based Three-Dimensional Scanning for Collision Reconstruction Using 123D Catch." System.

Fröhlich, C., and Mettenleiter, M. (2004). "Terrestrial laser scanning–new perspectives in 3D surveying." Laser-Scanners for Forest and Landscape Assessment ISPRS, 7–13.

Goor, B. Van. (2011). "Change detection and deformation analysis using Terrestrial Laser Scanning." Master Thesis.

Green, M. F., and Cebon, D. (1994). "Dynamic Response of Highway Bridges to Heavy Vehicle Loads: Theory and Experimental Validation." Journal of Sound and Vibration, 170(1), 51–78.

Guo, H., Xiao, G., Mrad, N., and Yao, J. (2011). "Fiber optic sensors for structural health monitoring of air platforms." Sensors, 11(4), 3687–3705.

Hobbs, B., and Tchoketch Kebir, M. (2007). "Non-destructive testing techniques for the forensic engineering investigation of reinforced concrete buildings." Forensic Science International, 167(2–3), 167–172.

José, J. S., and Fernández-Martin, J. (2007). "Evaluation of structural damages from 3D Laser Scans." XXI CIPA International …, (2002), 1–6.

Kalasapudi, V. S., and Tang, P. (2015). "Condition Diagnostics of Steel Water Tanks Using Correlated Visual Pattern." 5th Internaltional COnstruction Specialtiy Conference, ICSC15 – The Canadian Society for Civil Engineering's 5th International/11th Construction Specialty Conference.

Kalasapudi, V. S., Tang, P., and Turkan, Y. (2014a). "Toward Automated Spatial Change Analysis of MEP Components Using 3D Point Clouds and As-Designed BIM Models." 2014 2nd International Conference on 3D Vision, IEEE, 145–152.

Kalasapudi, V. S., Tang, P., Zhang, C., Diosdado, J., and Ganapathy, R. (2014b). "Adaptive 3D Imaging and Tolerance Analysis of Prefabricated Components for Accelerated Construction." Proceeding of the 3rd International Conference on Sustainable, Design, Engineering and Construction (ICSDEC 2014).

Kim, M.-K., Sohn, H., and Chang, C.-C. (2014). "Automated dimensional quality assessment of precast concrete panels using terrestrial laser scanning." Automation in Construction, Elsevier B.V., 45, 163–177.

Kovačič, B., Kamnik, R., Štrukelj, A., and Vatin, N. (2015). "Processing of signals produced by strain gauges in testing measurements of the bridges." Procedia Engineering, 800–806.

Lee, H. M., and Hyo, S. P. (2013). “Stress Estimation of Beam Structures Based on 3D Coordinate Information from Terrestrial Laser Scanning.” Proceedings of the Third International Conference on Control, Automation and Systems Engineering, Atlantis Press, Paris, France, (Case), 81–83.

Mabsout, M. E., Tarhini, K. M., Frederick, G. R., and Tayar, C. (1997). “Finite-Element Analysis of Steel Girder Highway Bridges.” Journal of Bridge Engineering, 2(3), 83–87.

Moore, M., Phares, B., Graybeal, B., Rolander, D., and Washer, G. (2001). “Reliability of Visual Inspection for Highway Bridges.” Journal of Engineering Mechanics, II(FHWA-RD-01-020), 486.

Mosalam, K. M., Takhirov, S. M., and Park, S. (2014). “Applications of laser scanning to structures in laboratory tests and field surveys.” Structural Control & Health Monitoring, 21(1), 115–134.

Olsen, M. J., Kuester, F., Chang, B. J., and Hutchinson, T. C. (2009). “Terrestrial Laser Scanning-Based Structural Damage Assessment.” Journal of Computing in Civil Engineering, 24(3), 264–272.

Park, H. S., Lee, H. M., Adeli, H., and Lee, I. (2007). “A New Approach for Health Monitoring of Structures: Terrestrial Laser Scanning.” Computer-Aided Civil and Infrastructure Engineering, 22(1), 19–30.

Tang, P., Chen, G., Shen, Z., and Ganapathy, R. (2015). “A Spatial-Context-Based Approach for Automated Spatial Change Analysis of Piece-Wise Linear Building Elements.” Computer-Aided Civil and Infrastructure Engineering, 31, 65–80.

Tang, P., Huber, D., Akinci, B., Lipman, R., and Lytle, A. (2010). “Automatic reconstruction of as-built building information models from laser-scanned point clouds: A review of related techniques.” Automation in Construction, Elsevier B.V., 19(7), 829–843.

Tang, P., Shen, Z., and Ganapathy, R. (2013). “Automated Spatial Change Analysis of Building Systems Using 3D Imagery Data.” 30th CIB W78 International Conference - October 9-12, Beijing, China, Proceedings of the 30th CIB W78 International Conference, 252–261.

Xiong, X., Adan, A., Akinci, B., and Huber, D. (2013). “Automatic creation of semantically rich 3D building models from laser scanner data.” Automation in Construction, Elsevier B.V., 31, 325–337.

Yi, T. H., Li, H. N., and Gu, M. (2013). “Experimental assessment of high-rate GPS receivers for deformation monitoring of bridge.” Measurement: Journal of the International Measurement Confederation, 46(1), 420–432.

Zogg, H.-M., and Ingensand, H. (2008). “Terrestrial Laser Scanning for Deformation Monitoring--Load Tests on the Felsenau Viaduct (CH).” International Archives of Photogrammetry and Remote Sensing, 37, 555–562.

CHAPTER 2

COMPUTATIONALLY EFFICIENT SPATIAL CHANGE DETECTION OF LARGE-SCALE BUILDING SYSTEMS USING 3D LASER SCANNING DATA

Introduction

Frequent changes in construction projects pose challenges to design-construction collaboration due to cascading interactions between design changes and field adjustments (Parvan et al. 2012). Incomplete design information, improper field operations, and unexpected site conditions may result in deviations between as-designed and as-built conditions of building components, which may lead to misalignments between components (Kalasapudi et al. 2014a; Wang et al. 2015; Xiong and Huber 2010). Therefore, developing computationally efficient change detection tool that can identify deviations between as-designed and as-built conditions is crucial in performing reliable spatial change analysis of large-scale building systems as discussed in the "Motivating Case" section in Chapter 1. In addition, undetected deviations may propagate along networks of building elements (e.g. ductworks), and cause cascading effects that are difficult to track. The propagation of design-built deviations among building elements usually requires a significant amount of change coordination efforts among multiple stakeholders. Improper change management could cause reworks, wastes, delays during construction while increasing construction costs (Park and Pena-Mora 2003). Furthermore, poor change coordination may also create interruptions in decision-making processes during Operations and Maintenance (O&M) phase. O&M planning can become challenging if detailed changes between as-built and as-designed conditions and

information about how spatial changes propagate along the spatial and temporal domains are missing (Xiong and Huber 2010). Construction engineers, therefore, have to analyze design changes and field adjustments causing design-built differences and find ways to control the impacts of such changes on project performance (Cai and Rasdorf 2008; Hindmarch et al. 2010).

Recent technological advancements, such as Building Information Modeling (BIM), enabled construction engineers and managers to coordinate design and construction activities of multiple trades involved in a project (Azhar et al. 2008). Commercial BIM software facilitates the visualization of building elements including Mechanical, Electrical, and Plumbing (MEP) systems for coordination purposes so that potential clashes among building elements can be resolved virtually before constructability problems occur on site ("Project Review Software | Navisworks Family | Autodesk" 2007). Some BIM tools support the comparison of multiple versions of as-designed models to detect changes between versions and record design change histories for change management (Seppo 2013). However, manual updates of as-designed BIM could be error-prone and may miss certain spatial changes occurring in the field. As a result, only using design-oriented BIM tools could hardly track differences between as-designed and as-built conditions (Han et al. 2012).

Chapter 1 highlights the potential of 3D laser scanning technology as an emerging technology that can capture very accurate as-built geometries promptly and discusses the use of such in capturing as-built geometry of a steel water tank in the "Motivating Case" section. In the domain of change analysis using 3D laser scanning technology, Tang et al. conducted a study which identified the challenges associated with detecting and

classifying spatial changes during design and construction processes (Tang et al. 2013). That study concluded that a robust spatial change detection and classification approach would enable reliable automatic diagnosis of the propagative effects of changes that cause reworks and construction quality problems. In addition, the author also discussed the limitation of traditional change detection algorithms which relied on "nearest neighbor searching" in the "Motivating Case" section in Chapter 1. Recent studies of the author explored the application of relational graphs to match and compare objects from 3D as-designed models with the objects in the corresponding 3D as-built model accurately (Kalasapudi et al. 2014a; Tang et al. 2015; Xiong and Huber 2010), which has significant advantages over data-model comparison tools that are available in commercial 3D data processing and reverse engineering environments, such as InnovMetric Polyworks (Innovmetric Software 2016). However, comparing relational graphs generated from as-designed models and 3D laser scan data of large-scale building systems (e.g., hundreds of inter-connected ductworks) involves computational complexity that grows exponentially with the number of building elements (Tang et al. 2015).

This chapter presents a novel approach that combines multiple algorithms to achieve a reliable and computationally efficient comparison of as-designed model and as-built models derived from laser scan data. This approach first calculates the distances between as-designed model objects and their corresponding geometries in the as-built model using the nearest neighbor algorithm, which derives a "data-model deviation map." The algorithm then uses the deviation map to isolate parts of the as-designed model that contain deviations larger than a threshold and applies reliable but

computationally expensive relational graph matching to those isolated parts. The algorithm finally utilizes the connectivity and spatial relationship between building elements to correct mismatches produced in the first step of "nearest neighbor matching," making sure that parts that have small deviations are all correct matches. This last step is necessary to avoid cases when certain as-designed and as-built objects that are not corresponding but happen to occupy the same space and have similar geometries. In brief, the developed approach leverages the computational efficiency of the nearest neighbor searching while narrowing the scope of executing computationally expensive relational graph matching to isolated model parts that contain significant changes. The objective is to achieve reliable data-model matching while maintaining computational efficiency.

The following section first provides a comprehensive review of challenges associated with the current design – construction change analysis and management methodologies. The methodology section of this chapter details the proposed novel approach for efficient and reliable change detection. Next, the validation and results section uses the as-designed model and laser scan data of a large-scale ductwork of an educational building to validate the efficiency and reliability of the proposed approach. Finally, the author discusses (Discussion and Conclusion) research findings, draw conclusions, summarize advantages and drawbacks of the proposed approach, and recommend future research directions.

Background

Construction industry adopted various technologies such as BIM and 3D imaging for managing changes in construction projects. The following paragraphs reviews the

literature on change management approaches employed in current design and construction practice. Spatial changes can originate even during the design phase of a construction project and inability to track changes originating in the design phase might influence the overall construction quality. Design changes have various impacts on the quality and performance of a construction project (Parvan et al. 2012). Poor communication among different trades and poor documentation practices lead to design changes and rework during construction (Wang et al. 2015). In current practice, design changes are documented as "Change Orders" as per the procedures defined by the American Institute of Architects (AIA) ("AIA Homepage - The American Institute of Architects" 1857; Hao et al. 2008). Architects follow these guidelines and manually log all the design change orders, which is time-consuming and error-prone.

BIM technology addresses the difficulties associated with design change coordination by enabling synchronization of multiple trade design models in a central BIM for clash detection and coordination (Azhar et al. 2008). Langroodi & Staub-French (Langroodi and Staub-French 2012) conducted a case study to exploit the benefits of using BIM for design change management of a fast-track project. Akinci and Boukamp (Akinci and Boukamp 2003) concluded that BIM can document different design alterations, but could hardly address the propagative impacts of changes that collectively influence the construction quality, cost, and productivity. Also, BIM tools mainly focus on design change coordination, while engineers are required to update as-designed BIM manually according to the as-built conditions to analyze the impact of field changes on the project performance. This practice is tedious and error-prone.

As discussed in the above paragraph, several commercial software has the capability to track and analyze spatial changes during the design phase of a construction project fail to associate the final updated design model with the as-built condition. Chapter 1 discussed the advantages as well as the limitations of the widely adopted change detection paradigm – nearest neighbor searching, which forms the basis of many previously published change detection methods in the domain of construction engineering and management. The following paragraph briefly discusses previous studies on change detection of individual components of a building system that rely on the nearest neighbor searching principle.

Previous studies focused on automated modeling of as-built pipelines from laser scan data for construction quality assessment and monitoring purposes (Bosché et al. 2014; Lee et al. 2013; Son et al. 2015). Construction project managers would use these as-built models to investigate any dimensional deviations between the individual objects of the as-built and as-designed models. Several studies investigated the integrated use of 3D imaging technologies and BIM for detecting and analyzing spatial changes that occur in the field. Tang et al. reviewed a broad range of algorithms and techniques that are used for the recognition and reconstruction of building elements from 3D laser scan data for as-built modeling (Tang et al. 2010). Based on this review, Xiong et al. developed methods that automatically create semantically rich BIM from 3D laser scan data using voxel representation to make the as-designed and as-built BIM comparison more efficient (Xiong et al. 2013). Similar concepts inspired a study that developed an approach for automated spatial change analysis of linear building elements (Tang et al. 2015). Bosché developed a robust point matching method for as-built dimension calculation and control

of 3D CAD model objects recognized in laser scans (Bosché 2010). Based on this work, Turkan et al. developed an automated progress monitoring system that combines 4D BIM and 3D laser scan data for change detection and management (Turkan et al. 2012). In the similar domain, Son et al. developed an automated schedule updating system that provides critical schedule information by comparing an as-built point cloud data and a 4D BIM model that includes an as-planned schedule of an actual construction site (Son et al. 2017). Nahangi and Haas developed an automated deviation detection approach for pipe spools based on scan-to-BIM registration (Nahangi and Haas 2014). This study employed an automated registration step for quantifying the deviations in the defective parts of the pipe spool assemblies. Bosché et al. coupled Scan-versus-BIM, and Scan-to-BIM approaches to track and diagnose changes of densely packed cylindrical MEP (Mechanical, Electrical, and Plumbing) elements (Bosché et al. 2015).

The majority of the studies described above utilizes nearest-neighbor searching algorithms for detecting spatial deviations and changes between as-designed and as-built conditions and thus inherit the limitations of this algorithm. In many cases, especially when several similar objects packed in small spaces (e.g., several ducts packed in a mechanical room), the change detection results of nearest neighbor searching may contain mismatches that associate data points with the wrong objects in the as-designed model (Tang et al. 2015). As a result, relying on unreliable change detection results will significantly affect the overall spatial change analysis study.

A previous study by the author (Kalasapudi et al. 2014a; Tang et al. 2015) matched “spatial contexts” of building components, e.g. ducts, captured in as-designed and as-built models to achieve more reliable association between as-designed model and

as-built data and to reduce the mismatches generated by the nearest neighbor searching algorithm. That study first constructs "relational graphs" that depict spatial relationships between objects extracted from as-designed models or as-built models created based on 3D laser scan data. More specifically, a relational graph is a network representation of the objects in a model, in which the nodes represent the objects and the edges connecting them represent spatial relationships between objects (Figure 7). Each node can have attributes to describe the properties of the object, called "local attributes" (e.g., shape, size, or color). The spatial relationships of an object with other objects represent the "spatial context" of that object. After obtaining two relational graphs that respectively represent the as-designed model and the as-built model, the algorithm matches these two relational graphs and associate as-designed objects with as-built model elements (e.g., surfaces and lines extracted from laser scan data) based on the similarity of their attributes and spatial contexts. More details of this algorithm are in (Kalasapudi et al. 2014a; Tang et al. 2015). These two studies showed that this relational-graph-based approach could achieve automatic and reliable change detection of relatively small ductworks (< 20 ducts) in a mechanical room (Kalasapudi et al. 2014a; Tang et al. 2015).

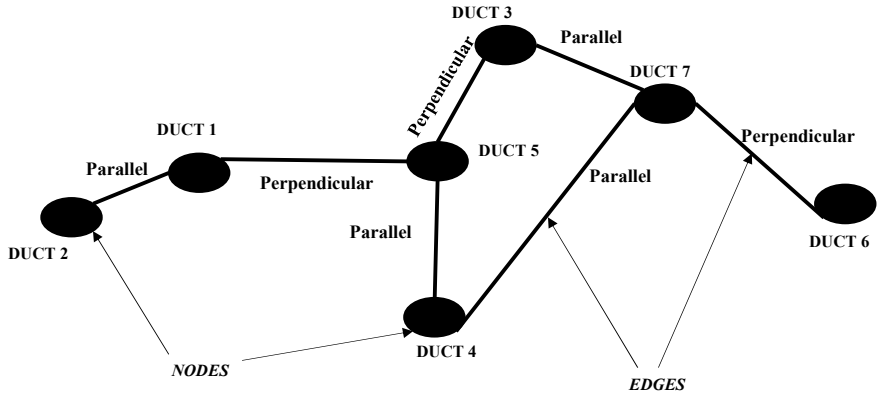

Figure 7. Example of a relational graph network

The two studies described above used cases that involve ten ducts to validate the relational-graph-based approach. Unfortunately, the computational complexity of extracting and matching relational graphs from large datasets increase exponentially with the number of objects in the as-designed and as-built models. A step forward is thus improving the computational efficiency of the relational-graph-based approach.

Methodology

The proposed improvement of the relational-graph-based approach integrates nearest neighbor searching and the relational-graph-based matching approaches to achieve a computationally efficient change detection for large as-designed models and as-built laser scan data of building systems composed of hundreds of elements (e.g., ductworks).

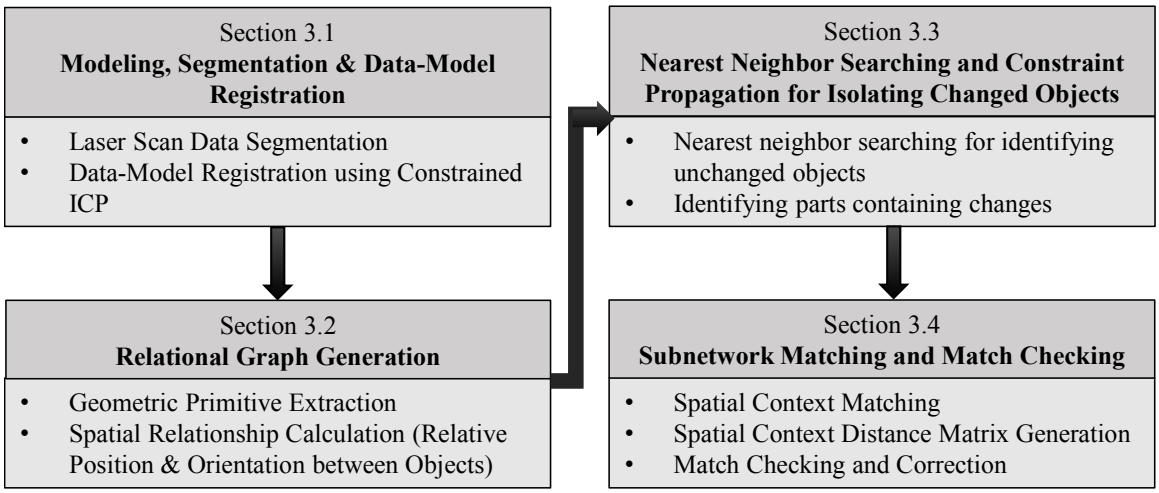

Figure 8. Framework for change detection between as-designed model and as-built model

Figure 8 presents four steps of the new method: 1) modeling, segmentation, and data-model registration, 2) relational graph generation, 3) nearest neighbor searching and constraint propagation for isolating subnetworks that contain significant changes or

deviations, and 4) subnetwork matching using spatial contexts and match checking, as detailed below.

Modeling, Segmentation, and Data-Model Registration

This step involves preprocessing of 3D laser scan data to remove redundant information and segments out relevant data for reliable change detection (Rabbani et al. 2006). Commercially available software tools for 3D laser scan data processing, such as Leica Geosystems HDS™ Cyclone, 3DReshaper, and ClearEdge^{3D} EdgeWise^{TM}, include segmentation and modeling tools (ClearEdge 3D 2011; Geosystems 2006; Technodigit 2009). In this study, the author used Clear Edge's EdgeWise 3D Plant Suite™ software to extract 3D objects (e.g., ducts) from 3D laser scan data (ClearEdge 3D 2011). This process is referred to as Scan-to-BIM, where the final product is a 3D as-built model. Clear Edge's Edgewise 3D Plant^{TM} software considers occlusions when implementing cylinder-fitting algorithms for extracting ducts from 3D laser scan data. Our testing results confirmed that the cylinder fitting algorithm implemented in Clear Edge's Edgewise 3D Plant^{TM} software can accurately extract cylindrical ducts from 3D laser scan data even if only partial surfaces of the cylindrical shapes are scanned. Such occlusion-tolerant algorithms ensure that the axes of ducts used for change analysis between the as-designed and as-built ductworks are reliable. Next, the author align the as-designed model against the as-built model using a Constrained Iterative Closest Point (ICP) registration technique so that to bring the as-designed and as-built models to the same coordinate system (Tang and Rasheed 2013). This process requires users to first manually align larger ducts with a radius larger than 0.1 meters between the as-designed and as-built models, and then apply the constrained ICP algorithm by utilizing a

maximum distance value of 0.3 meters. This "maximum distance" value of 0.3 m means that the registration algorithm would not search corresponding objects beyond a neighborhood of 0.3 m (a sphere with a radius of 0.3 for searching corresponding objects). Narrowing the closest point search in such a 0.3 m spherical neighborhood ignores the parts of the model with significant deviations for improved computational efficiency. This data-model registration is a preparation necessary for the following data-model comparison that integrates the nearest neighbor searching and relational graph matching.

Relational Graph Generation

This step aims at automatically extracting local attributes of objects (e.g., lengths and radii of duct sections) and spatial relationship between objects for generating relational graphs based on the as-designed model and the as-built model created based on laser scan data. The algorithm first detects the attributes of all objects present in both models, and then automatically generates relational graphs for both models by computing spatial relationships between objects. Algorithm 1 below shows the pseudo code of this relational graph generation process. To generate the nodes and edges of relational graphs, algorithm 1 requires the geometric representations of all objects present in both the as-designed and as-built models. The focus of this study is change detection of cylindrical ductworks packed in relatively small mechanical rooms so that the author focus on the geometric representations of ductworks. Specifically, the author used "Line" as a geometric primitive to represent cylindrical ducts present in the as-designed and as-built models. The developed algorithm thus needs to automatically extract the axes of the cylindrical duct sections in the as-designed and as-built models and represents them as

lines to generate the relational graphs. Because the geometric representation of duct sections in as-designed and as-built models are surfaces of cylindrical objects, the extraction of axes of cylinders need to implement a method for fitting lines based on the surface geometry.

Algorithm 1: Pseudo Code for Relational Graph Generation

```
1.  //Sampled duct components of As-designed model
2.  for each sampled as-designed duct
3.      Use Principle Component Analysis to extract line segments (best fit)
4.      Calculate the line segment's center point P(x,y,z)
5.      Calculate relative positions (Eq 1) & orientations (Eq 2) between extracted line segments
6.  end
7.  //Sampled duct components of As-built model
8.  for each sampled as-built model duct
9.      Use Principle Component Analysis to extract line segments (best fit)
10.     Calculate the line segment's center point P'(x,y,z)
11.     Calculate relative positions (Eq 1) & orientations (Eq 2) between extracted line segments
12. end
```

Relative Position between center points P(x,y,z) and P(x_1,y_1,z_1)

$$Rp = (x - x_1, y - y_1, z - z_1) \quad (1)$$

Relative Orientation between Line Segments a = (a_1,a_2,a_3) and b = (b_1,b_2,b_3)

$$Ro = a \times b = (a_2b_3 - a_3b_2, a_3b_1 - a_1b_3, a_1b_2 - a_2b_1) \quad (2)$$

The author's implementation is to use the "sample points on mesh" tool of the CloudCompare™ software (Girardeau-Montaut 2011) to uniformly sample points on the surfaces of as-designed and as-built model objects. That process converts surfaces of objects into point clouds. The Principle Component Analysis (PCA) method then extracts lines from the 3D points sampled on surfaces of duct sections. Figure 9 shows an

example of sampled as-designed model ducts (Red). The algorithm then detects changes between the as-designed/as-built lines extracted from the uniformly sampled as-designed/as-built point clouds. In the past, researchers found that fitting geometric primitives against 3D point cloud data with varying data densities will produce geometric primitives that are distorted towards parts having higher data densities. Therefore, using resampled point clouds will avoid inaccurate geometric primitives extracted from raw point clouds that have varying data densities.

In the modeling step, the author focus on modeling the straight duct sections from the as-designed and as-built models, because analyzing the changes of those sections can serve as a major step forward to further analysis of joints and valves. More specifically, matching lines (straight duct sections) between the models pave the path toward automatically recognizing the connections between those lines (e.g., elbows, joints) and matching the as-designed and as-built objects relevant to those connections (valves installed on those connected parts). Keeping the cylindrical ducts as the focus in this chapter, the number of points required for identifying cylindrical duct sections is set to be 100 pts per square meter. The author conducted experiments on 3D imagery data used in this research and found that using this threshold could successfully eliminate elbow connections, valves, and tee joints between ducts while keeping straight sections of ducts in both the as-designed and as-built models. This process of modeling (Scan-to-BIM) and uniform sampling is robust when extracting straight cylindrical duct sections even if the duct is occluded in the 3D laser scan data. The next step is to extract the best-fit line (geometric primitive) of straight cylindrical duct sections using the PCA algorithm and then generate the relational graph.

Given relational graphs that represent the spatial relationships between duct sections (lines), the relational-graph-generation algorithm finally generates a spatial context for each line or each duct section in both the as-designed and as-built models. The algorithm automatically uses the position and orientation information of lines to calculate the relative position (e.g., above, below, left, right) and orientation (e.g., parallel, perpendicular) between lines and the spatial contexts of lines. A spatial context of a line represents how many lines are above, below, to the left/right, parallel with and perpendicular to that line. These spatial contexts would play critical roles in the step of relational graph matching presented later.

Nearest Neighbor Searching and Constraint Propagation for Isolating Change Parts

The generated relational graphs provide a basis for the detection of differences between the as-designed and as-built models. In the change detection step, the algorithm first uses the nearest neighbor searching to associate the objects (ducts) that did not have significant deviations between the as-designed and as-built models. The algorithm then follows a hierarchical process to isolate parts of the ductworks that have significant deviations and apply computationally expensive but reliable relational graph matching. Such hierarchical process reduces the amount of computation by first establishing most of the data-model associations through the rapid nearest neighbor search, leaving the context matching on smaller parts of the large network of ductworks.

Algorithm 2 below shows the pseudo code of this process. In Algorithm 2, i represents the i-th as-designed line, and j represents the j-th as-built line; diff_distance (i,j) represents the distance between center points of lines i and j; diff_orientation (i,j) stands for the dot-product of the orientation vectors of lines i and j (i.e., 1 means that two

lines are parallel). CM is the Correlation Matrix that indicates the association between as-designed and as-built lines – if CM(i,j) equals to 1, then the i-th as-designed line is corresponding to the j-th as-built line, while 0 represents no association. Table 1 shows an example of a correlation matrix presenting the matching results of the as-designed and as-built models shown in Figure 9.

Algorithm 2: Pseudo Code for Change Detection using the nearest neighbor searching

```
1.  Define diff_distance (i,j)=zeros; (i is the i-th as-designed line, j is the j-th as-built line)
2.  Define diff_orientation (i,j)=zeros; (i is the i-th as-designed line, j is the j-th as-built line)
3.  Define CM(i,j)=zeros; (Correlation matrix between diff_distance and diff_orientation)
4.  for each ducts center point from both as-designed model and as-built model
5.      Calculate the distance "D" between each pair i,j's center points and store it in
        diff_distance(i,j)
6.      Calculate the dot product between each i,j's line segments and store it in
        diff_orientation(i,j)
7.    if  diff_distance(i,j) <0.15 && diff_orientation ==1
8.        CM(i,j) ==1
9.    else
10.       CM(i,j) ==0
11.   end
12. end
```

In Algorithm 2, the algorithm first eliminates parts of the ductworks that have no significant deviations based on the deviation map produced by the nearest neighbor searching process. The remaining parts would then contain large deviations and be much smaller than the complete duct network for carrying out computationally expensive relational graph matching process. The algorithm first uses the relative position and orientation of the lines (duct sections) to associate duct sections that have similar locations and orientations. Specifically, the algorithm calculates the center of each extracted line from the as-designed model and the as-built model, and determines that

two lines be corresponding lines in the as-designed and as-built models based on two conditions: 1) the distance between the two lines' center points are less than 0.15 m, and 2) the two lines are parallel with each other. The author found that this 0.15 m threshold could effectively identify most pairs of lines that have less or no changes between as-designed and as-built models. Figure 9 shows an example of an as-designed model (red) and its corresponding as-built model (blue). In Figure 9, the distance between the centers of the line (duct) 14 (as-designed) and line 12' (duct) (as-built) is within 0.15 m, and they are parallel with each other. Thus, the algorithm associates these two lines (Table 1).

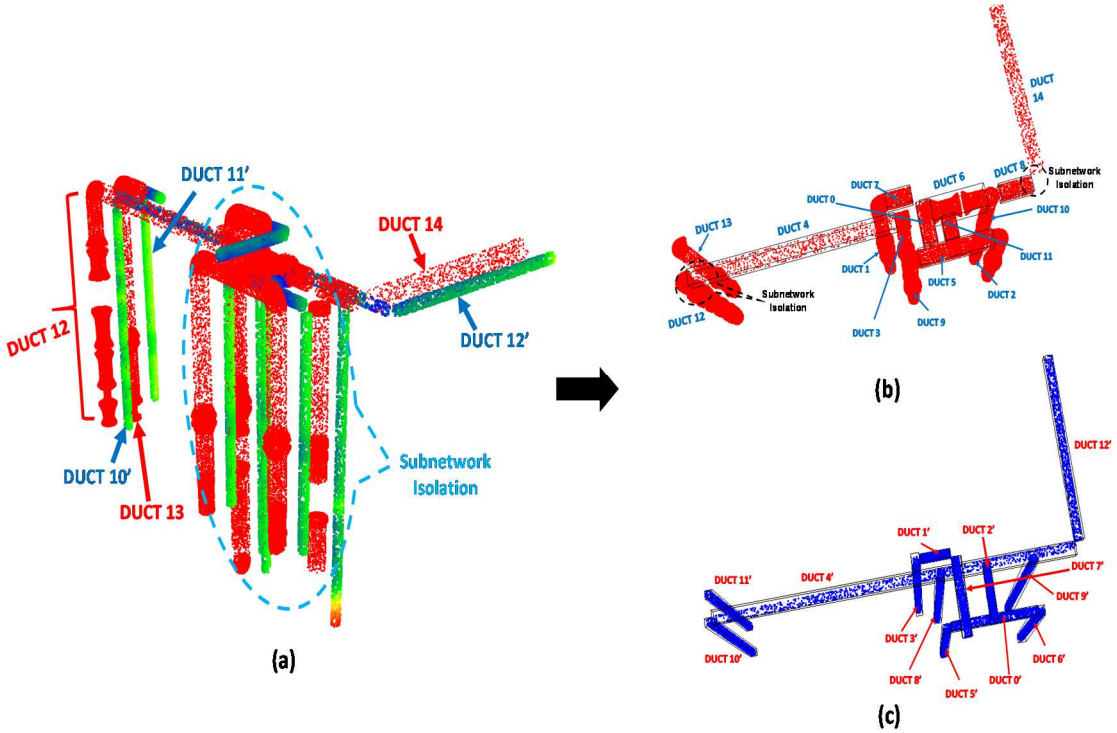

Figure 9. (a) Nearest neighbor matching between (b) As-designed model (Red) and (c) As-built model (Blue)

Table 1. Correlation matrix for subnetwork 1 ("1" means a match, "0" means no match)

As-Designed/ As-Built	DUCT 0'	DUCT 1'	DUCT 2'	DUCT 3'	DUCT 4'	DUCT 5'	DUCT 6'	DUCT 7'	DUCT 8'	DUCT 9'	DUCT 10'	DUCT 11'	DUCT 12'
DUCT 0	1	1	1	0	1	0	0	1	0	0	0	0	0
DUCT 1	0	0	0	1	0	0	0	0	1	0	0	0	0
DUCT 2	0	0	0	0	0	0	1	0	0	1	0	0	0
DUCT 3	0	0	0	1	0	1	0	0	1	0	0	0	0
DUCT 4	0	0	0	0	1	0	0	0	0	0	0	0	0
DUCT 5	1	0	0	0	0	0	0	1	0	0	0	0	0
DUCT 6	0	0	1	0	0	0	0	0	0	0	0	0	0
DUCT 7	0	1	0	0	1	0	0	0	0	0	0	0	0
DUCT 8	0	0	0	0	0	0	0	0	0	0	0	0	0
DUCT 9	0	0	0	0	0	1	0	0	1	0	0	0	0
DUCT 10	0	0	0	0	0	0	1	0	0	1	0	0	0
DUCT 11	1	0	1	0	0	0	0	1	0	0	0	0	0
DUCT 12	0	0	0	0	0	0	0	0	0	0	1	0	0
DUCT 13	0	0	0	0	0	0	0	0	0	0	1	1	0
DUCT 14	0	0	0	0	0	0	0	0	0	0	0	0	1

The nearest neighbor searching step matches most of the duct sections that do not change in the as-designed and as-built models and assign "1"s to the elements of the Correlation Matrix to indicate these matches. On the other hand, such simple nearest neighbor and orientation checking have the following limitations:1) if the models consist of duct sections packed in small spaces, the algorithm will associate multiple as-designed ducts within 0.15 m with a single as-built duct while only one of these as-designed ducts is the correct match, and vice versa; 2) if significant changes occurred during construction, the nearest neighbor searching can't automatically associate as-designed and as-built objects that move out of the neighborhood due to changes; 3) if the occlusions in the as-built model split a duct into multiple sections and cause significant dislocations of the center points of duct sections, which would not be within 0.15 m of any as-designed ducts and thus remain unmatched; 4) if a change causes an as-built duct occupy the same space of an as-designed duct that is actually not corresponding to the as-built duct, the algorithm incorrectly associates these two ducts. The following paragraphs

will introduce new techniques that could resolve these limitations based on spatial relationship and context information available in relational graphs.

A "constraint propagation" step can overcome the first limitation of the nearest neighbor searching process. For example, in Figure 9(a), the as-designed duct 13 is the nearest neighbor to both as-built duct 10' and duct 11'. The correlation matrix indicates that duct 13 in the as-designed model matches with both duct 10' and duct 11' in the as-built model (Table 1). The constraint propagation process found that duct 10' is the only match of duct 12, so it applies constraint propagation to resolve the ambiguous match between duct 10' and duct 13 (Highlighted in Table 1) and determines that duct 13 should be paired with duct 11'. Such sequential matching eliminates multiple associations and increases the accuracy of matching. After executing the nearest neighbor searching and constraint propagations, the correlation matrix still has unmatched ducts or incorrect matches. Figure 9(a) clearly shows that few ducts (dash line) are close to each other, where the nearest neighbor matching fails and leave certain lines as "unmatched." Once the algorithm identifies these matched and unmatched lines, it automatically isolates smaller subnetworks that contain unmatched lines (Figure 9(b)&(c)) breaks from the entire relational graph. Such subnetwork isolation utilizes the results of the nearest neighbor searching and constraint propagation along with the connectivity information between the adjacent ducts. Specifically, the unmatched Duct 4 in the as-designed model is connected to an unmatched Duct 3 and a matched Duct 12. Since Duct 12 is matched using both the nearest neighbor searching and the constraint propagation, the algorithm will use the connection between Duct 4 and Duct 12 to isolate the sub-network (Figure 9(b)-Highlighted in Black). Similarly, the subnetwork isolation approach identified the

connection between the unmatched Duct 8 and matched Duct 14 to identify interconnected unmatched ducts (Figure 9(b)-Highlighted in Black). Using this subnetwork isolation approach, the algorithm isolated Ducts 0-11 in the as-designed model and Ducts 0'-9' in the as-built model (Figure 9(b)&(c)) for further spatial context matching, as detailed in the next subsection.

Subnetwork Matching Using Spatial Contexts, and Match Checking

A combined use of connectivity information that indicates the adjacent ducts through connections and spatial contexts of ducts that indicate relative position and orientation between ducts can help address the second limitation of nearest neighbor searching – the difficulty in associating changed ducts in the as-designed and as-built models. The developed algorithm first detects areas that have interconnected unmatched ducts (lines). The algorithm then either traces the connected ducts or identifies ducts with similar spatial contexts to associate unmatched as-built ducts with their likely correspondents in the as-designed model. Figure 10 shows an example of tracing connected ducts for identifying corresponding ducts between the as-designed and as-built models. In this case, a subnetwork contains three connected ducts.

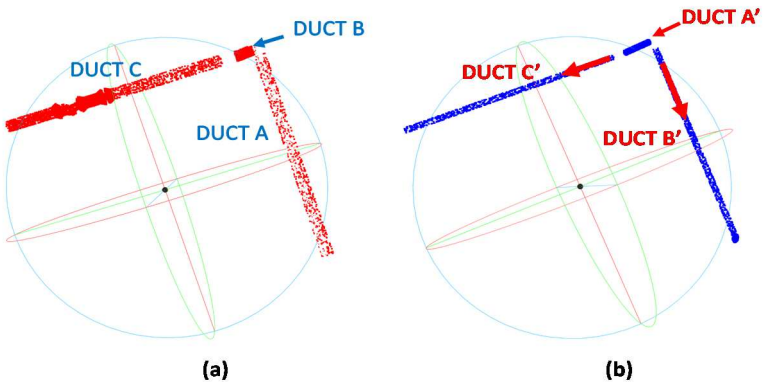

Figure 10. (a) As-designed model ducts (b) As-built model ducts

Algorithm 3: Pseudo Code for Subnetwork Matching using spatial context

```
1.  // For each duct in the Subnetwork (As-designed model and As-built Model)
2.  Define r_fnt, l_fnt, r_bk, l_bk (Initial Value=0)
3.  for each Unmatched duct's center point
4.      if Difference between the x-coordinate of an as-designed line and an as-built line >0
5.          if  Two lines are parallel
6.              l_fnt = l_fnt + 1
7.          else
8.              r_fnt = r_fnt +1
9.          end
10.     end
11.     if Difference between the x-coordinate of an as-designed line and an as-built line <0
12.         if  Two lines are parallel
13.             l_bk = l_bk + 1
14.         else
15.             r_bk = r_bk +1
16.         end
17.     end
18. end
19. //Repeat the above loop for y, z coordinates of the line's (As-designed and as-built models)
    center points by defining r_rt, l_rt, r_lft, l_lft, r_ab, l_ab, r_blw, l_blw
20. // Generate "Spatial Context Matrix" for each line (duct) using all the variables defined
    above.
21. // Find the absolute sum of differences between spatial context matrix of each line (duct)
    from the as-built model to each line (duct) from the as-designed model.
22. // Generate the spatial context distance matrix.
23. //Use the least distance value to match corresponding ducts from the as-built model with
    ducts from the as-designed model.
```

The nearest neighbor matching process associated duct C (as-designed) with duct C' (as-built), and duct A (as-designed) with duct B' (as-built). Duct A' in the as-built model is short but still twice longer than its corresponding as-designed object (duct B); so that the nearest neighbor matching could not match these two short ducts. The connection tracking method can associate duct B with duct A' through the check of the connections

with ducts already matched – two adjacent ducts both have known matches in the as-built model, then duct B should be duct A', which connect the two matched as-built ducts. More generally, the connection tracking algorithm can grow the network of matched ducts (along the red arrows in Figure 10(b)) through connections for identifying more matches until filling unmatched "gaps" between matched ducts.

Unfortunately, tracing the connections could become unreliable if large numbers of unmatched duct sections connect because any mismatches along the connectivity chain could cause a series of mismatches along the chain of connected objects. In such cases, a more reliable but more computationally expensive spatial context matching is necessary for identifying corresponding as-built ducts that have similar spatial contexts as unmatched as-designed ducts. More specifically, the algorithm will first examine the total number of ducts in the as-designed model that form a connected component of unmatched ducts, if that number is more than three, then the algorithm will apply spatial context matching detailed in Algorithm 3.

Algorithm 3 generates a "local" spatial context for each duct in the isolated parts of duct networks that undergo significant changes between their as-designed and as-built models. Such isolated parts of ducts are "subnetworks" of larger duct networks of the as-designed and as-built model. A "local" spatial context represents the relative spatial locations and orientations of a duct with respect to other ducts in the subnetwork that contains the considered duct (Kalasapudi et al. 2014a). Table 2 formally defines the concept of local spatial context - every row represents the relative positions of the considered duct with respect to other ducts in the subnetwork along the X, Y, and Z-axes. Here "r" represents the number of lines perpendicular to it; "l" represents the number of

lines parallel to it. Along the x-axis, “fnt” means front, “bk” means back. Along the y-axis, “rt” means to the right, “lft” means to the left. Along the z-axis, “ab” means above, and “blw” represents below the corresponding duct. Therefore, “l_{fnt}” stands for the number of ducts in front of and parallel to the considered duct.

Table 2. Spatial Context matrix

Axis	**Spatial Context**			
x	r_{fnt}	l_{fnt}	r_{bk}	l_{bk}
y	r_{rt}	l_{rt}	r_{lft}	l_{lft}
z	r_{ab}	l_{ab}	r_{blw}	l_{blw}

$$D_{ij} = \text{Sum}\left(\left|C_{ii} - C'_{ii}\right|\right) \quad (3)$$

The spatial context matching process calculates the spatial context distance between two ducts and identifies as-designed and as-built ducts that have the most similar spatial contexts as matches. The spatial context distance is the absolute sum of the differences between the local spatial context matrices of the as-designed duct (*C)* and the as-built duct (C'), as shown in Equation 3. The spatial context matching process associates all remaining unmatched ducts in the as-built model with ducts in the as-designed model that have the most similar spatial contexts as theirs. The distances between the local spatial contexts are elements in a “spatial context distance matrix.” In a spatial context distance matrix, the rows represent the ducts from the as-designed model, and the columns represent the ducts from the as-built model. The matrix elements contain values of the spatial context distances between the corresponding pairs of as-designed and as-built ducts.

Table 3. Spatial context distance matrix generated for ducts shown in Figure 12

As-Designed/ As-Built	DUCT 0'	DUCT 1'	DUCT 2'	DUCT 3'	DUCT 4'	DUCT 5'	DUCT 6'	DUCT 7'	DUCT 8'	DUCT 9'
DUCT 0	12	24	19	18	20	16	16	**8**	13	10
DUCT 1	28	16	14	**4**	18	21	18	16	24	20
DUCT 2	20	12	15	19	19	36	**7**	18	36	24
DUCT 3	12	20	24	13	29	33	19	19	**5**	16
DUCT 4	13	28	24	16	**6**	23	30	26	33	12
DUCT 5	**6**	20	14	28	27	27	23	21	24	20
DUCT 6	24	13	14	20	**9**	19	22	22	14	28
DUCT 7	18	**2**	19	24	36	18	19	12	14	24
DUCT 8	15	19	18	16	**7**	16	18	20	19	24
DUCT 9	13	14	20	9	19	**3**	16	19	13	14
DUCT 10	10	16	36	18	10	24	28	22	10	**4**
DUCT 11	24	20	**10**	20	24	20	20	29	24	19

Table 3 presents the spatial context distance matrix generated for the isolated subnetworks case shown in Figure 9. This table indicates that the local spatial context matching approach can achieve a reliable match in certain cases. For example, ducts 4, 6, and 8 from the as-designed model are correctly associated with one duct in the as-built model (duct 4'). The spatial context matching can handle such "n to one" matching cases. Actually, for the case shown in Figure 9, the spatial context matching correctly associate all ten as-built ducts with the corresponding as-designed ducts, while the nearest neighbor searching could only correctly match eight of these ten ducts.

Above discussions indicate that a combined use of connection tracing and spatial context matching can address the second limitation of the nearest neighbor searching (cannot establish reliable matches between as-designed and as-built ducts when significant changes occur). Overall, the algorithm will classify the subnetworks of ducts into two categories: Category 1 – subnetworks that have three or less connected ducts, and category 2 – subnetworks that have more than three connected ducts. Once the algorithm extracts all subnetworks containing unmatched ducts between the as-designed

and as-built model, it separates them into these two categories. The algorithm uses the connection tracking for growing subnetworks falling into category 1 for filling the unmatched duct sections between matched parts of the duct network. When the subnetwork has more than three ducts and becomes a category 2 subnetwork, the algorithm will apply the local spatial context matching for achieving more reliable matching. The last two limitations of the nearest neighbor searching described at the beginning of this subsection cause mismatches – those ducts that are matched in the nearest neighbor searching step could be wrong. An addition step of match checking is thus necessary for correcting such nearest neighbor mismatches. Such a match-checking step traces the connections between ducts available in the as-designed and as-built models for verifying the consistency of the matching results. For example, when two connected as-designed ducts are matched with two as-built ducts that are not connected, the algorithm will detect that inconsistency, and trigger a back-tracking of the connection relationships for correcting the mismatch.

Performance Metrics and Comparative Analysis of Algorithms for Change Detection

The fast and computationally efficient change detection approach presented in this chapter accurately associates the as-designed and as-built model objects, as discussed above. Based on previous studies of assessing the performance of change detection algorithms (Clarkson 2006; Kalasapudi et al. 2014a), the author propose to validate the performance of the approach presented in this chapter against the nearest neighbor searching approach (NN approach hereafter) and a spatial-context matching approach (SC approach hereafter) presented by the author in (Kalasapudi et al. 2014a). In this comparative analysis of the three change detection approaches, the author use the amount

of computation time and precision as two metrics to compare the performance of these three algorithms. The computation time only includes the time after the data-model registration step because all three compared approaches use the same data-model registration step and the critical performance difference between these algorithms lie in the steps related to data-model matching. Equation 4 defines the metric of precision.

$$Precision\ (P) = \frac{Number\ of\ Correctly\ Matched\ Ducts}{Total\ Number\ of\ Modeled\ As{-}Built\ Ducts} \quad (4)$$

The precision refers to the percentage of correctly matched as-built ducts in this study. The author manually associated as-built ducts with as-designed ducts to create the ground truth necessary for calculating the "number of correctly matched ducts" and derive the precision of matching between as-built and as-designed models.

Validation and Results

Experiment Design

To validate the proposed approach in this chapeter, the author collected as-designed information and as-built data of an educational building located at Iowa State University campus. The building is a four-story structure with 16,260 square meter space. The experiment conducted here was focused on the mechanical room of the building. The general contractor of the project provided the as-designed model of the mechanical room, while the author collected the as-built data using a Trimble® TX5 phase-based laser scanner. Figure 11 presents the 3D laser scan data of the mechanical room as well as its corresponding up-to-date BIM, which was updated multiple times during construction

due to design changes. Appendix A provides more details about the collected as-designed and as-built data of the mechanical room of the educational building.

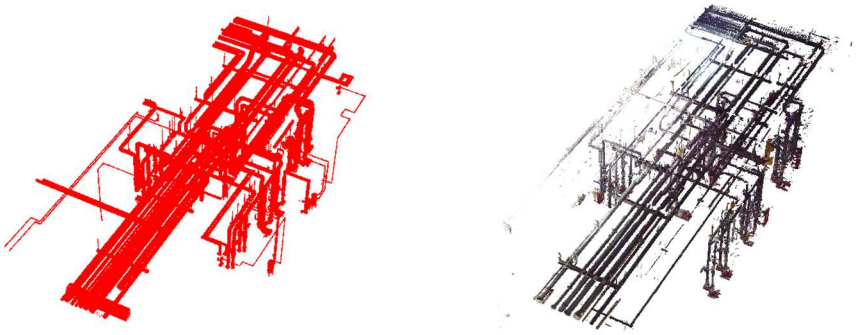

(a) (b)

Figure 11. (a) As-designed model (b) 3D Laser scan data

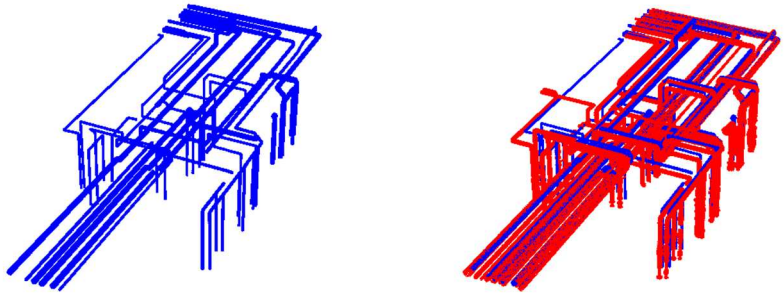

(a) (b)

Figure 12. (a) As-built model (b) Registered as-designed model and as-built model

The four-step process presented in the methodology section of this chapter was applied to the dataset described above to match the ducts captured in the as-designed model and the 3D laser scan data. The first step is to use the ClearEdge3D™ point cloud processing software to extract ducts present in the laser scan data. The software roughly aligned the design model and as-built data and was able to detect 66% (109 out of 165) of the as-designed ducts that were visible in the 3D laser scan data (Figure 12). The validation experiments presented below thus use that 109 ducts for comparing the data-

model matching the performance of the method presented in this chapter (NN + SC method) against the nearest neighbor searching (NN method) and spatial context matching (SC method) methods examined in previous studies.

Experiment Results

Upon completion of the as-built modeling process, the nearest neighbor searching and the constraint propagation algorithms were able to detect deviations between the as-designed and as-built models. In the test case, the nearest neighbor searching and constraint propagation algorithms matched (77%) 84 out of 109 of the ducts between two models while detecting and isolating ducts with large deviations between the as-designed and as-built models. Figure 13 shows areas of duct network having large deviations (Major isolated subnetworks). Table 4 lists all subnetworks isolated for this test case.

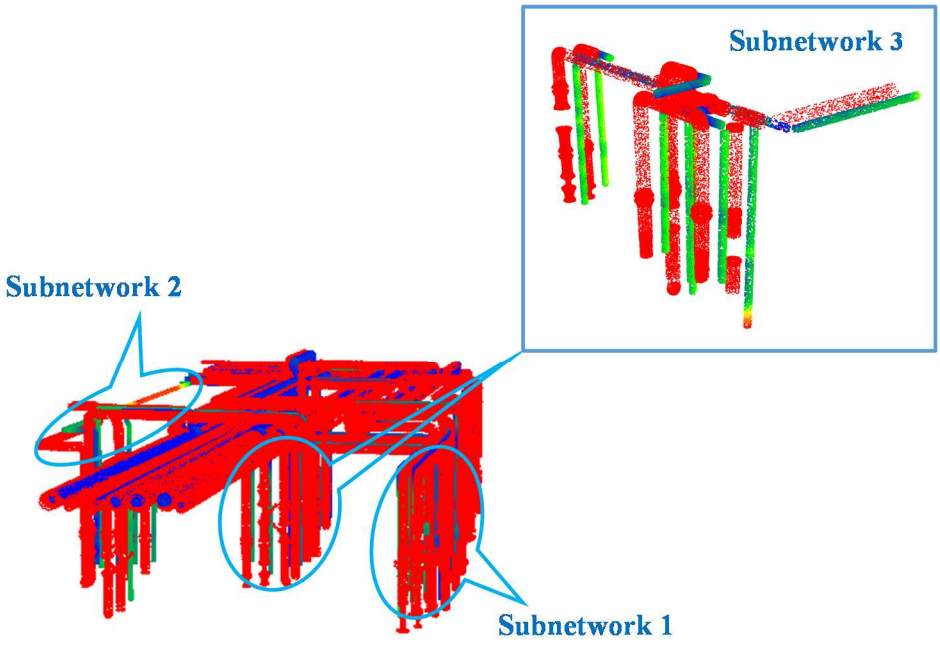

Figure 13. Areas with large deviations (Major Isolated Subnetworks)

Table 4. Subnetworks isolated by the nearest neighbor searching and constraint propagation process

Subnetwork	No. of ducts in the subnetwork (As-Designed model)	No. of ducts in the subnetwork (As-Built model)
Subnetwork 1	8	8
Subnetwork 2	6	6
Subnetwork 3	12	10
Subnetwork 4	5	5
Subnetwork 5	4	4
Subnetwork 6	3	3
Subnetwork 7	3	3

Comparison of the Developed Algorithm with NN and SC Methods

Figure 14 provides a comparison between the algorithms in terms of processing time and precision; where "NN" is the nearest neighbor searching approach, while "SC" is the spatial context algorithm presented in (Kalasapudi et al. 2014a), and "NN&SC" refers to the algorithm proposed in this study. To ensure the generality of the comparative performance analysis of these algorithms, the author conducted a set of experiments using 10, 20, 39, 69, and 109 ducts respectively. The experimental results (Figure 14) indicate that the proposed NN&SC algorithm is more precise compared to NN and SC algorithms. Figure 14 shows that when the number of ducts increases, the processing time required for matching using NN algorithm increases while the precision decreases significantly. On the other hand, the processing time required for matching using NN&SC algorithm increases but not exponentially while maintaining the precision of matching.

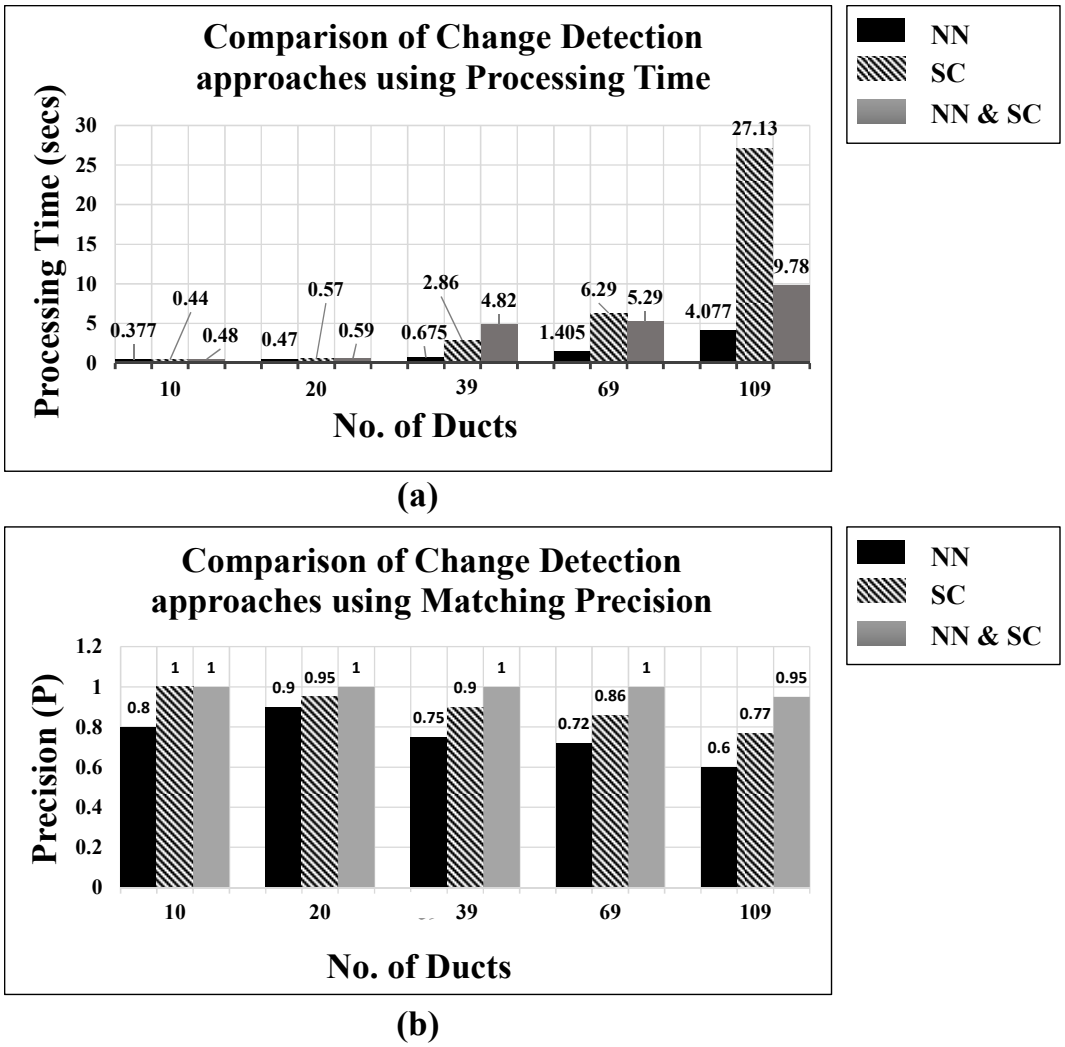

Figure 14. Comparison of change detection approaches using (a) Processing Time (secs) and (b) Matching Precision (Equation 2)

Discussion and Direction for Future Research

Extension of the presented new change detection algorithm could enable some domain applications that require a fast and reliable comparison between as-designed and as-built conditions. At the same time, the algorithm itself does have a few aspects that deserve further investigation. The paragraphs below present how the presented relational-graph-based approach enables real-time constructability analysis of installing

prefabricated building components in accelerated construction projects and discusses a few other issues of the algorithm that deserve further studies.

Fast and reliable detection of design changes could help detect "fit-up" issues (miss-alignment between components) during the accelerated construction process. Prefabrication of building components has become popular in recent years and shows the potentials in improving the overall construction workflow. However, current methods for monitoring dimensional and installation errors of prefabricated components can hardly capture how those errors accumulate in the field and result in misalignment. As a result, engineers lack tools for real-time control of the error accumulation in the field. As detailed below, an extension of the proposed change detection approach could generate tolerance networks to assist with prefabricated components' installation process to avoid "fit-up" problems.

A comparison of the relational graphs generated from the as-designed and as-built models could help identify manufacturing and installation errors for each component involved in the accelerated construction process. Those errors of components could form into "tolerance network" that is useful for predicting how errors interact with each other and accumulate into misalignments. A tolerance network analysis could help engineers in identifying strategies in adjusting installation processes for minimizing the impacts of the manufacturing and installation errors of prefabricated components. Figure 9 shows an example of a tolerance network that shows dimensional errors on the nodes that represent building elements (e.g., SEGMENT of ducts, "SEG" in the figure), and shows the rotation and displacement errors of joints between building elements. Specifically, $\Delta\theta$ represents the deviation of a joint from its as-designed orientation, while Δx, Δy, and Δz

represent the dislocation of joint from its as-designed location. Given fabrication errors of all connected components and errors at the connections between building elements, this tolerance network can predict how those errors accumulate into misalignment between building elements and predict how engineers could adjust position and rotation parameters during installation for alleviating misalignments.

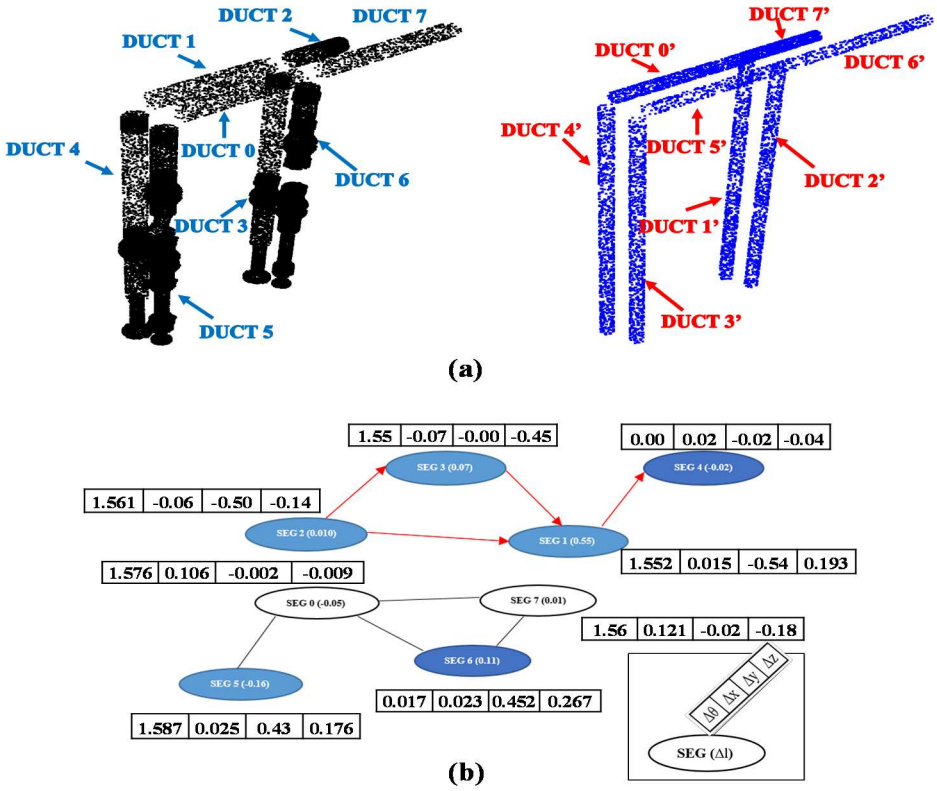

Figure 15. (a) Subnetwork 1 (b) Tolerance Network

Figure 15(b) is the tolerate network generated for the data and model shown in Figure 15(a) (Subnetwork 1 discussed in the previous section). Eight nodes in Figure 15 represent the eight as-designed ducts in this case. Each node contains a Δl to indicate the prefabrication error that causes the deviation of the length of a duct from its as-designed length. Each edge linking two nodes contains four numbers (Δθ, Δx, Δy, Δz) that indicate the deviations of the joint between the two ducts from its original orientations and

locations. Observing the fabrication errors and joint errors in Figure 15, one could identify a "flow" of errors that originates from section 2 (SEG 2) and ends at section 4 (SEG 4). In the future, the author plans to develop automatic tolerance network analysis algorithms that can automatically recognize such flow of errors in a tolerance network and predict how to best control the error propagation and avoid misalignment between prefabricated building elements. The author has already presented some initial results of such an automatic tolerance network analysis approach in (Kalasapudi and Tang 2015b).

The developed spatial change detection approach reliably detects spatial changes of the mechanical duct network as shown in Figure 12 contains ducts having 90^0 degree angles between each other duct. However, there can be situations having duct networks having different angles between the interconnected ducts sections that cause failure in the developed matching using spatial context approach. Similarly, the author would like to consider cases having change in the global orientation between the as-designed model and the as-built data of entire duct network with respect to its surrounding environment. Such change in the overall global orientation of the duct network may create errors while matching using nearest neighbor searching and irregular spatial context representations of the duct sections. In future, the author would like to develop a more generalized spatial context representation that can represent duct sections having different angle between each other and handle global change in the orientation between the spatial changed ducts networks. Such generalization will significantly improve the robustness of the developed spatial change detection approach for handling different types of closely-packed building systems.

The author has detected spatial changes of the straight cylindrical duct sections between the as-designed and the as-built models by eliminating the interconnected flange/valve sections. The future work will include testing the hypothesis mentioned in the methodology section of this chapter that states that matching the cylindrical duct sections would serve as the basis of detecting and matching flange/valve sections connected to the matched duct sections in the as-designed and as-built models. Finally, the author would like to point out that the accuracy of the algorithm depends on the accuracy of the alignment between the models. In this study, a constrained ICP registration approach was utilized to align both models roughly. The future work should also test bundle adjustment and progressive registration approaches to test whether they improve the results (Swart et al. 2011; Tang and Rasheed 2013).

Conclusions

This chapter presented a computationally efficient approach that implements a combination of nearest neighbor searching and spatial context algorithms to reliably associate as-designed and as-built models to detect changes in complex, large-scale building systems such as building duct networks. The proposed approach utilizes both local and global attributes of duct objects and generates a relational graph between their as-designed and as-built models. An automated relational-graph generation process then uses the position and orientation information of the duct objects (presented as lines) to associate the ducts between the models. If there are significant differences between the associated as-designed and as-built duct objects, the proposed algorithm isolates the relational network into subnetworks to isolate areas that contain large deviations. The algorithm then matches these subnetworks between both models using the spatial

contexts of the duct objects. Spatial context matching between subnetworks corrects possible mismatches produced at the end of the first step of the algorithm, which only uses the position and orientation information for matching.

The change detection approach presented in this chapter is an improvement over the previous one presented in (Kalasapudi et al. 2014a) as it significantly improves the computational efficiency and achieves fully automated change detection between as-designed and as-built models. The future work will include classifying the detected spatial changes based on its actual cause (Chapter 3). Such changes include global rigid body motions (e.g., translations and rotations of structural elements) and local shape changes (e.g., bending and torsional deformations of bridge elements). The author would like to resolve the problem of detecting mixed global and local changes by comapring two sets of 3D laser scanning data of a structure collected at different times. Such diagnosis is critical for engineers to understand the underlying reasons for design changes, and take actions to control those changes. The author expect that such a workflow would increase the construction quality while reducing or eliminating potential rework and costs associated with fit-up issues.

References

"AIA Homepage - The American Institute of Architects." (1857). <http://www.aia.org/> (Nov. 4, 2014).

Akinci, B., and Boukamp, F. (2003). "Representation and Integration of As-Built Information to IFC Based Product and Process Models for Automated Assessment of As-Built Conditions." Proceedings of 19th International Symposium on Automation and Robotics in Construction, IAARC, Washington, D.C., 543–550.

Azhar, S., Nadeem, A., Mok, Y. N. J., and Leung, H. Y. B. (2008). "Building Information Modeling (BIM): A New Paradigm for Visual Interactive Modeling and Simulation for

Construction Projects." First International Conference on Construction in Developing Countries (ICCIDC–I), 435.

Bosché, F. (2010). "Automated recognition of 3D CAD model objects in laser scans and calculation of as-built dimensions for dimensional compliance control in construction." Advanced Engineering Informatics, 24(1), 107–118.

Bosché, F., Ahmed, M., Turkan, Y., Haas, C. T., and Haas, R. (2015). "The value of integrating Scan-to-BIM and Scan-vs-BIM techniques for construction monitoring using laser scanning and BIM: The case of cylindrical MEP components." Automation in Construction, Elsevier B.V., 49, 201–213.

Bosché, F., Guillemet, A., Turkan, Y., Haas, C. T., and Haas, R. (2014). "Tracking the Built Status of MEP Works: Assessing the Value of a Scan-vs-BIM System." Journal of Computing in Civil Engineering, American Society of Civil Engineers, 28(4), 5014004.

Cai, H., and Rasdorf, W. (2008). "Modeling Road Centerlines and Predicting Lengths in 3-D Using LIDAR Point Cloud and Planimetric Road Centerline Data." Computer-Aided Civil and Infrastructure Engineering, 23(3), 157–173.

Clarkson, K. L. (2006). "Nearest-neighbor searching and metric space dimensions." Nearest-Neighbor Methods for Learning and Vision: Theory and Practice, (April), 15–59.

ClearEdge 3D. (2011). "EdgeWise Plant Suite | ClearEdge 3D."

Geosystems, L. (2006). "'Leica Cyclone 5.4 Technical Specifications.' product literature."

Girardeau-Montaut, D. (2011). "CloudCompare-Open Source project." OpenSource Project.

Han, S., Lee, S., and Peña-Mora, F. (2012). "Identification and Quantification of Non-Value-Adding Effort from Errors and Changes in Design and Construction Projects." Journal of Construction Engineering and Management, 138(1), 98–109.

Hao, Q., Shen, W., Neelamkavil, J., and Thomas, R. (2008). "Change Management in Construction Projects." CIB W78 International Conference on Information Technology in Construction, 1–11.

Hindmarch, H., Gale, A., and Harrison, R. (2010). "A Proposed Construction Design Change Management Tool To Aid in Making Informed Design Decisions." 26th Annual Association of Researchers in Construction Management Conference, (September), 21–29.

Innovmetric Software. (2016). “PolyWorks | InnovMetric Software.” <http://www.innovmetric.com/en/about/about-innovmetric>.

Kalasapudi, V. S., and Tang, P. (2015). “Automated Tolerance Analysis of Curvilinear Components Using 3D Point Clouds for Adaptive Construction Quality Control.” Computing in Civil Engineering 2015, American Society of Civil Engineers, Reston, VA, 57–65.

Kalasapudi, V. S., Tang, P., and Turkan, Y. (2014). “Toward Automated Spatial Change Analysis of MEP Components Using 3D Point Clouds and As-Designed BIM Models.” 2014 2nd International Conference on 3D Vision, IEEE, 145–152.

Langroodi, B. P., and Staub-French, S. (2012). “Change Management with Building Information Models: A Case Study.” Construction Research Congress 2012, American Society of Civil Engineers, Reston, VA, 1182–1191.

Lee, J., Son, H., Kim, C., and Kim, C. (2013). “Skeleton-based 3D reconstruction of as-built pipelines from laser-scan data.” Automation in Construction, Elsevier B.V., 35, 199–207.

Nahangi, M., and Haas, C. T. (2014). “Automated 3D compliance checking in pipe spool fabrication.” Advanced Engineering Informatics, 360–369.

Park, M., and Pena-Mora, F. (2003). “Dynamic change management for construction: Introducing the change cycle into model-based project management.” System Dynamics Review, 19(3), 213–242.

Parvan, K., Rahmandad, H., and Haghani, A. (2012). “Estimating the impact factor of undiscovered design errors on construction quality.” Proceedings of the 30th International Conference of the System Dynamics Society, 1–16.

“Project Review Software | Navisworks Family | Autodesk.” (2007). .

Rabbani, T., van den Heuvel, F. a, and Vosselman, G. (2006). “Segmentation of point clouds using smoothness constraint.” International Archives of Photogrammetry, Remote Sensing and Spatial Information Sciences - Commission V Symposium “Image Engineering and Vision Metrology,” 36(5).

Seppo, T. (2013). “Change detection in BIM models – Computing diffs between versions.” Built Environment Innovations.

Son, H., Kim, C., and Kim, C. (2015). “3D reconstruction of as-built industrial instrumentation models from laser-scan data and a 3D CAD database based on prior knowledge.” Automation in Construction, Elsevier B.V., 49, 193–200.

Son, H., Kim, C., ASCE, A. M., Cho, Y. K., and Asce, M. (2017). “Automated Schedule Updates Using As-Built Data and a 4D Building Information Model.” *Journal of Management in Engineering*, 1–13.

Swart, A., Broere, J., Veltkamp, R., and Tan, R. (2011). “Refined Non-rigid Registration of a Panoramic Image Sequence to a LiDAR Point Cloud.” Lecture Notes in Computer Science, 73–84.

Tang, P., Chen, G., Shen, Z., and Ganapathy, R. (2015). “A Spatial-Context-Based Approach for Automated Spatial Change Analysis of Piece-Wise Linear Building Elements.” Computer-Aided Civil and Infrastructure Engineering, 31, 65–80.

Tang, P., Huber, D., Akinci, B., Lipman, R., and Lytle, A. (2010). “Automatic reconstruction of as-built building information models from laser-scanned point clouds: A review of related techniques.” Automation in Construction, Elsevier B.V., 19(7), 829–843.

Tang, P., and Rasheed, S. H. (2013). “Simulation for characterizing a progressive registration algorithm aligning as-built 3D point clouds against as-designed models.” 2013 Winter Simulations Conference (WSC), IEEE, 3169–3180.

Tang, P., Shen, Z., and Ganapathy, R. (2013). “Automated Spatial Change Analysis of Building Systems Using 3D Imagery Data.” 30th CIB W78 International Conference - October 9-12, Beijing, China, Proceedings of the 30th CIB W78 International Conference, 252–261.

Technodigit. (2009). “3DReshaper (Home) |About Technodigit | Contact.”

Turkan, Y., Bosche, F., Haas, C. T., and Haas, R. (2012). “Automated progress tracking using 4D schedule and 3D sensing technologies.” Automation in Construction, Elsevier B.V., 22, 414–421.

Wang, J., Sun, W., Shou, W., Wang, X., Wu, C., Chong, H.-Y., Liu, Y., and Sun, C. (2015). “Integrating BIM and LiDAR for Real-Time Construction Quality Control.” Journal of Intelligent & Robotic Systems, 79(3–4), 417–432.

Xiong, X., Adan, A., Akinci, B., and Huber, D. (2013). “Automatic creation of semantically rich 3D building models from laser scanner data.” Automation in Construction, Elsevier B.V., 31, 325–337.

Xiong, X., and Huber, D. (2010). “Using Context to Create Semantic 3D Models of Indoor Environments.” Proceedings of the British Machine Vision Conference 2010, British Machine Vision Association, 1–11.

CHAPTER 3

AUTOMATIC MULTI-LEVEL 3D DATA REGISTRATION FOR RELIABLE SPATIAL CHANGE CLASSIFICATION OF SINGLE-PIER BRIDGES

Introduction

Monitoring spatial changes of bridges is an important aspect of bridge management (Committee 2012). Examples of such spatial changes include deformation, deflection, or rotation of individual elements of bridge structures and structural elements (e.g., girders, piers) (Patjawit and Kanok-Nukulchai 2005). Changes in the materials properties of elements, loading on the elements or changes in the structures boundary conditions may cause spatial changes of a bridge structure. Changes of individual bridge elements often influence each other through connections between these elements. Failure to identify such spatial changes could cause unreliable condition assessment that may result in recognizing abnormal stiffness changes and its corresponding structural defects in bridge structures (Raghavendrachar and Aktan 1992). In general, spatial changes of a bridge structure can be classified as: 1) local deformation of individual bridge elements, and 2) rigid body motion (global deviation hereafter) of structural elements (Maragakis and Jennings 1989; Wakefield et al. 1991). The local deformation analysis can help engineers assess the internal forces and possible damages of individual elements; the rigid body motion of structural elements can help engineers analyze the interactions between structural elements and the environments (e.g., interactions between girders, interactions between soil and foundations) and system-level behavior of structures (Chang et al. 2003). Local and global changes could influence each other – element-level damages, deformations would reduce the stiffness of the structural elements and trigger

the redistribution of loads to structural elements connected to the damaged elements, which cause local deformation, and displacements of those connected structural elements. Displacements of connected structural elements can aggregate into large translations and rotations of the whole structure. On the other hand, global displacements of structural elements (e.g., settlements of foundations) can trigger displacements and deformation of structural elements connected to them. Analyzing both the local and global spatial changes of bridge structures is thus necessary for effective condition assessment of bridge structures.

The current practice of spatial change monitoring can hardly provide local and global spatial change analysis of bridge structural elements in an efficient and effective manner. Most bridge engineers conduct a visual inspection of bridges (Moore et al. 2001; Zanyar et al. 2012). Visual inspection methods are tedious and heavily rely on the experience of the bridge engineer (Moore et al. 2001). Some inspectors use contact sensors such as accelerometers, laser interferometers, and global positioning systems (GPS) for measuring spatial changes of bridges (Yi et al. 2013). Contact sensors, such as accelerometers, can only collect spatial data (e.g., locations, accelerations) at the locations where the sensors are, and require either careful sensor location planning for capturing critical structural responses and deformations related to structural defects (Park et al. 2010). Engineers who lack structural engineering knowledge and experiences of using sensors for structural condition assessment could put sensors at locations that provide limited geometric details for structural defect detection. Also, contact-sensor-based methods could only report changes at sensors' locations and could not capture

detailed shapes of structures and thus have limitations in reliably analyzing global and local changes of bridges in detail (Wahbeh et al. 2003).

Numerical simulation studies such as Finite Element Analysis (FEA) could perform faster assessment studies than contact-sensor-based methods through simulating detailed geometric changes based on as-designed geometries and material properties, and given loading conditions. However, FEA assume that the as-designed information of the structures is an accurate representation of the actual physical structure so that the simulation could produce reliable predictions of the actual deformation of physical structures. Unfortunately, in reality, the as-designed information of structures could significantly deviate from as-is physical conditions (Tang et al. 2015). Some researchers use conventional surveying equipment, such as total stations, which could also measure the required geometric information of the structure (Fröhlich and Mettenleiter 2004). Such surveying equipment could only collect tens of 3D point per second and need hours for capturing geometric details of a structure. Moreover, such equipment requires a licensed professional to operate for collecting accurate geometric data (Erickson et al. 2013).

In recent years, engineers started using 3D imaging technologies, such as 3D laser scanning, photogrammetry, and videogrammetry techniques, for capturing and analyzing spatial changes of various buildings, facilities, and civil infrastructures (Park et al. 2007; Wahbeh et al. 2003). For instance, the applications of 3D imaging technologies in bridge inspection and management showed some potentials while revealing challenges related to efficient and reliable change analysis based on 3D imagery data (Olsen et al. 2009). With the development of efficient and effective image processing algorithms, structural health

monitoring domain started employing imaging and photogrammetry techniques (Agdas et al. 2012; Basharat et al. 2005; Park et al. 2007). Most of these studies focused on local deformation analysis of an individual building or structural elements. In practice, the comparison of geometries of a structure will produce a "deviation map" that shows the deviations between two geometries. That deviation map contains both the deviation patterns caused by local deformation of the elements (local deviation patterns) and deviation patterns caused by the global deviations of the element (global deviation patterns). Additionally, global deviations often are larger than local deformations and making it difficult for engineers to recognize local deformations. Thus, resolving the mixed patterns to identify global deviations and local deformations separately is important for civil engineers to use 3D imagery data for comprehending how global and local changes influence each other to determine the structural integrity.

An example shown in Figure 16 illustrates the correlated changes of the bridge structure and can help illustrate the challenges described above. Figure 16 shows the deviation map of the bridge structure that has undergone several geometric spatial changes that include the global displacement of the entire bridge (Figure 16(c)&(e)), and local deformation of the girder of the bridge (Figure 16(g)). This deviation map contains mixed deviation patterns (Figure 16 & 17 shows mixed deviation pattern 1, 2 & 3) that can either be due to external loading or change in the connectivity between elements. These results will mislead a civil engineer about the actual internal forces of the girder and cause uncertainties in determining the structural behavior. A mix of both the rigid body motion (global deviation) and the observed local deformation of the individual element cause difficulties in interpreting the deviation map into a structure behavior. A

method that can reliably separate global deviations and local deformation are crucial for assisting civil for interpreting the deviation map (Park et al. 2010).

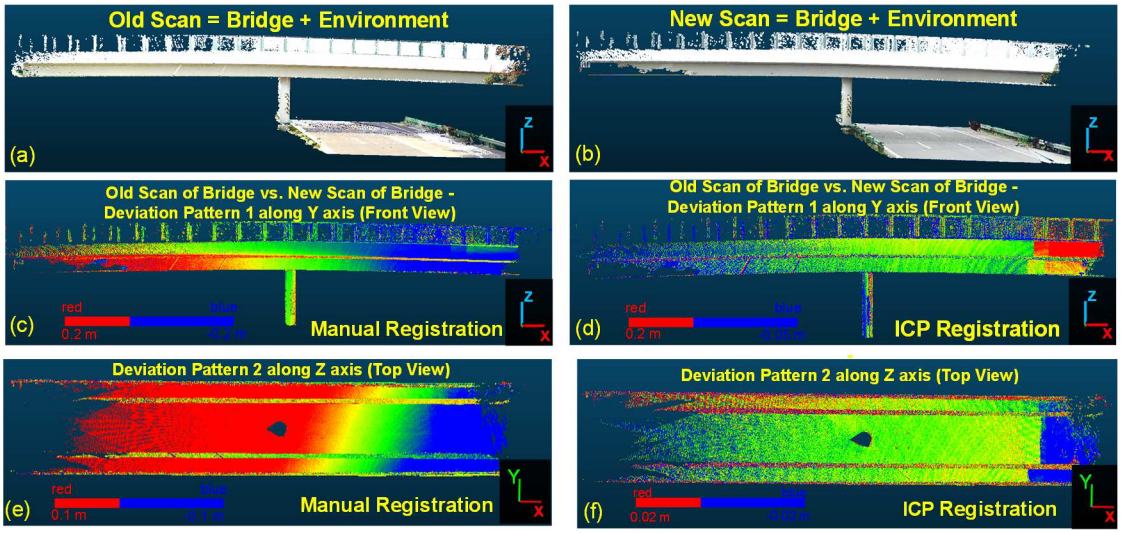

Figure 16. Deviation maps showing comparison between old scan and new scan of a single pier bridge (Deviation patterns - blue color for negative deviations to red color for positive deviations along each coordinate axis)

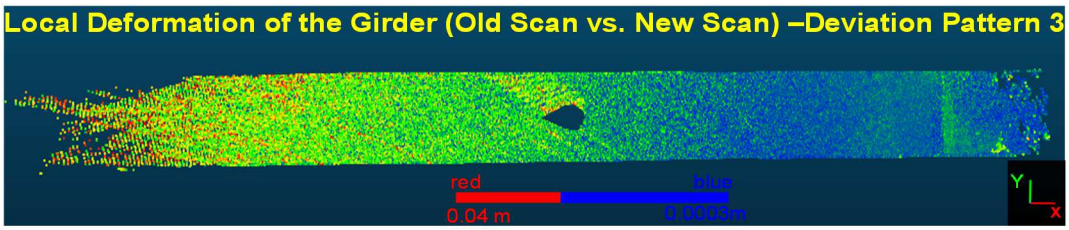

Figure 17. Deviation pattern of the local deformation of the girder (old scan of girder vs. new scan of girder)

The scientific challenge to establish such a method that enables reliable global and local change analysis based on 3D imagery data is two-folded:

1. The lack of a robust 3D data registration method that can automatically ignore changed parts of the scanned scenes while using unchanged parts only for aligning the data collected at different times cause difficulties of identifying global rigid body changes of a structure. Previous registration methods require the tedious setup of unchanged control networks for referring the compared data sets

to the common coordinate system and then detect global motions of objects; ICP registration use all data points without considering that significantly changes objects, especially global changes, can mislead the registration and result in inaccurate deviation map (as shown in Figure 16(d)). Figure 16 ((c) and (d)) shows the registration of an old scan with the new scan of the bridge using manual registration, and ICP registration approaches. The author performs the manual registration by manually aligning the old and the new scan using both the bridge and its surrounding environment. It is easier for a structural engineer to identify the spatial changes of the bridge structure using the deviations patterns detected from the manual registration process (Figure 16(c) shows the spatial change along y-axis & Figure 16(e) shows the spatial change along z-axis of the bridge structure). However, the automatic ICP registration process generates complicated deviation patterns making it harder for engineers to identify and classify the spatial changes of the bridge structure (Figure 16(d) & (f)).

2. The lack of an automatic change classification approach that can reliably identify structure-level deviations and classify element-level deformations. The inability to accurately classify these mixed deviation patterns (Figure 16 & 17 shows mixed deviation pattern 1,2&3) cause difficulties of identifying global rigid body motions of the structure and structure elements. As described above, most existing methods focus on local deformation analysis of individual structure elements assuming the global motions have been addressed before analyzing local deformation patterns. Figure 16(c) shows the deviation pattern between the old and new bridge scans (global rigid body motion) and Figure 17 shows the

deviation pattern between the scans of the old and new girder of the bridge (local deformation). This shows that the global deviation patterns of the girder (Figure 16 (c) & (e))) are overwhelming the local deviation patterns (Figure 17) thus making it extremely difficult for engineers to assess the internal forces in the bridge elements and eventually complicating the structure behavior.

This chapter presents a novel multi-level 3D laser scanning data registration method for reliable spatial change classification of bridge structures that addresses the two limitations described above. The robust registration approach automatically identifies unchanged environmental features surrounding the bridge structure, and use those features to accurately register the two sets of 3D laser scanning data collected at different times. Then a structure-level registration isolates the global rigid body motion of the entire bridge (G1) and aid in detecting structure/element level spatial changes. An element-level registration approach identifies relative rigid body motions of individual bridge elements (G2) and automatically removes the global deviation of each individual bridge element for classifying local deformations of individual bridge elements (L). Then the pattern classification approaches classify individual bridge elements as deformed shapes due to tension, compression, bending, and torsion. The author tested this approach using two sets of 3D laser scanning data of a highway bridge structure collected in 2015 and 2016 respectively.

The following section reviews and details the challenges of traditional contact/non-contact and imagery sensors for spatial changes monitoring for identifying global displacement and local deformations of a structure. Then the author describes the framework that integrates two new methods that address the two challenges described

above: 1) robust registration for separating rigid body motion 2) pattern classification method that classifies deformation patterns of individual elements of the structure. The author has utilized the developed approach to investigate spatial changes of 2 highway bridges and validating the findings against the assessment results from an experienced structural engineer researcher. Finally, the chapter concludes by summarizing research findings, discusses limitations, and recommends future research directions.

Literature Review

Civil infrastructure facilities often undergo changes during their operation and maintenance phase. Such changes include material changes, geometric changes, soil behavior changes, and environmental condition changes, etc. (Fruchter et al. 1993; Lattanzi and Miller 2012; Tessler et al. 1993). It is difficult to identify such spatial changes in advance and are often detected after the structure has undergone significant visual deformation or damage (Kalasapudi et al. 2014a). *The following sections detail existing studies on spatial change monitoring and several technological advancements that can aid in controlling such spatial changes well in advance.*

Contact/non-contact Sensor Methods for Spatial Change Monitoring

Recent years saw the use of GPS receiver sensors for conducting spatial change monitoring and detecting the rigid body motion of the structure (Moschas and Stiros 2011; Yi et al. 2013). Such sensors are used to measure and monitor real-time displacement measurement of a structure under different loading conditions (Yi et al. 2013). Accelerometers also provide accurate measurement of acceleration levels of the elements of the civil infrastructure to identify its rigid body motion under loading, but are limited to measuring

short term dynamic displacement instead of long term displacement monitoring. Additionally, one of the limitation of using GPS receivers and accelerometers is it requires accurate sensor network planning in order to mount sensors across all the elements of the structure. If the sensor network is improper, the output is inaccurate due to the resulting numerical integration errors (Park et al. 2007). Majority of the traditional deformation measurement techniques either detect local changes of the structure or use a sensor network to detect its overall displacement (global deviation). For instance, non-destructive techniques measure the variations at a particular location of the structure to detect the change in a structures' material properties (Lattanzi and Miller 2012). Similarly, GPS sensors detect the displacement at the mounted location on the structure but do not identify the interaction between the detected displacement and surrounding environment. Hence, currently, available deformation monitoring techniques are constrained to detect and measure localized deformations and lack data about the correlation of such deformation with the surrounding environment of the structure (Koh and Dyke 2007; Zeibak and Filin 2007).

Total station and laser projection sensing are predominantly used non-contact sensor methods to monitoring long term displacement of civil structures (Cross et al. 2012; Zhao et al. 2015). Such sensor methods collect data at several locations of a structure and measure the displacement at regular intervals for understanding the long-term change of a structure. Several researchers conducted displacement measurements annually of bridge structure to understand the long-term rigid body motion using a total station sensor (Cosser et al. 2003). However, the major disadvantage of using such sensors is its data density (Deruyter 2013). Total station sensor require intense manual data collection activity and

large amount of time to collect geometric data of a structure a several locations (Riveiro et al. 2013). In cases having large-scale structures such as bridges, these non-contact sensor methods involve tedious manual data collection process that generally produces lower data density for measuring the displacement of structures. Advanced imaging technologies aid in automating visual inspection of large civil infrastructures (Zogg and Ingensand 2008). The major advantage of using imaging technology is its ability to capture large amount of data points and measure millimeter level changes of the structures (Vezočnik et al. 2009). The following section details vision-based methods for performing long-term spatial change monitoring of civil infrastructures. Recent years saw the use of GPS receiver sensors for conducting spatial change monitoring and detecting the rigid body motion of the structure (Moschas and Stiros 2011; Yi et al. 2013). Such sensors are used to measure and monitor real-time displacement measurement of a structure under different loading conditions (Yi et al. 2013). Accelerometers also provide accurate measurement of acceleration levels of the elements of the civil infrastructure to identify its rigid body motion under loading but are limited to measuring short-term dynamic displacement instead of long-term displacement monitoring. Additionally, one of the limitations of using GPS receivers and accelerometers is it requires accurate sensor network planning in order to mount sensors across all the elements of the structure. If the sensor network is improper, the output is inaccurate due to the resulting numerical integration errors (Park et al. 2007). The majority of the traditional deformation measurement techniques either detect local changes of the structure or use a sensor network to detect its overall displacement (global deviation). For instance, non-destructive techniques measure the variations at a particular location of the structure to detect the change in a structures' material properties (Lattanzi

and Miller 2012). Similarly, GPS sensors detect the displacement at the mounted location on the structure but do not identify the interaction between the detected displacement and surrounding environment. Hence, currently, available deformation monitoring techniques are constrained to detect and measure localized deformations and lack data about the correlation of such deformation with the surrounding environment of the structure (Koh and Dyke 2007; Zeibak and Filin 2007).

Total station and laser projection sensing are predominantly used non-contact sensor methods to monitoring long-term displacement of civil structures (Cross et al. 2012; Zhao et al. 2015). Such sensor methods collect data at several locations of a structure and measure the displacement at regular intervals for understanding the long-term change of a structure. Several researchers conducted displacement measurements annually of the bridge structure to understand the long-term rigid body motion using a total station sensor (Cosser et al. 2003). However, the major disadvantage of using such sensors is its data density (Deruyter 2013). Table 1 highlights the limitations of several non-contact sensors for collecting detailed geometric data of a structure. Total station sensor requires intense manual data collection activity and a large amount of time to collect geometric data of a structure at several locations (Riveiro et al. 2013). In cases having large-scale structures such as bridges, these non-contact sensor methods involve tedious manual data collection process that generally produces lower data density for measuring the displacement of structures. Advanced imaging technologies aid in automating visual inspection of large civil infrastructures (Zogg and Ingensand 2008). The major advantage of using imaging technology is its ability to capture a large amount of data points and measure millimeter

level changes of the structures (Vezočnik et al. 2009). The following section details vision-based methods for performing long-term spatial change monitoring of civil infrastructures.

Vision-based Methods for Spatial Change Monitoring

2D and 3D imagery technology provides faster data collection of large-scale civil infrastructures. Stephen et al. conducted static and dynamic displacement measurements from video-based monitoring of a bridge structure under standard loading conditions (Stephen et al. 1993). This approach tracks the motion of structural components to determine the deck displacements using a real-time video tracking system. With the development of 3D imaging capture, researcher started exploring change-based structural health monitoring techniques (Liang-Chien 2010; Su et al. 2006; Vezočnik et al. 2009; Zeibak and Filin 2007). Cabaleiro et al. utilized LiDAR data for conducting beam deformation modeling (Cabaleiro et al. 2015). It utilizes a polynomial surface fitting algorithm to model the deformations of beams caused by bending and torsional deflections. Therefore, such studies validated the ability of using imaging technologies to detect millimeter level geometric changes and adopting them for performing continuous deformation monitoring of structures (Beskhyroun et al. 2011; Cabaleiro et al. 2015; Riveiro et al. 2011b; Zogg and Ingensand 2008). Identifying changes between two sets of point cloud data can help in detecting geometric spatial changes that aid in the long-term monitoring of a structure.

Detecting spatial changes between two sets of 3D laser scanning data collected at different time intervals will help in performing bridge deformation monitoring and damage prevention (Cabaleiro et al. 2014). However, the reliability of the spatial change detection depends on the process of registering the collected two data sets (Vezočnik et al. 2009).

This registration process will bring both the collected 3D laser scanning data sets into one global coordinate system for detecting spatial changes of the bridge. Several researchers generated control points, and geodetic networks using surveying methods such as Total Station sensors to establish a reference network for comparing 3D laser scanning data sets collected at different time intervals (Hsiao et al. 2004; Vezočnik et al. 2009). The major disadvantage of using control networks is in the process of setting up the control network and ensuring a minimum number of the control network points are visible on all the scans. This process is tedious and sometimes becomes impractical in situations such as scanning underneath bridge structures submerged in water (Zeibak and Filin 2007). 3D laser scanning data provides the capability to generate virtual control network by manually selecting several common feature points between the two set of 3D laser scanning data. In general, feature points in a 3D laser scanning include points on both the surrounding (environment feature points) that include signs/railings on roads, mile markers, etc. and on the bridge structure (bridge feature points).

Several previous studies developed automated, robust registration algorithms that identify common feature points to perform point cloud registration (Barnea and Filin 2008; Poreba and Goulette 2015). Such algorithms identify common feature points and use closest point-to-point registration (ICP registration) approaches to overlap two set of point cloud data. However, if such feature point registration algorithms identify certain feature points that have also undergone spatial changes along with a bridge structure, the applied registration approach outputs several errors in measuring changes or deformation of the bridge structure. For instance, identifying the corner of a signboard that has deformed due to wind loading as a feature point in the registration process will result in the improper

measurement of spatial changes and unreliable decision making by structural engineers. Such improper registration of the data sets may lead to detecting inaccurate spatial changes and unreliable deviations/deformation measurements. Hence, it is extremely important to identify and isolate those feature points that have not undergone spatial changes between the two sets of point cloud data and then use them for performing closest point-to-point registration.

Previous studies performed several case studies such as beam deformation, girder deformation monitoring, etc. but failed to detect the overall rigid body motion of structure or the deviations of the element itself. The first step in these studies starts with registering two sets of data using commercially available registration algorithms that are fast and readily available (Yang et al. 2010). This registration will accurately align the two 3D laser scanning data sets but fail to identify the interaction between the structure and its surrounding environment. Hence, none of previous studies that relied on 3D laser scanning addressed the limitation of identifying mixed deviations patterns that contain both the global (rigid body motion) and local deformations (bending, tension etc.). To address all the limitations (Table) of current contact/non-contact and vision-based change monitoring methods, the author proposed a systematic spatial change classification framework to identify the change in the interaction between a bridge structure and its surrounding environment along with classify the local deformation patterns for each element of the bridge structure. 2D and 3D imagery technology provide faster data collection of large-scale civil infrastructures. Stephen et al. conducted static and dynamic displacement measurements from video-based monitoring of a bridge structure under standard loading conditions (Stephen et al. 1993). This approach tracks the motion of structural components

to determine the deck displacements using a real-time video tracking system. With the development of 3D imaging capture, researcher started exploring change-based structural health monitoring techniques (Liang-Chien 2010; Su et al. 2006; Vezočnik et al. 2009; Zeibak and Filin 2007). Cabaleiro et al. utilized LiDAR data for conducting beam deformation modeling (Cabaleiro et al. 2015). It utilizes a polynomial surface fitting algorithm to model the deformations of beams caused by bending and torsional deflections. Therefore, such studies validated the ability of using imaging technologies to detect millimeter level geometric changes and adopting them for performing continuous deformation monitoring of structures (Beskhyroun et al. 2011; Cabaleiro et al. 2015; Riveiro et al. 2011b; Zogg and Ingensand 2008). Identifying changes between two sets of point cloud data can help in detecting geometric spatial changes that aid in the long-term monitoring of a structure.

Detecting spatial changes between two sets of 3D laser scanning data collected at different time intervals will help in performing bridge deformation monitoring and damage prevention (Cabaleiro et al. 2014). However, the reliability of the spatial change detection depends on the process of registering the collected two data sets (Vezočnik et al. 2009). This registration process will bring both the collected 3D laser scanning data sets into one global coordinate system for detecting spatial changes of the bridge. Several researchers generated control points, and geodetic networks using surveying methods such as Total Station sensors to establish a reference network for comparing 3D laser scanning data sets collected at different time intervals (Hsiao et al. 2004; Vezočnik et al. 2009). The major disadvantage of using control networks is in the process of setting up the control network and ensuring a minimum number of the control network points are visible on all the scans.

This process is tedious and sometimes becomes impractical in situations such as scanning underneath bridge structures submerged in water (Zeibak and Filin 2007). 3D laser scanning data provides the capability to generate virtual control network by manually selecting several common feature points between the two set of 3D laser scanning data. In general, feature points in a 3D laser scanning include points on both the surrounding (environment feature points) that include signs/railings on roads, mile markers, etc. and on the bridge structure (bridge feature points).

Several previous studies developed automated, robust registration algorithms that identify common feature points to perform point cloud registration (Barnea and Filin 2008; Poreba and Goulette 2015). Such algorithms identify common feature points and use closest point-to-point registration (ICP registration) approaches to overlap two set of point cloud data (Table 1). However, if such feature point registration algorithms identify certain feature points that have also undergone spatial changes along with a bridge structure, the applied registration approach outputs several errors in measuring changes or deformation of the bridge structure. For instance, identifying the corner of a signboard that has deformed due to wind loading as a feature point in the registration process will result in the improper measurement of spatial changes and unreliable decision making by structural engineers. Such improper registration of the data sets may lead to detecting inaccurate spatial changes and unreliable deviations/deformation measurements. Hence, it is extremely important to identify and isolate those feature points that have not undergone spatial changes between the two sets of point cloud data and then use them for performing closest point-to-point registration.

Previous studies performed several case studies such as beam deformation, girder deformation monitoring, etc. but failed to detect the overall rigid body motion of structure or the deviations of the element itself. The first step in these studies starts with registering two sets of data using commercially available registration algorithms that are fast and readily available (Yang et al. 2010). This registration will accurately align the two 3D laser scanning data sets but fail to identify the interaction between the structure and its surrounding environment. Hence, none of the previous studies that relied on 3D laser scanning addressed the limitation of identifying mixed deviations patterns that contain both the global (rigid body motion) and local deformations (bending, tension, etc.). To address all the limitations highlighted in Table 1 using current contact/non-contact and vision-based change monitoring methods, the author proposed a systematic spatial change classification framework to identify the change in the interaction between a bridge structure and its surrounding environment along with classifying the local deformation patterns for each element of the bridge structure.

Table 5. Limitations of Existing Spatial Change Monitoring Methods

Spatial Change Monitoring Methods	Technology Examples/Sensors	Limitations	Citations
Contact Methods	Tape, NDT's	Intense manual work, Measures local defects	(Moore et al. 2001), (Patil and Patil 2008)
Non-contact Methods	GPS, Laser Projection, Total Station	Low data density, No local change/deformation measurement	(Cross et al. 2012), (Zhao et al. 2015), (Cosser et al. 2003), (Deruyter 2013)
Vision-based Methods	2D Images, 3D Laser Scanning	Relies on ICP for alignment, Contain mixed deviation patterns	(Park et al. 2007), (Olsen et al. 2009), (Monserrat and Crosetto 2008a)

Methodology

The proposed spatial change classification approach accurately registers two 3D laser scanning data sets to identify global deviation (deviation due to rigid body motion) and classifies the local spatial changes of a civil infrastructure as tension, compression, bending, and torsion etc. Figure 18 presents a detailed flowchart that consists of four major steps: 1) Robust registration approach to accurately register two 3D laser scanning data sets, 2) Structure level registration to identify global deviation of bridge, 3) Element level registration to identify element level global deviation, 4) Pattern classification approach to classify element level local deformations.

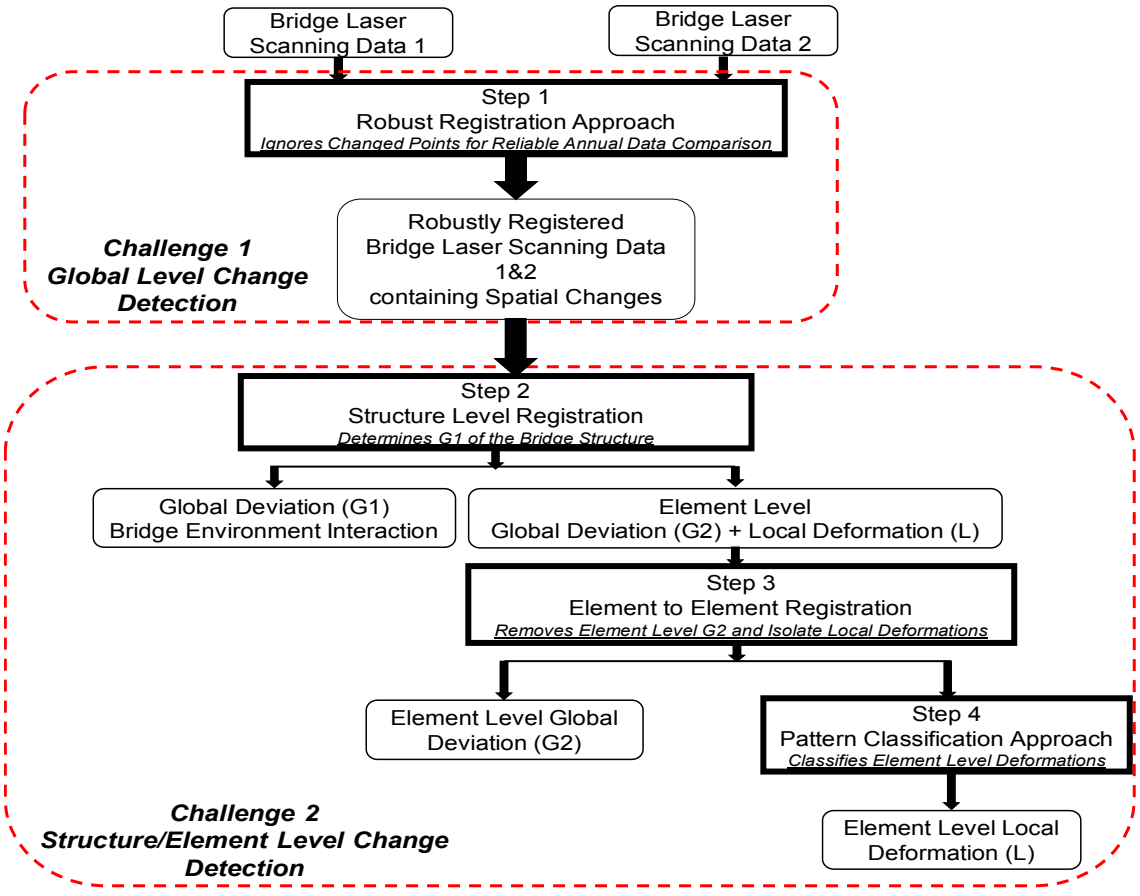

Figure 18. Framework for geometric spatial change classification of a bridge structure

A Robust Registration Algorithm for Automatic and Reliable Geometric Change Detection of Bridges using 3D Laser Scanning Data

3D laser scanning data provides the capability to generate virtual control network by manually selecting several common feature points between the two set of 3D laser scanning data. In general, feature points in a 3D laser scanning include points on both the surrounding (environment points) such signs on bridges/roads, railings on the roads, mile markers, etc. and the bridge structure (bridge feature points). Figure 19 shows an example of few points on the bridge and its surrounding.

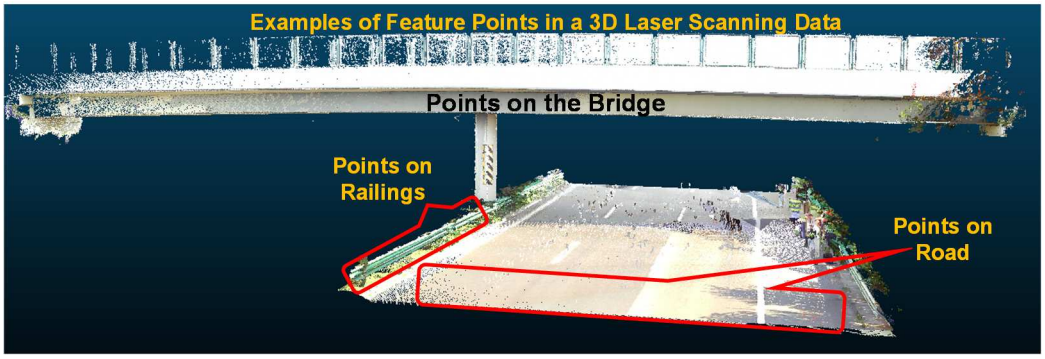

Figure 19. Points for performing robust 3D laser scanning data registration

However, periodic investigation of the bridge structure using 3D laser scanning data requires manually aligning two sets of point cloud data collected at different times. Such aligned process is termed as registering two point cloud data sets into one single coordinate system. Such manual alignment process may significantly affect the analysis results. Unreliable or inaccurate registration of 3D laser scanning datasets of a bridge collected at different times (e.g., from year to year, or from month to month) can lead to improper detections of spatial changes and eventually leading to unreliable condition

assessment of bridge structures. Failure to accurately detect spatial changes may lead to incorrect decision-making and wastage of maintenance resources.

Traditionally 3D laser scanning data processing software utilize common feature points between several scans of a bridge structure to perform the automatic registration process ("FARO Laser Scanner Software - SCENE - Overview" 2010). Based on this principle, several previous studies developed automated algorithms based on robust feature point registration for aligning two sets of 3D laser scanning data (Barnea and Filin 2008; Poreba and Goulette 2015). Such algorithms identify common feature points between two data sets and align them using an Iterative Closest Point (ICP) registration method that minimizes the difference between the two point cloud data sets (Gvili 2010). However, these algorithms were developed for aligning 3D data sets collected within a short time (e.g., within the same day) and need the collected data sets share a significant amount of unchanged features (e.g., within the same day, most parts of a job sites remain unchanged). On the other hand, the author found that the long-term change analysis of bridges requires registration of data sets collected from data collection sessions that are months or even years apart from each other, which can contain large amounts of gradual changes of bridges and environments. Therefore, utilizing conventional feature-based algorithms for registering 3D laser scanning data sets collected from different times can lead to significant registration errors and eventually leads to detecting geometric changes reflected by such registration error. In the following section, the author provides the details about the steps taken to implement the registration using manual feature point selection and limitations of using traditional registration approach.

Limitations of traditional registration approach

This section presents a motivating case to highlight the necessity and contribution of the study described in this chapter. Figure 19 shows the 3D laser scanning data of a two-lane pre-stressed concrete bridge located in Mesa, Arizona collected in 2015 and 2016. As per the 2D drawings, the bridge is 396.25 meters long and 13.5 meters wide and consists of 18 spans. Each span is 19.8 meters long that is supported by four 32 meters long columns. The author first removes the unwanted data in both the 3D laser scanning data sets. Such unwanted data are mostly from objects in the environments, such as trees, hills, traffic noise (moving cars), water under the bridge, etc. Performing the registration with these unwanted data will significantly affect the registration results, as these objects can change significantly compared with bridge structures. The author manually removes all unwanted data points in both the two 3D laser scanning data sets to be compared using the interactive segmentation tool found in CloudCompare (Girardeau-Montaut 2011). The 3D laser scanning data collected in 2015 consists of around 657 million points whereas the data collected in 2016 consists of about 335 million points. However, both data sets have the same number of scans. Such data collection process shows that the point cloud data collected in 2015 have scans having higher data densities (spatial resolutions), which eventually leads to parts of data having denser and more number of points. During the registration, denser parts of the point clouds provide more data points for matching data from two years, and the algorithm will tend to bias towards those parts having denser point clouds. Automatic registration methods such as Iterative Closest Point (Tang and Rasheed 2013) or registration methods would generate results biased towards denser data parts and high errors in parts of the scene that have sparser or

missing data. Figure 20 (a) highlights the denser parts of data collected in 2015. This figure shows that the registration will be biased towards the highlighted areas and produce registration errors in parts that have fewer data points. Primarily, such registration errors will affect the change analysis of the bridge structure and lead to improper decision-making. Therefore, a subsampling method that can generate 3D laser scanning data sets which have similarly distributed points around the point cloud data is thus necessary for overcome this issue (similarly distributed data density between the point cloud data sets).

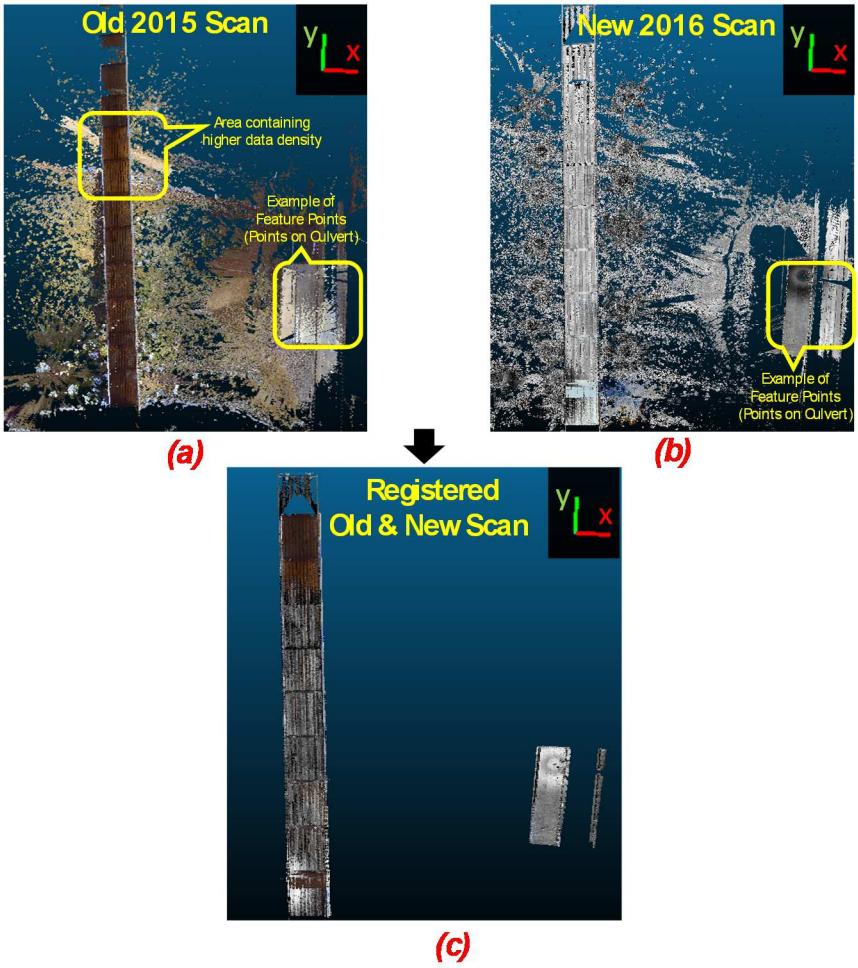

Figure 20. Registered 3D laser scanning data collected in 2015 and 2016 using traditional approach

Another way to overcome the bias issues caused by varying data densities is to perform registration by manually selecting common feature points between both the 3D laser scanning data sets. Such features include railing ends, signs on bridges, etc. Varying data densities of the point cloud data generally do not affect the traditional registration approach that relies on common feature points because those algorithms only use selected feature points not all the points in the point cloud. Figure 20(a & b) highlights few common feature points that can be utilized for performing the registration between the 2015 and 2016 3D laser scanning data sets using manual feature point selection (Figure 19 (c)). This manual approach can be utilized for change analysis of the bridge structure but has few limitations. First, the amount of time invested in manually selecting common features is high. Another major limitation of this approach is the assumption that the manually selected feature points would not change significantly when compared with changes of the bridge structure. Selecting feature points that have large spatial changes than the bridge structure's changes will mislead the change analysis as well. A novel registration approach that performs reliable registration between two 3D laser scanning data sets containing spatial changes is in need.

Several researchers combined the use of Total Station data, and the data collected the 3D laser scanners to establish a control network of points that would not change. This process involves scanning the bridge structure along with the use of a total station to establish a control network that will not change significantly between the data collection sessions. This process of scanning the bridge structure along with the established control points helps in aligning 3D laser scanning data collected at different times. However, the process of establishing the control network is tedious and becomes impractical when a

bridge submerged in water (Monserrat and Crosetto 2008b). Additionally, checking and ensuring that at least three control points are visible from any pair of registered laser scans is also tedious and could hardly be practical for complex outdoor jobsites. For instance, scanning a control point that has been setup far away from the bridge structure requires high-resolution scans that generate a large amount of raw data for pre-processing.

The author in this chapter presents a novel robust registration approach that automatically registers two sets of 3D laser scanning data collected at different times that are one year apart from each other. First, the approach extract bridge features from two 3D laser scanning point clouds and roughly register two bridge data sets by matching salient bridge features. Next, the algorithm extracts feature points from both the surroundings and on the bridge structure and then use a new robust 3D data registration algorithm that automatically identifies changed features between two data sets through a robust fitting method. Finally, the algorithm utilizes the robustly registered feature points to perform accurate registration of the point clouds and label changed parts between two point clouds. The author tested this robust registration approach using 3D laser scanning data of a highway bridge collected in 2015 and 2016 respectively. The following section briefly reviews previous studies on conventional 3D data registration methods. The author describes the developed methodology in detail and presents registration results of the new method on the data collected on a highway bridge. The author then validates the new approach by comparing it with conventional 3D data registration method that uses manually selected feature points for aligning 3D data sets from different data collection sessions and concludes by summarizing the results and discussing the limitations.

Previous Studies on 3D Laser Scanning Data Registration

Recent developments in the field of computer vision (2D & 3D imagery data) applications in civil engineering enable spatiotemporal information retrieval from imagery data for engineering decision support on construction sites (Park et al. 2007). Spatiotemporal changes observed in point cloud data sets collected at different times provides detailed visual information for monitoring changes and analyzing structural deformations (Girardeau-Montaut and Roux 2005; Monserrat and Crosetto 2008a). Lindenbergh and Pfeifer utilized terrestrial laser data of a lock (sea entrance of a harbor) for statistical deformation analysis (Lindenbergh and Pfeifer 2005). The statistical analysis consists of calculating the deformation of the lock detected between two point clouds scanned at the exact same position. Such analysis concluded that terrestrial laser scanners could achieve deformation detection in the order of 9 mm. However, the major limitation of the statistical analysis study for deformation monitoring is that the researchers conducted the experiment by fixing the scanner's position. This is a limitation in cases having to detect deformation of civil infrastructures at larger time gaps and unable to access previous scan position for the next data collection. Numerous studies conducted change detection studies using two sets of point cloud data scanned within 24 hours (Girardeau-Montaut and Roux 2005). Girardeau-Montaut et al. detected changes between two sets of point cloud data collected every day (Girardeau-Montaut and Roux 2005). The change detection study utilized the point cloud data to monitor applications on a building site by registering two 3D laser scanning data sets having shared points nearly not moved. Such registration process consists of using a minimum threshold value for the shared points and then utilizing the Iterative Closest Point (ICP) approach to perfectly

align them. The major disadvantage of using such approach is to detect changes in structures that undergo significant spatial changes over the time period such as a bridge structure.

Researchers also conducted studies to monitor complex deformation of objects having complicated shapes (Antova 2015; Cabaleiro et al. 2015; Vezočnik et al. 2009). Antova (Antova 2015) discussed several registration processes that can perform deformation monitoring using laser scan data in the field containing objects having complicated shapes. These registration processes automatically generate targets using planes in overlapped scanned for performing the registration. However, the accuracy of the registration results is dependent on the percentage of overlapping between the scans. Other studies involved combining terrestrial laser scanning technology with static GNSS positioning and Tacheometry point-wise surveying techniques. Vezocnik et al. conducted long-term high precision deformation monitoring of underground pipelines subjected to high-pressure conditions and concluded that the combined use of laser scanning and point surveying techniques is a valid solution for monitoring deformation in a 3D space (Vezočnik et al. 2009). The limitation of using such techniques is the amount of time invested in the data acquisition and processing and in assuming that the selected surveying point do not change over a few months. Therefore, the author developed a novel robust registration approach to reduce the amount of time needed in data acquisition and to accurately register 3D laser scanning data collected at different times. The following section presents the developed approach in detail.

Robust Registration Approach

The developed robust registration algorithm automatically registers two sets of 3D laser scanning data collected in different years (Figure 21). It utilizes points that are common and are less likely to change between two 3D laser scanning data sets of the bridges and registers them into one global coordinate system. The major advantage of this robust registration algorithm is that it automatically identifies such common points that do not have significant changes between two years' data. These automatically identified points aid in performing reliable registration of the two 3D laser scanning point clouds in order to accurately detect the geometric changes of bridges from year to year. The first step in the robust registration approach is to perform rough registration of the two 3D laser scanning data sets. This rough registration can be either performed manually or using commercially available registration software tools (e.g., Leica Cyclone). Next, the author manually removes redundant data found in 3D laser scanning data. Inaccurate segmentation of such redundant data may cause unreliable registration. The following section details the data preprocessing and 3D point cloud subsampling process.

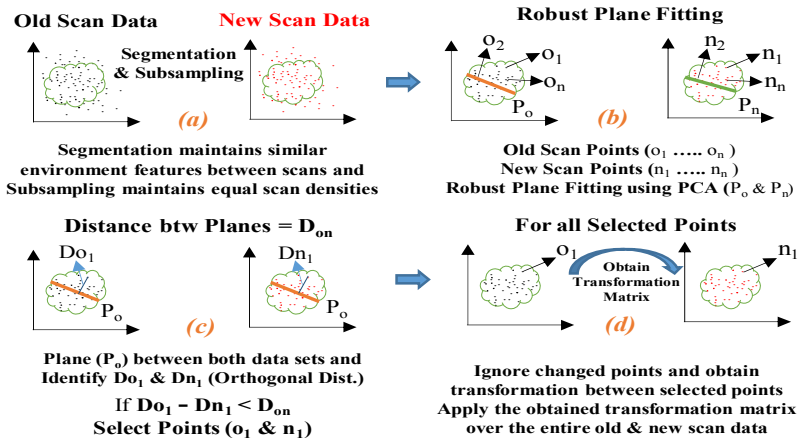

Figure 21. Robust registration approach to register old and new scan data

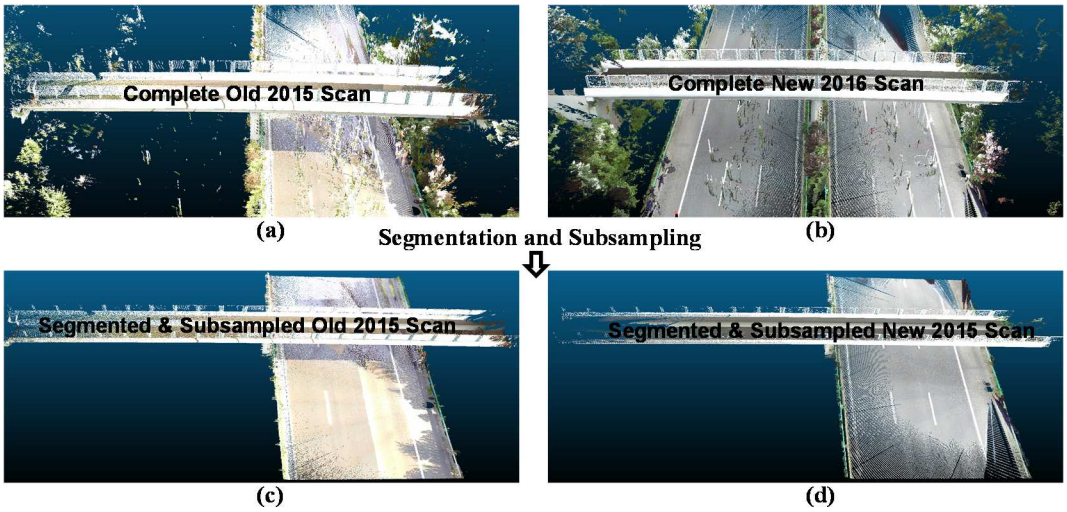

Figure 22. Segmentation and subsampling process of 3D laser scanning data for robust registration

Data Preprocessing and Subsampling

The process of segmentation removes all unwanted data, but it is very important that both the data sets have similar data densities to avoid biases of the registration towards denser parts of data. Hence, the author uses a two-step process to subsample both the 3D laser scanning data sets to maintain similar data densities across the point clouds. The two-step process firstly subsamples both the 3D laser scanning data sets to maintain uniform spacing between points. This process will subsample the 3D laser scanning data sets by maintaining a similar number of neighbors around a point in denser areas and not altering points in parts having sparser data points. The next step is to interpolate the sparser parts of the point cloud data and increase its density to the same level as other parts keeping similar densities across point clouds. The author conducted these two steps using the subsample tool available in CloudCompare (Girardeau-Montaut 2011). Figure 22 (c & d) shows an example of a subsampled 3D laser scanning data sets collected in 2015 and 2016 having uniformly distributed points. After the segmentation

and subsampling process, the robust registration approach detailed in the following section will align 3D data sets from different years for change detection.

Robust Registration Algorithm

3D laser scanning data collected at different times enable spatial change detection of the bridge structure. Examples of these spatial changes include overall deviation of the bridge structure (rigid body motion), deviations of individual bridge elements, and deformation of the individual bridge elements. However, the first step is to identify the rigid body motion of the bridge structure, which can help in identifying the other spatial changes. Such rigid body motion of the bridge can be identified by accurately registering 3D laser scanning data collected at different times. The collected 3D laser scanning data sets contain several common features and other additionally captured features of objects around the bridge structure. There may be cases that one point cloud data may contain features that might be missing in other point cloud data set. If a registration process is implemented during such case, the registration result will be biased toward the additional features, which is missing in one of the captured point cloud data. Hence, the reliable registration approach must segment both the point cloud data sets so that both contain exact same environment and bridge features that improve the quality of the registration results. The following paragraph details the process of segmenting both the point cloud data sets to contain exact same environment and bridge features that utilize a robust plane fitting approach to identify unchanged data points between the collected data sets. Failure to accurately segment the point cloud data sets will affect the plane fitting step that eventually affects the overall robust registration approach.

Algorithm 4: Robust Registration Algorithm

1. // Subsampled Old Laser Scanning Data (Points o_1, o_2, o_3… o_n)
2. **for** all the points of the old scan
3. Use Principle Component Analysis to robustly fit a plane (P_O)
4. Calculate the orthogonal distance (Eq. 5) between all the points and best-fit plane (P_O)
5. Orthogonal Distance's: Do_1, Do_2, Do_3 … Do_n
6. **end**
7. // Subsampled New Laser Scanning Data (Points n_1, n_2, n_3… n_n)
8. **for** all the points of the new scan
9. Use Principle Component Analysis to robustly fit a plane (P_n)
10. Calculate the orthogonal distance (Eq. 5) between all the points and old scan best-fit plane (P_O)
11. Orthogonal Distance's: Dn_1, Dn_2, Dn_3 … Dn_n
12. **end**
13. // Calculate the orthogonal distance between plane P_O and P_n = D_{on} (say)
14. **for** each point in the old scan (o_1, o_2, o_3… o_n), calculate its corresponding closest in the new scan (n_1, n_2, n_3… n_n)
15. **if** $|Do_1 - Dn_1| < D_{on}$ (say Po_1 is closest to point Pn_1 using nearest neighbor association)
16. inliers = [Po_1 , Pn_1]
17. **else** outliers
18. **end**
19. **end**
20. // Obtain the **Transformation Matrix** (Eq. 6) using the **ICP** between new scan inlier and old scan inlier points
21. // Apply the Transformation Matrix to the entire new and old 3D laser scanning data sets

The orthogonal distance (D_{on}) between the plane $ax + by + cz + d = 0$ and a point $xo = (x, y, z)$ is

$$D_{On} = \frac{|ax+by+cz+d|}{\sqrt{a^2+b^2+c^2}} \quad (5)$$

The transformation matrix transforms points (o_1, o_2, o_3) to (n_1, n_2, n_3) using the below equation

$$\begin{bmatrix} n_1 \\ n_2 \\ n_3 \\ 1 \end{bmatrix} = \begin{pmatrix} R_{11} & R_{12} & R13 & T_x \\ R_{21} & R_{22} & R_{23} & T_y \\ R_{31} & R_{32} & R_{33} & T_z \\ 0 & 0 & 0 & 1 \end{pmatrix} \times \begin{bmatrix} o_1 \\ o_2 \\ o_3 \\ 1 \end{bmatrix} \quad (6)$$

The segmented and subsampled 3D laser scanning data sets contain several common points between them. Manually identifying unchanged points between two data sets is tedious. Hence, the author developed an automatic method (Algorithm 4) that utilizes all the points in the point clouds to automatically and accurately identify unchanged parts between the two compared 3D laser scanning data sets (e.g., data collected in 2015 and 2016). First, the algorithm utilizes a robust plane fitting approach to fit a plane between all the points found in both the old (Points o_1, o_2, o_3… o_n) and new (Points n_1, n_2, n_3… n_n) 3D laser scanning data. The robust plane fitting approach utilizes the Principle Component Analysis (PCA), which minimizes the perpendicular distances between the points and the fitted plane (Elliot 2015). Using such plane fitting approach, the author robustly fit one plane between the points from the old (P_O) data collected in 2015 and an another plane between the points from the new (P_n) data collected in 2016.

The output of the plane fitting process is the center of the plane and the orthogonal distances between the fitted plane and all the points. However, if either of the point clouds contains data points that capture objects in one of the point cloud data and is not captured in the other point cloud, the robust plane fitting approach may generate a plane biased towards such additionally captured data parts that are missing in one of the compared point clouds. That plane would not well represent the overall trends of data points in the data set that have parts of data missing, making the comparison of two point clouds not on the same basis. In order to avoid such issues, the author only keeps data

points that are visible in both of the compared point clouds. That process segments both point clouds such that they share the exact same boundary, which contains the captured bridge and environmental features. Such segmentation is important so that a robustly fitted plane from one point cloud can be a good basis to assess the changes of the other data set. These two data sets capturing similar parts of the scene should have similar trends represented by a robustly fitted plane for analyzing differences between 2015 and 2016 point clouds which contain several spatial changes. The author utilizes the cross-section segmentation tool found in CouldCompare (Girardeau-Montaut 2011), which utilizes a bounding box to edit and segment 3D laser scanning data sets. The cross-section segmentation process consists of maintaining the exact same size of the bounding box, which eventually helps in maintaining similar features between the two 3D laser scanning data sets. This step will aid in improving the overall quality of the robust registration algorithm. Figure 21 shows an example of a segmented 3D laser scanning data of a bridge structure collected in 2015 and 2016 respectively. The author performed the segmentation process such that both the 3D laser scanning data sets contain the similar parts of the scene.

Since both the 3D laser scanning data sets are roughly registered and in the same global coordinate system, the algorithm then calculates the orthogonal distances between the data points in the old point cloud collected in 2015 and the old plane that is derived from old point cloud (Do_1, Do_2, Do_3 … Do_n hereafter). Similarly, the algorithm calculates the distances between the data points in the new point cloud collected in 2016 and the old plane that is derived from old point cloud (Dn_1, Dn_2, Dn_3 … Dn_n hereafter). Such process of calculating the orthogonal distance between the old and new points with the same old

plane derived from old point cloud will help to identify unchanged points among the old and new point clouds. The author now calculates the distance between the two fitted planes P_O and P_n, say $D_{on.}$ The next step in the robust registration algorithm is to associate every point in the old point cloud (2015 point cloud) to each point in the new point cloud (2016 point cloud) using the nearest neighbor approach. The nearest neighbor approach associates each individual old point to each new point based on the smallest distance between them.

The rough registration approach brings both the data sets into a single global coordinate and the nearest neighbor approach associates each point in the old point cloud (2015 point cloud) to its corresponding closest point in the new point cloud (2016 point cloud). Assuming that o_1 is the nearest neighbor to n_1, o_2 is the nearest neighbor to n_2 and so on for all other points. Now, the algorithm calculates the difference between orthogonal distances of the all the associated nearest neighbors such as $D_{O1} - D_{n1,}$ $D_{O2} - D_{n2,}$ etc. If one of the calculated orthogonal difference is smaller than $D_{on,}$ then the algorithm identifies those corresponding points as unchanged. For instance, if $D_{O1} - D_{n1} < D_{on}$, the algorithm identifies that the corresponding point D_{O1} and D_{n1} remain unchanged between old and new point cloud data.

Hence, the algorithm identifies all corresponding old and new points that have the difference in the orthogonal distances smaller than $D_{on.}$ This process now eliminates all the changed points and extracts only those unchanged points that are utilized for automatic registration between both the collected 3D laser scanning data sets. The algorithm now utilizes an Iterative Closest Point (ICP) registration (Tang and Rasheed 2013) to register unchanged old and new points and determine its corresponding

transformation matrix. This transformation matrix provides the translation and rotation values required to accurately align the new points to their corresponding old points and eventually to register the entire old and new 3D laser scanning data from which those points were extracted. Therefore, this process determines the transformation matrix between the unchanged old and new points and algorithm uses this transformation matrix to register both the collected 3D laser scanning data sets required for reliable geometric change detection of bridges.

Validation of the Developed Robust Registration Approach

To validate the developed robust registration approach, the author compared its registration results with the traditional registration approach, which relies on matching features points between two sets of 3D laser scanning data. The comparison process relies on comparing the transformation matrix generated by the robust registration approach with that of the transformation matrix generated by the traditional registration approach. A transformation matrix consists of translation parameters that consist of displacement along x, y, and z coordinates and rotation parameters that consists of rotation along α (rotation around the x-axis), β (rotation around the y-axis), and γ (rotation around the z-axis) that helps to register the 2015 3D laser scanning data with the 2016 3D laser scanning data (Gentle 2007). The final output of the robust registration approach is the transformation matrix, which is compared with the registration results of the traditional registration approach. The following section provides details about generating the transformation matrix using the traditional registration approach.

The author executed a registration approach that iteratively selects unchanged feature points between the two data sets. The improved manual feature point selection

approach utilizes manually selected feature points on the bridge and its surrounding common in the 3D laser scanning data collected in 2015 (old data) and 2016 (new data) respectively. Specifically, the author selected several feature points on a nearby culvert and few feature points on the part of the bridge structure. The process of manually selecting feature points involves selecting few common feature points between the old and the new 3D laser scanning data. For instance, the author has selected 11 common feature points (bridge & environment) between the two data sets. Then the author select three points each from the previously selected set of 11 common feature points such that the triangle formed by connecting the three feature points in the old data is similar to the triangle formed by the feature points in the new data. Here, the similarity between the two triangles can be obtained by maintaining the equal length of the sides of the triangle. Now the author performs the registration between the old and the new 3D laser scanning data using these three selected feature points to obtain the transformation matrix. After this registration step, the author calculates the change in the distance between the remaining 8 feature points from the old 3D laser scanning data with their corresponding 8 feature points from the new 3D laser scanning data. Such calculation will provide information about those features points that have undergone significant changes after the first registration step.

Next, the author identifies the least changing common feature point between the old and the new 3D laser scanning data. After identifying the least changing feature point, the author again performs the registration between the original old and new 3D laser scanning data using the previously identified 3 common feature point and the least changing common feature point. This registration step generates another transformation

matrix. The author calculates the difference in the new transformation matrix (4 feature point registration) and the old transformation matrix (3 feature point registration) and identifies if any of the translation (translation along x, y or z coordinate directions) value difference is above a certain threshold. The author set 30 cm as value for the threshold. Here, the author ignored the rotation values from the transformation matrix, as these rotation values are significantly smaller. If the difference between both the transformation matrices is above the threshold, then the author continues the registration process by calculating the change in the distance of the remaining 7 feature points from the old scan with their corresponding 7 feature points from the new scan to identify the least changed feature point.

In the next step, the author again performs another registration between the original 3D laser scanning data sets using the four previously selected feature points and the new identified least changed feature point to obtain another transformation matrix. If the difference between the new transformation matrix and the previous transformation matrix is below the threshold value, then the author end this registration process and treat the new transformation matrix as final. If the difference between the new transformation matrix and the previous transformation matrix is above the threshold value, then the author continues the registration process by again identifying another least changed feature point among the remaining common feature points. The above described registration using manual feature point selection approach iteratively identifies least changing feature points by gradually registering both the old and the new 3D laser scanning data. This iterative registration approach can be utilized in cases of a bridge data having no similar environmental feature points to perform the robust registration

approach. The author validated the developed robust registration approach using a case study of a highway bridge structure detailed in the following section.

Case Study for Validating the Developed Robust Registration Approach

First, the author segmented, subsampled, and roughly aligned both the 2015 and 2016 3D laser scanning data sets (Figure 23). Now the author applied the robust registration algorithm to accurately register both the 2015 and 2016 3D laser scanning data (Figure 23 (c)). Figure 23 shows the obtained transformation matrix (Table 6), which contain the translation and rotation parameters to robustly register both the 3D laser scanning data sets. These robustly registered 3D laser scanning data sets to aid in reliable geometric change detection of bridges for performing accurate condition diagnosis. Therefore, the changes detected from such robustly registered 3D laser scanning data sets reflect the actual geometric changes of a bridge structure rather reflecting changes due to registration errors between the two data sets. Now the author implements the improved feature point registration approach to manually register both the 2015 and 2016 3D laser scanning data. To implement the improved traditional registration approach, the author initially selected 11 feature points and then identified that there is no significant change in the obtained transformation matrix when using 6 least changed commonly identified feature points. Table 6 shows the final transformation matrix using the 6 identified feature points, and its comparison with the transformation matrix generate using robust registration approach.

Table 6. Comparison of the registration results (Robust Registration vs. Manual Registration)

REGISTRATION TYPE	TRANSLATION VALUES			ROTATION VALUES		
	X	*Y*	*Z*	α	β	γ
Robust Registration Approach	1.123	-2.308	-0.1014	0.0053	0.0024	-0.0009
Registration using Improved Manual Feature Point Selection	1.208	-2.743	-0.0812	0.0078	0.0026	-0.0001

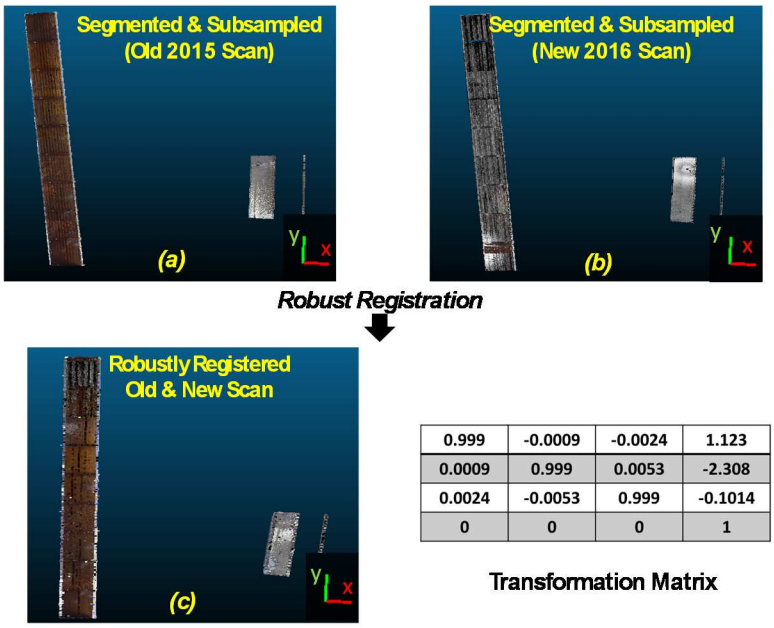

Figure 23. Segmented, subsampled and robustly registered 3D laser scanning data of the highway bridge (z-axis along elevation).

The comparison results show that the developed robust registration approach is qualitatively same but slight vary from the registration results using manual feature point selection. This means that both the registration approaches output results that have the same direction of translation and the direction of rotation along all the coordinate axes. Additionally, the quantitative difference between all the registration results is very small and does not significantly affect the results of the geometric changes detected between the collected 3D laser scanning data sets. This comparison study validates the robust nature of the developed robust registration approach and its substantial advantage for

performing automatic and reliable geometric change detection of the bridges using 3D laser scanning data over other traditional approaches.

Structure level Registration for Finding Global Change Type 1 (G1) – Global Rigid Body Motion of the Whole Bridge Structure

This step aims at detecting the global deviation of the bridge structure when comparing two 3D laser scanning data sets. After the robust registration of the two 3D laser scanning data sets, the detected spatial changes will help identify geometric changes of the bridge structure during the time between the two scans. However, such geometric changes can be due to a mix of rigid body motion (global deviation G1) and local deformation of individual bridge elements (L). To resolve the mix of global and local geometric changes, the author first perform a feature based point cloud registration technique. Using the common feature points (shown in Figure 24) extracted from the bridge structure, the developed approach aligns the two point cloud data of the bridge structure using a pairwise point-to- point registration. The point-to-point registration approach generates a transformation matrix that contains the translation and rotation information of the bridge after the alignment process. These transformation and rotation matrices provide information about the bridge's displacement along x, y, and z coordinates and rotation along α (rotation around the x-axis), β (rotation around the y-axis), and γ (rotation around the z-axis). Figure 24 shows a structure-level registration approach for identifying global deviation of the bridge using a single-pier highway bridge structure as an example. After generating the transformation matrix, this process will remove the global deviation detected between the two 3D laser scanning data sets. The identified translation and rotation of the bridge structure is a geometric change caused

due to the rigid body motion of the entire bridge (global deviation G1) when compared to its surrounding environment.

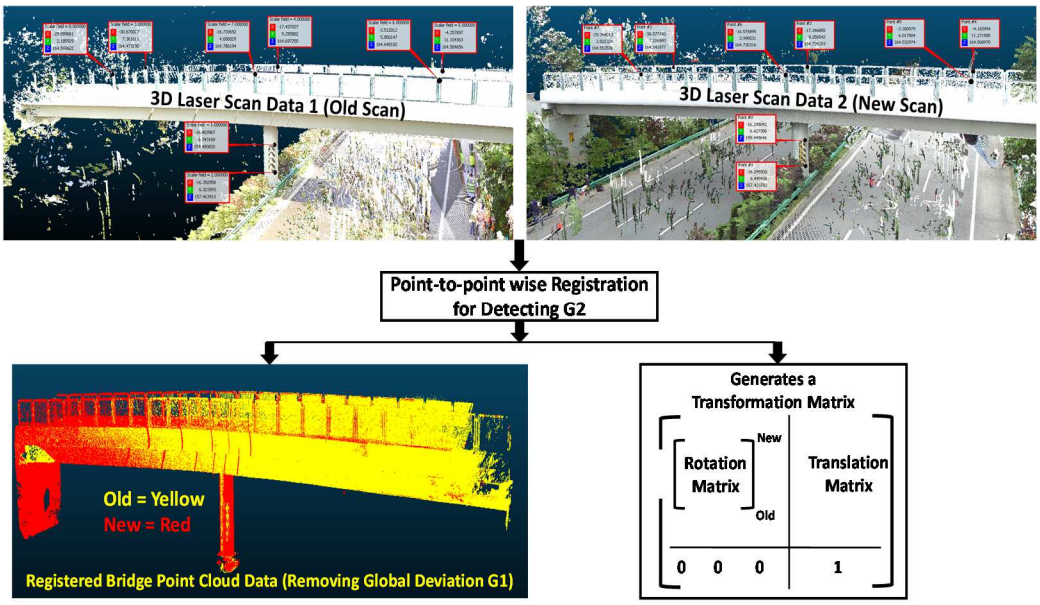

Figure 24. Detecting global deviation (G1) of the bridge structure

Figure 25. Detected global deviation (twist of the bridge)

Element Level Registration for Finding Global Change Type 2 (G2) – Relative Displacement between Structural Elements

Global deviation (G1) of the bridge structure provides the details about the change in rotation/translation of the entire bridge. Similarly, individual elements of the bridge also undergo changes in their position, which is a dependent on the element's global deviation and the properties of element-to-element connectivity (boundary conditions). For instance, a pinned girder of a bridge undergoes different changes (deflects) when

compared to a girder supported by roller supports. Figure 6 provides the steps to identify and classify element level global deviations (G2) of the single pier bridge structure using element-level registration approach. First, the author segment each element of the bridge structure into individual girders, columns, pier caps, etc. Then the author utilize the end points (extracted from point cloud data) of each element to perform precise pair wise point-to- point registration to identify the element-wise change in position. This registration approach will generate a transformation matrix that provides the details about the translation and rotation parameters of the element (shown in Figure 26). This pointwise registration will remove the element level global deviation (G2), and now the point cloud data will only contain information about element level local deformation (e.g. bending, torsion, tension, etc.).

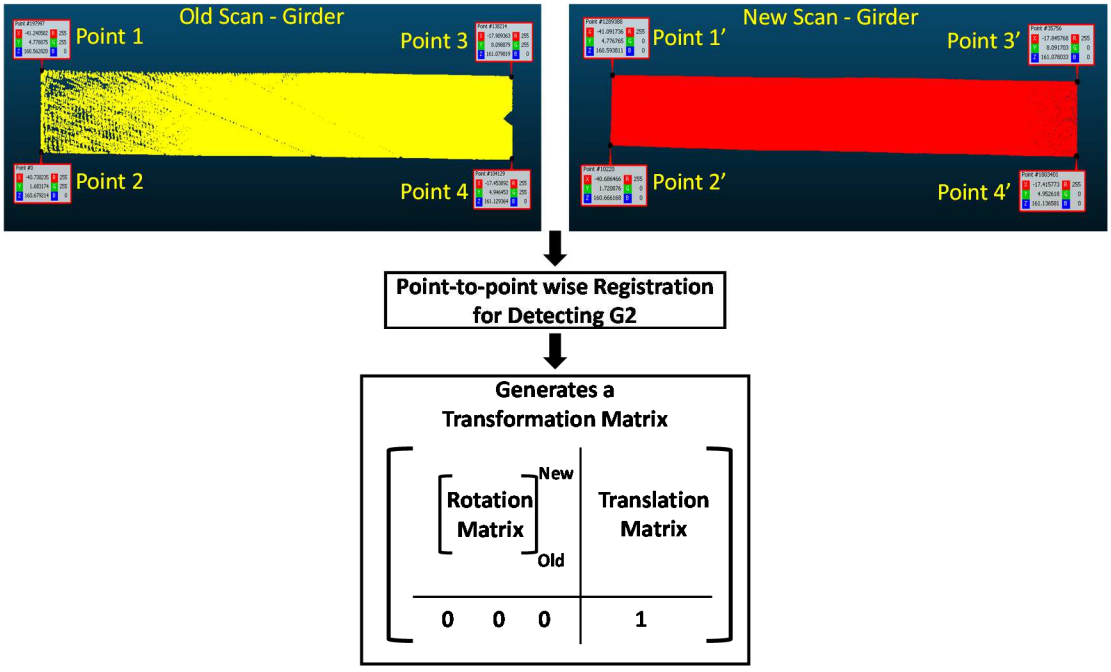

Figure 26. Detecting global deviation (G2) for each element of the girder

Pattern Classification for Classifying Local Shape Changes (L) – Element-Level Local Deformations

This step aims to identify element level local deformation that is primarily due to bending, torsion, tension, or compression of individual elements of the bridge structure. After performing element-wise registration to identify and remove its global deviation (G2), the author will identify the element level local deformation (L) using ends (joints) of the element in the point cloud data. For example, the ends of the element will provide the information about the length of each element, which can help in detecting changes due to compression or tension of the investigated element. In general, an increase in the length of the element is associated with deformation due to tension and the decrease in the length of the element is associated with deformation due to compression. However, detecting deformation due to bending or torsion is difficult when compare to detecting deformation due to compression or tension. To identify the deformation due to bending/torsion along with detecting its corresponding change in direction, the author developed a pattern classification algorithm that utilizes the information of the normal of a fitted plane for each element of the bridge structure. The change in the direction of the normal will provide the information about the change in the direction of bending or torsion of the element. Figure 27 shows the detailed systematic process that consists of extracting planes, generating normals, computing the change in the direction of normals, and detecting deformation due to bending/torsion.

Detecting local deformation of the elements due to bending: The developed algorithm first splits the entire girder/column from both the point cloud data sets into several small strips of equal size and generates the normal for each strip. A girder is split along its length

whereas a column is split along its height. Then the algorithm computes the change in the direction of the normals to identify the change in rotation at the joints of each element (girder/column) to recognize the direction of bending. For instance, if the left joint of the girder is rotating anticlockwise and the right joint of the girder is rotating clockwise, the girder is bending downward (Figure 27(a)). Such information will provide the direction of bending (upward or downward) and identify the local deformation of all the elements. Hence, a girder having a decrease in its length and bending downward has a combination of bending and compression as its local deformation. The following section will provide the details about identifying the direction of torsion.

Detecting local deformation of the girders due to torsion: The developed algorithm first extracts four planes at all the four corners of the girder's point cloud data. Then the algorithm generates the normal to all the four extracted planes and computes the change in the angle between the normals of the girders of the bridge structure from both the 3D laser scanning data sets. Figure 27(b) shows the steps taken by the algorithm to detect local deformation due to bending or torsion. In general, bending is a deformation of the girder along its central axis whereas torsion is deformation perpendicular to the central axis of the girder. Hence, the extracted normals will provide the information for both the direction of bending deformation and torsion deformation by using different combinations of normals. Figure 27(b) shows that computing the change in the direction of normals N1-N4 vs. N1'-N4' will provide the direction of torsion of the girder.

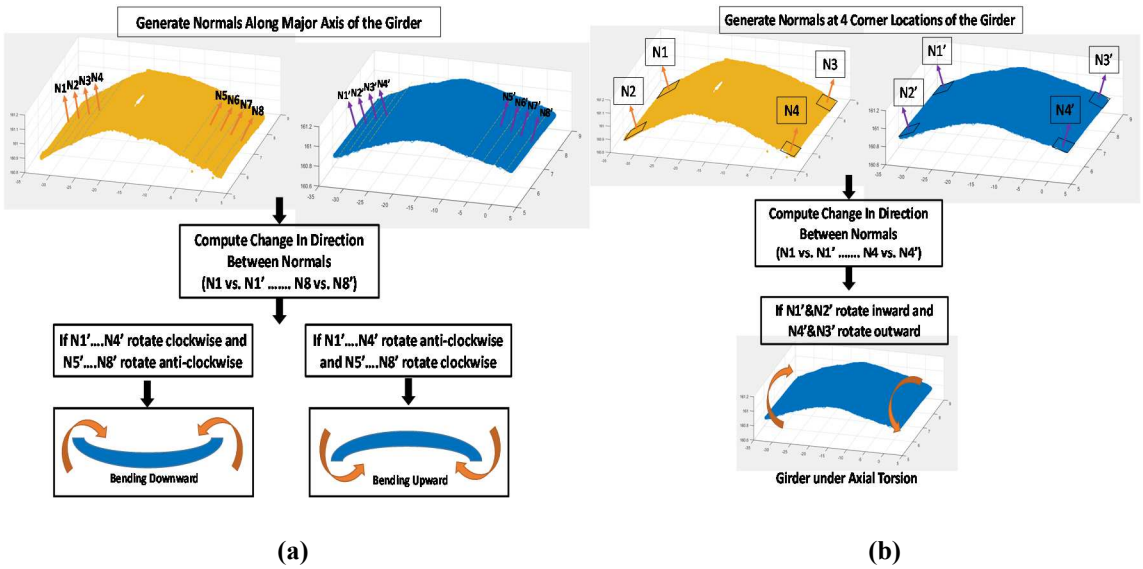

Figure 27. Pattern classification approach for detecting (a) Bending (b) Torsion

Using the above-described methodology, the developed approach aligns two sets of 3D laser scanning data, detects spatial changes, identifies global deviation of the bridge (G1), recognizes global deviation of elements of the bridge (G2), and detects element level local deformations (L).

Validation

The developed multi-level 3D data registration algorithm helps in reliable spatial change classification of single-pier bridges as global deviations and local deformations. This section details the results of the spatial change classification approach of 2 highway bridges using 3D laser scanning data collected in 2015 and 2016 respectively. The author applied the four-step approach detailed in the methodology section to classify the observed spatial changes for both the highway bridges. However, the author first discuss the validation process to validate the robustness of the developed automatic robust

registration approach to register two sets of 3D laser scanning data scanned at different times and to detect the global rigid body motion of the bridge structure.

Validation of Global Level Change Detection Approach

The developed robust registration approach utilizes all the feature points in a point cloud data for performing automatic registration between 2 sets of 3D laser scanning data collected at different time. To validate the robustness of the developed robust registration approach, the author compared its registration results with traditional registration using manual feature point selection. In addition, the author also compared the global rigid body motion of the bridge structure between the 2 sets of registered 3D laser scanning data using the robust registration approach and the manual feature point selection approach. Manual feature point selection consists of picking common points on the objects around a bridge structure that are available in the both the sets of 3D laser scanning data. The author manually selected common points from both the environment (environment feature points) and on the bridge structure (bridge feature points) in both data sets. The manual feature point selection process consists of selecting those feature points that may undergo significantly smaller spatial changes when compared to the bridge structure. Figure 28 shows the manually selected feature points, the registration process, and the obtained global rigid body transformation matrix for highway single-pier bridge 1. Similarly, Figure 29 shows the robust registration approach, the registration process, and the obtained global rigid body transformation matrix for highway single-pier bridge 1. The author compared the generated results (G1) between the registration using manual feature point selection approach and the robust registration approach in Table.

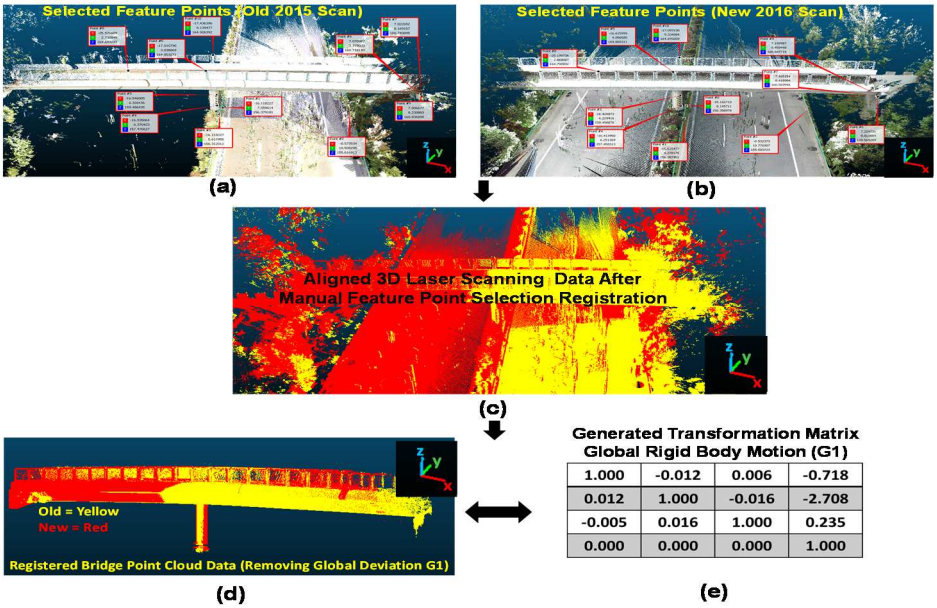

Figure 28. Registration Using Manual Feature Point Selection of Highway Bridge 1

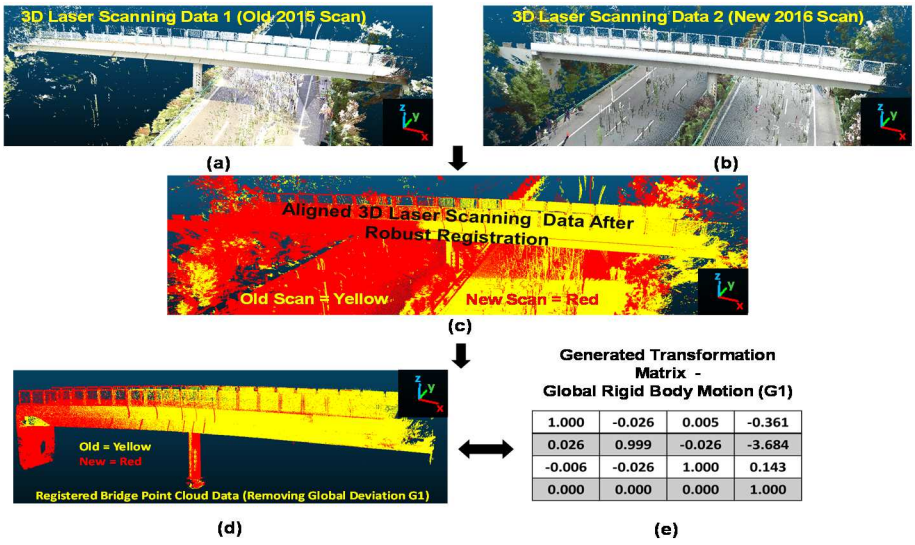

Figure 29. Robust Registration Approach for Identifying Global Rigid Body Motion of Highway Single-Pier Bridge 1

Table 7. Comparison of Registration Results using Robust Registration and Registration using Manual Feature Point Selection Approaches of Highway Bridge 1

REGISTRATION TYPE (Highway Single-Pier Bridge 1)	TRANSLATION VALUES			ROTATION VALUES		
	X	Y	Z	α	β	γ
Robust Registration (RR)	-0.0481	0.9247	-0.0456	-0.0058	-0.0002	-0.001
Registration Using Manual Point Selection (PP)	-0.408	1.027	-0.063	-0.006	-0.003	-0.01

Table 8. Comparison of the Global Rigid Body Motion of Highway Bridge 1 based on Robust Registration and Registration using Manual Feature Point Selection

Global Rigid Body Motion (G1) (Highway Single-Pier Bridge 1)	TRANSLATION VALUES			ROTATION VALUES		
	X	Y	Z	α	β	γ
G1 (Robust Registration)	-0.361	-3.684	0.143	-0.026	-0.005	-0.026
G1 (Manual Feature Point Selection)	-0.718	-2.708	0.235	-0.016	-0.006	-0.012

Automated Change Analysis Highway Single-Pier Bridges

This section details the results of the robust registration and spatial change classification approach on the 3D laser scanning data of two single pier Highway Concrete Bridges collected in 2015 and 2016 respectively. In the previous section, Figure 29 ((a) & (b)) shows the 3D laser scanning data of the Highway Bridge 1 collected in 2015 and 2016 respectively, wherein the bridge comprises of a single circular column (pier) of length 5.13 meters and 1.3 meters in diameter that supports a simply supported girder having length 47.82 meters and width 3.15 meters approximately. The author collected a total of 2 scans in 2015 and 4 scans in 2016 and applied the robust registration approach to accurately align the 3D laser scanning data of Highway Bridge 1 (Figure 29 (c)) and identified the global rigid body motion of the bridge structure (Figure 29 (d) &(e)). Similarly, Figure 30 shows the 3D laser scanning data of the highway bridge two collected in 2015 and 2016 respectively (Figure 30 (a) & (b)). The bridge comprises of 2 circular columns (pier) of length 3.23 meters and 1.8 meters in diameter that support a continuous simply supported girder of length 63 meters and width 9 meters approximately. The author collected a total of 7 scans in 2015 and 9 scans in 2016 and utilized the robust registration approach to accurately align the registered scans into one

global coordinate (Figure 30(c)) that automatically identifies the global rigid body motion of the bridge structure (Figure 30 (d) & (e)).

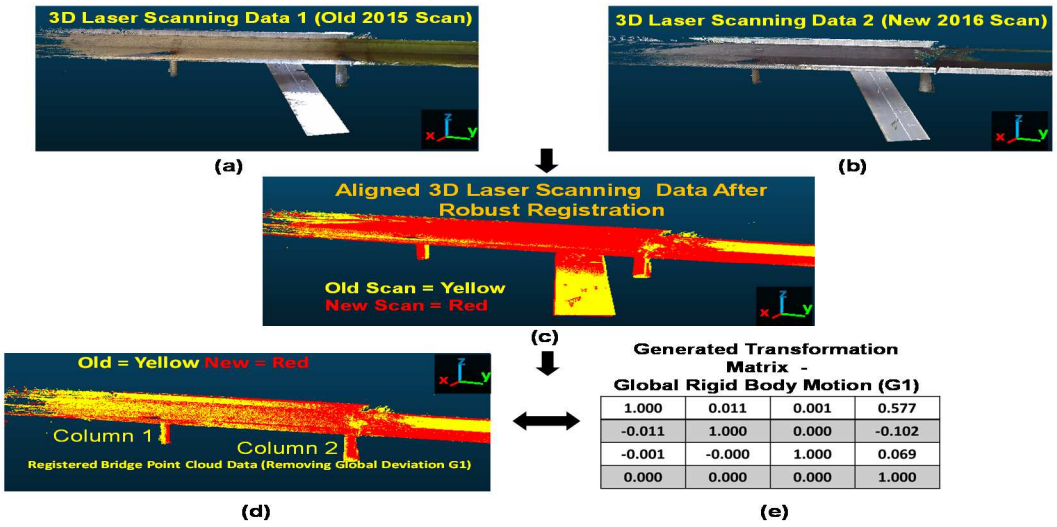

Figure 30. Robust Registration Approach for Identifying Global Rigid Body Motion of Highway Single-Pier Bridge 2

The robust registration approach accurately aligns two sets of 3D laser scanning data collected at different times and the structure level registration identifies the global rigid body motion of the bridge structure as shown in the above figures. Now, the registered 3D laser scanning data of the bridges contain element level global deviations (G2) and local deformations as the structure level registration approach removes the global rigid body motion (G1) of the bridge structure. The author now applies the element level registration for identifying the global deviation of individual elements of the bridge structure (G2) highlighted in Table 9 & 10 for highway single pier bridge 1 and 2 respectively.

Table 9. Global Deviations (G2) of the Element of Highway Single-Pier Bridge 1

ELEMENT	TRANSLATION (meters)			ROTATION (degrees)		
	x	y	z	α	β	γ
GIRDER	0.039	-0.362	0.022	0.002	0	0
COLUMN	-0.083	-0.032	-0.009	0	-0.001	0

Table 10. Global Deviations (G2) of the Element of Highway Single-Pier Bridge 2

ELEMENT	TRANSLATION (meters)			ROTATION (degrees)		
	x	y	z	α	β	γ
GIRDER	-0.467	0.045	-0.055	0.000	0.002	0.002
COLUMN 1	-0.640	0.174	-0.002	0.001	0.002	0.001
COLUMN 2	-0.214	-0.275	-0.024	-0.001	0.001	0.002

Finally, the author utilizes the developed pattern classification approach to identify the element level local deformations (L) for both the girder and column of the bridge structures. The pattern classification approach first identifies deformation due to tension and compression for each individual bridge element by comparing its length/height from 2015 3D laser scanning data with that of 2016 3D laser scanning data. Then the author applies the normal based pattern classification approach that classifies element level local deformations due to bending and torsion. Figure 31 highlights all the classified local deformations of highway bridge 1 and Figure 32 highlights all the classified local deformations of highway bridge 2 respectively.

Figure 31. Classified Local Deformations of Highway Single-Pier Bridge 1

Figure 32. Classified Local Deformations of Highway Single-Pier Bridge 2

Validating the detected multi-level against domain experts interpretation of single pier bridge changes

The author detected and classified the spatial changes of two highway single pier bridges using 3D laser scanning data. This change analysis study will help in revealing the mechanisms of deterioration of the single pier bridges based on the spatial changes detected using 3D laser scanning data collected in 2015 and 2016 respectively. The developed spatial change classification approach will provide the cause of an observed spatial change (global or local). This classification will help structural engineers understand the correlation between the detected global and local changes, which lead to structural deteriorations. It also enables structural engineers to recognize the deterioration mechanism of the single pier bridges by identifying the abnormal changes in the boundary conditions and loading conditions of such bridges. The developed spatial change classification approach on the two highway single-pier bridges achieved the following observations:

- The single pier bridge undergoes global rigid body motion with respect to the environment. This shows the long-term change in the interaction between the bridge structure and its surrounding environment. The change in rigid body

motion of bridge may also indicate a change in boundary condition between the bridge structure and the surrounding environment.

- The individual elements of the single pier bridge experiences change in the rotation and translation changing the geometric relationship (relative displacement) between connected bridge elements. Such change in the geometric relationship may cause changes in the boundary conditions between the bridge elements. Excessive unidirectional loading from vehicles may cause such change in relative rotation between connected bridge elements resulting in the overturning collapse of the bridge. For instance, unidirectional loading may lead to twisting of the girder causing the change in the thickness of the pier cap (deformation of pier cap) connecting the bridge girder and the column. The gradual long-term increase in the deformation of the pier cap may result in the collapse of the entire single pier bridge.
- The detected change in the local deformations of bridge elements may be due to change in the material property of the elements or due to uneven loading conditions. However, it is difficult to identify if such local shape change signifies general deformation under loading or long-term creep of the element.

Discussions

Limitations of the Developed Spatial Change Classification Approach

The developed spatial change classification approach has few limitations and assumptions when identifying and classifying the geometric spatial changes, which are detailed as following.

When evaluating the interaction between the bridge and its surrounding environment for detecting global deviation (G1), the author assumes that the surrounding environment has significantly much fewer changes when compared with changes in the bridge structure. In general, the surrounding environment around a bridge structure such as railings on roads, mile markers, etc. also undergoes day-to-day spatial changes. However, such spatial changes are geometrically very small when compared to the geometric changes of a bridge structure under constant loading and unloading. Therefore, the author has utilized these less changing environmental features for performing robust registration of two 3D laser scanning datasets collected at different time intervals.

The author has manually picked common feature points (ends of girder/column) to execute the registration between the bridge structures or between two individual elements of the bridge structures. The density of the collected data of the bridge structure will significantly influence the registration results and generate errors while calculating the global and local changes. For instance, if the 3D laser scanning data is dense in the right part of the bridge and sparse at its left part. The registration result will be dominated by the denser area of the bridge and generates unreliable spatial change detection and classification results.

Directions for Future Research

Spatial changes such as deformations of individual elements cause changes in the structures loading behavior. If individual elements of a structure undergo larger deformations, the structure may eventually lose its load carrying capacity. It is necessary to identify elements in the loading path that have abnormal deformations. If there is a change in the structures loading path, it may suggest that the few elements along the

loading path have anomalous behavior. Correlated spatial changes can help in identify the loading path of the structure and detecting changes that highly correlate with particular types of structural failure. Such loading path connectivity analysis approach can help in identifying elements that are abnormally behaving under loading and are on the verge of its structural collapse. However, the major challenge is to identify the patterns of change that correlate with the loading behavior of the structure. Several deformations are caused due to environmental conditions; accidents etc. that are difficult to detect. Hence, it is important to identify correlating spatial changes that occur together and cause changes in the structure loading behavior. However, no previous studies have investigated in the direction of structure's loading behavior and its correlation with the visual change patterns. Such knowledge is crucial in performing accurate and reliable condition diagnosis of a structure. Traditional local defect identification techniques cannot determine the effect of such defect on the loading performance of the entire structure.

The future work will include developing an algorithm that uses the correlated spatial changes of individual elements to determine the structures loading path. The author plans to utilize a 3D laser scanning data of a highway bridge under a loading test to detect the spatial changes of a bridge under systematic loading conditions. Such loading test data will provide the basis for understanding the spatial changes (deformation) of individual elements and the correlations between the spatial changes of connected elements of a bridge. Using the results from the loading test data, the author developed an algorithm that can automatically detect the correlations between the identified spatial changes of elements from the 3D laser scanning data of 2 highway bridges collected in 2015 and 2016 respectively.

Conclusion and Future Work

This chapter presented a novel robust registration approach that automatically detects unchanged common points between two sets of 3D laser scanning data and accurately registers them into one global coordinate. The developed approach first segmented redundant data and subsampled both the 3D laser scanning data sets. Then a robust registration algorithm automatically extracted unchanged points on both the bridge and its surrounding environment to perform a point-to-point registration. Such process does not require any manual intervention or the tedious process of manually selecting unchanged points. The author applied the developed registration approach on highway pre-stressed Concrete Bridge and validated the registration results by comparing it with the traditional manual feature point selection registration approach.

Next, the author developed a reliable and accurate spatial change classification approach for classifying the observed geometric spatial changes of a highway bridge structure as global deviations (G1&G2) and local deformations of elements. The developed approach identifies the interactions between the bridge structure and its surrounding environment to detect the global deviation of the bridge (G1). The author removes the detected global deviation (G1) and then identify the global deviation of each individual element of the bridge (G2) using a point-to-point registration approach. Such registration approach will remove all the global deviations of the bridge and its connected elements. Then a local deformation detection algorithm detects the change in the length of each element of the bridge and utilizes the normal of the point cloud data to detect the change in the direction of bending/torsion of all the elements (L). This hierarchical change classification approach accurately classifies all the detected changes and aids in

performing reliable condition diagnosis of the bridge structure. This change classification approach is a significant improvement over traditional deformation monitoring, and geometric change detection approaches as it provides the cause of an observed spatial change, which can be a helpful tool for a structural bridge engineer.

The developed robust registration algorithm utilizes several environment feature points that surround the bridge structure. However, in some cases, these environment feature points undergo higher spatial changes than the bridge structure. In the future, the author plan to study the effect of spatial changed environmental feature points on the registration results. The author plan to use the surveying data collected using a Total Station sensor to establish several control point network using the environmental features around the bridge structure. These ground control points can aid in understanding the spatial changes of these environmental features that can be incorporated in registering two sets of 3D laser scanning data collected at different times. Hence, using both the data generated by the 3D laser scanners and the Total Station sensor can help in developing more robust registration approach that is not affected by the spatial changes of the environment surrounding a bridge structure.

References

ACSE. (2013). "Report Card for America's Infrastructure." American Society fo Civil Engineers, (March), 1–74.

Agdas, D., Rice, J. A., Martinez, J. R., and Lasa, I. R. (2012). "Comparison of Visual Inspection and Structural-Health Monitoring As Bridge Condition Assessment Methods." Journal of Performance of Constructed Facilities, 26(4), 371–376.

Antova, G. (2015). "Registration Process of Laser Scan Data in the Field of Deformation Monitoring." Procedia Earth and Planetary Science, 15, 549–552.

Barnea, S., and Filin, S. (2008). "Keypoint based autonomous registration of terrestrial laser point-clouds." ISPRS Journal of Photogrammetry and Remote Sensing, 63(1), 19–35.

Basharat, A., Catbas, N., and Mubarak Shah. (2005). "A Framework for Intelligent Sensor Network with Video Camera for Structural Health Monitoring of Bridges." Third IEEE International Conference on Pervasive Computing and Communications Workshops, IEEE, 385–389.

Beskhyroun, S., Wegner, L. D., and Sparling, B. F. (2011). "New methodology for the application of vibration-based damage detection techniques." Structural Control and Health Monitoring, (May 2011), n/a-n/a.

Briaud, L., and Diederichs, R. (2007). "Bridge Testing." Nondestructive Testing (NDT), 1–4.

Cabaleiro, M., Riveiro, B., Arias, P., and Caamaño, J. C. (2015). "Algorithm for beam deformation modeling from LiDAR data." Measurement: Journal of the International Measurement Confederation, 76, 20–31.

Choi, K., Lee, I., and Kim, S. (2009). "A Feature Based Approach to Automatic Change Detection from Lidar Data in Urban Areas." International Society for Photogrammetry and Remote Sensing Vol. XXXVIII, Part 3/W8, XXXVIII(C), 6.

Doebling, S., Farrar, C. R., and Prime, M. (1998). "A summary review of vibration-based damage identification methods." Shock and vibration digest, 1–34.

Elliot, N. (2015). "Using Principal Components Analysis to determine the best fitting plane from locations in a #PointCloud | Garrett Asset Management." New York Tech Journal, <https://elliotnoma.wordpress.com/2015/09/29/using-principal-components-analysis-to-determine-the-best-fitting-plane-from-locations-in-a-point-cloud/> (Mar. 7, 2017).

"FARO Laser Scanner Software - SCENE - Overview." (n.d.). <http://www.faro.com/en-us/products/faro-software/scene/overview> (Mar. 12, 2015).

Fruchter, R., Law, K. H., and Iwasaki, Y. (1993). "QStruc: an approach for qualitative structural analysis." Computing Systems in Engineering, 4(2–3), 147–157.

Gentle, J. E. (2007). Matrix Algebra: theory, computations, and applications in statistics. Books.Google.Com.

Girardeau-Montaut, D. (2011). "CloudCompare-Open Source project." OpenSource Project.

Girardeau-Montaut, D., and Roux, M. (2005). “Change detection on points cloud data acquired with a ground laser scanner.” International Archives of Photogrammetry, Remote Sensing and Spatial Information Sciences, 36, W19.

Gvili, R. (2010). “Iterative Closest Point.” Insight.

Kalasapudi, V. S., and Tang, P. (2015). “Automated Tolerance Analysis of Curvilinear Components Using 3D Point Clouds for Adaptive Construction Quality Control.” Computing in Civil Engineering 2015, American Society of Civil Engineers, Reston, VA, 57–65.

Kalasapudi, V. S., Turkan, Y., and Tang, P. (2014). “Toward Automated Spatial Change Analysis of MEP Components Using 3D Point Clouds and As-Designed BIM Models.” 2014 2nd International Conference on 3D Vision, IEEE, 145–152.

Kashif Ur Rehman, S., Ibrahim, Z., Memon, S. A., and Jameel, M. (2016). “Nondestructive test methods for concrete bridges: A review.” Construction and Building Materials.

Koh, B. H., and Dyke, S. J. (2007). “Structural health monitoring for flexible bridge structures using correlation and sensitivity of modal data.” Computers and Structures, 85(3–4), 117–130.

Lattanzi, D., and Miller, G. R. (2012). “Robust Automated Concrete Damage Detection Algorithms for Field Applications.” Journal of Computing in Civil Engineering, (April), 120917010504009.

Liang-Chien, C. (2010). “Change detection of building models from aerial images and lidar data.” International Society for Photogrammetry and Remote Sensing TC VII Symposium, 121–126.

Lindenbergh, R., and Pfeifer, N. (2005). “A statistical deformation analysis of two epochs of terrestrial laser data of a lock.” Proc. Of Optical 3D Measurement Techniques, Vol II, Vienna, Austria, 61–70.

Maragakis, E. A., and Jennings, P. C. (1989). “Analytical models for the rigid body motions of skew bridges.” Mathematical and Computer Modelling, 12(3), 377.

Mirzaei, Z., Adey, B. T., Klatter, L., and Kong, J. S. (2012). The Iabmas Bridge Managment Committee Overview of Existing Bridge Management Systems 2012 C EMS. IABMAS.

Monserrat, O., and Crosetto, M. (2008a). “Deformation measurement using terrestrial laser scanning data and least squares 3D surface matching.” ISPRS Journal of Photogrammetry and Remote Sensing, 63(1), 142–154.

Monserrat, O., and Crosetto, M. (2008b). “Deformation measurement using terrestrial laser scanning data and least squares 3D surface matching.” ISPRS Journal of Photogrammetry and Remote Sensing, 63(1), 142–154.

Moschas, F., and Stiros, S. (2011). “Measurement of the dynamic displacements and of the modal frequencies of a short-span pedestrian bridge using GPS and an accelerometer.” Engineering Structures, 33(1), 10–17.

Park, H. S., Lee, H. M., Adeli, H., and Lee, I. (2007). “A New Approach for Health Monitoring of Structures: Terrestrial Laser Scanning.” Computer-Aided Civil and Infrastructure Engineering, 22(1), 19–30.

Patjawit, A., and Kanok-Nukulchai, W. (2005). “Health monitoring of highway bridges based on a Global Flexibility Index.” Engineering Structures, 27(9), 1385–1391.

Poreba, M., and Goulette, F. (2015). “A robust linear feature-based procedure for automated registration of point clouds.” Sensors (Switzerland), 15(1), 1435–1457.

Raghavendrachar, M., and Aktan, A. E. (1992). “Flexibility by Multireference Impact Testing for Bridge Diagnostics.” Journal of Structural Engineering, 118(8), 2186–2203.

Riveiro, B., Morer, P., Arias, P., and De Arteaga, I. (2011). “Terrestrial laser scanning and limit analysis of masonry arch bridges.” Construction and Building Materials, Elsevier Ltd, 25(4), 1726–1735.

Ryan, T. W., EricMann, J., Chill, Z., and Ott, B. T. (2012). “Bridge Inspector’s Reference Manual.” Fhwa, BIRM 1, 1020.

Su, Y. Y., Hashash, Y. M. A., and Liu, L. Y. (2006). “Integration of Construction As-Built Data via Laser Scanning with Geotechnical Monitoring of Urban Excavation.” Journal of Construction Engineering and Management, ASCE, 132(12), 1234–1241.

Tang, P., and Rasheed, S. H. (2013). “Simulation for characterizing a progressive registration algorithm aligning as-built 3D point clouds against as-designed models.” 2013 Winter Simulations Conference (WSC), IEEE, 3169–3180.

Tessler, S., Iwasaki, Y., Law, K. H., and Shirley Tessler, Y. I. and K. L. (1993). “Qualitative Structural Analysis Using Diagrammatic Reasoning.” The Seventh International Workshop on Qualitative Reasoning about Physical Systems, 885–891.

Vezočnik, R., Ambrožič, T., Sterle, O., Bilban, G., Pfeifer, N., and Stopar, B. (2009). “Use of terrestrial laser scanning technology for long term high precision deformation monitoring.” Sensors, 9(12), 9873–9895.

Wakefield, R. R., Nazmy, A. S., and Billington, D. P. (1991). “ANALYSIS OF SEISMIC FAILURE IN SKEW RC BRIDGE.” Journal of Structural Engineering, 117(3), 972–986.

Yang, S., Wang, C., and Chang, C. (2010). “RANSAC Matching : Simultaneous Registration and Segmentation.” Robotics and Automation (ICRA), 2010 IEEE International Conference on, 1905–1912.

Yi, T. H., Li, H. N., and Gu, M. (2013). “Experimental assessment of high-rate GPS receivers for deformation monitoring of bridge.” Measurement: Journal of the International Measurement Confederation, 46(1), 420–432.

Zeibak, R., and Filin, S. (2007). “Change detection via terrestrial laser scanning.” Proceedings of the ISPRS Workshop, 430–435.

Zogg, H.-M., and Ingensand, H. (2008). “Terrestrial Laser Scanning for Deformation Monitoring--Load Tests on the Felsenau Viaduct (CH).” International Archives of Photogrammetry and Remote Sensing, 37, 555–562.

CHAPTER 4

A QUALITATIVE SHAPE-BASED REASONING APPROACH FOR AUTOMATED CORRELATED SPATIAL CHANGE ANALYSIS OF STRUCTURES

Introduction

The previous chapter focuses on classifying the detected spatial changes of a structure as global deviations and local deformations. In this chapter, the author plans to focus on automatically identifying local deformations of structure elements connected at joints that fail to satisfy the joint equilibrium for transferring load between elements.

Three-dimensional imagery data enables analyzing detailed spatial changes of structures. However, analysis of spatial changes of the structure elements connected at joints takes significant amount of time due to the large number of joints in a structure. More specifically, engineers manually assess the geometric changes of structural elements connected at joints to comprehend how forces transferred at joints and identify anomalous load transferring due to defective structural elements. Manually analyzing the correlations of changes occurring at multiple joints is even more time consuming but necessary for comprehending structure system behaviors. This fact is due to the lack of automated methods for rapidly assessing how deformations of connected elements influence each other and support engineers in evaluating correlated changes happening across multiple joints.

Previous studies examined the use of 3D imagery data for detecting the local deformations of structure elements, but limited studies were on automatically deriving the load transferring behaviors of joints based on the detected local deformation of elements. Jose and Fernandez-Martin developed a hybrid-view method for evaluating structural

damages of damaged buildings using a volumetric analysis display for assisting in restoration planning. Such hybrid-view method can only conduct volumetric analysis but failed to accurately identify the elements under structural damages (José and Fernández-Martin 2007). Additionally, researchers developed automated algorithms that utilize the quantitative data obtained from sensors such as 3D laser scanning to model the deformed structure and then perform reverse engineering to update the Finite Element (FE) model for performing structural analysis (Cabaleiro et al. 2015). The developed algorithm relied on a polynomial surface fitting modeling approach to model the deformation of the beam, detecting the effect of torsion, and bending deflections. However, this modeling study did not focus on the detecting the effects of such deflections on the joints where the load is transferred to other connected structure elements. One of the disadvantages of using quantitative geometric data is the amount of computational load for large-scale structures such as bridges. Utilizing huge amount of quantitative geometric data often predicts several possible loading combinations that are impossible for a structural engineer to manually check every possibility.

In general, several possible load combinations can cause the observed local deformations of the structure element such as compression, tension etc. A local spatial change of an element can be either due to direct loading on that element, due to the transfer of loading from its connected element or even due to external factors such as change in temperature etc. The advantage of identifying local deformation leading to failure of the equilibrium at joints will help to systematically eliminate improbable loading combinations casing such local deformations. Figure 33 shows a deformed truss

structure under numerous probable loading possibilities predicted by the author based on the deformed shape of the structure.

Here, the author specifically focuses on deformation due to external loading. For a simple truss structure having 8 joints, 4 possible loading directions (along +ve x&y, -ve x&y), the total number of loading combinations that may lead to the observed deformed shape of the structure is 4^8 combinations. Manually checking every possible load combinations leading to the observed deformation of the truss structure causing failure of the joint equilibrium condition is tedious and sometimes becomes impractical in cases having complicated structure. Hence, there is a need for the development of a spatial change correlation technique that automatically identifies contradicting local deformations of structure elements for eliminating improbable loading combinations and aid in determining the loading behavior of the structure.

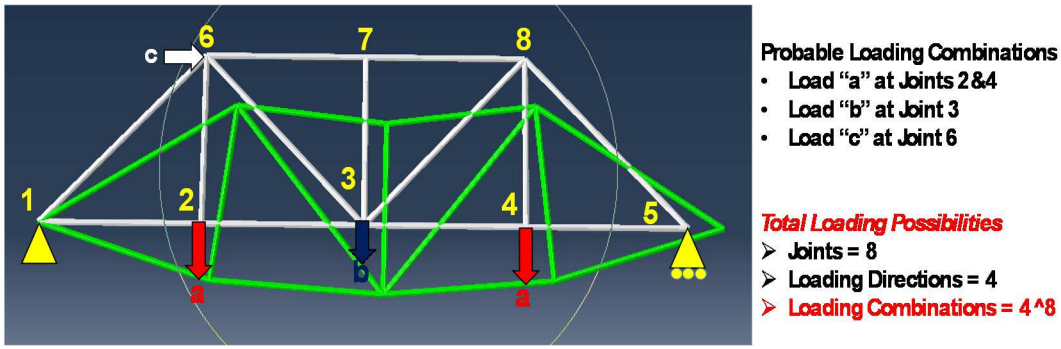

Figure 33. Probable loading combinations for deformation of a truss structure

This chapter presents a qualitative shape-based reasoning approach for automatically identifying correlation between the local deformations of connected structure element at joints. Such correlated spatial change analysis at joints can help to eliminate improbable load combinations that contradicts the joint equilibrium condition.

First, the author reviews previous studies that focused on identifying the structure systems identification and modeling studies based on the both the simulation and as-is data of the structure. Then the author describes the developed qualitative shape-representation that can help perform the joint analysis of a structure with computational efficiency. The developed qualitative shape-representation approach will help in spatial change correlation of simulated 2D truss models for identifying probable loading conditions at joints.

Literature Review

System Identification and Parameter Estimation Method to Predict Loading Condition

Recent developments in the domain of computer modeling have enabled simulating structural models that can study the dynamic behavior of a structure, material property changes of a structure, or even simulate damages due to collisions (Aghagholizadeh and Catbas 2015). Advancement in computational capabilities of computers enabled structural engineers to rigorously use the simulated structural model to analyze and predict the performance of a structure under the observed loading conditions. Based on the observed behavior of the structure, parameter identification studies update the simulation model of the structure to accurately identify the system properties (Banan and Hjelmstad 1994; Kim et al. 2012). Kim et al. investigated a highway bridge by collecting its vibration data under traffic and estimating its modal parameter (Kim et al. 2012). The modal parameter estimation study aimed to investigate the feasibility of parameter identification in the domain of structural health monitoring and damage prediction.

Banan and Hjelmstad proposed algorithms for estimating the properties of a FE model for predicting the behavior of structural systems (Banan and Hjelmstad 1994). Similarly, a research study developed an experimental case study for performing system identification of a structure under high impact loading (Kim et al. 2013). The experimental case study revealed that the systems identification framework produced similar results to that of the observed experimental results even under high impact loading. In the similar domain, Solari 1985 developed a mathematical model to predict wind loading on the building having rectangular geometry (Solari 1985). The proposed mathematical model can predict the wind load distribution that are from atmospheric turbulences and validated the proposed model by comparing the results from a previously developed research experiment that predicted wind loads on a square building model.

Several researchers developed theoretical models for predicting the behavior of structures (Banan and Hjelmstad 1994; Malek et al. 1998; Solari 1985). Such theoretical studies model building geometries, formulate the applied loading, and measure the corresponding outputs for achieving structural system identification. Majority of these studies are aimed at determining the properties of the studied structure such as dynamic frequencies, the stiffness of the elements, and identifying the severely damaged location on the structure (Adeli and Jiang 2006; Banan and Hjelmstad 1994). The advantage of using a system identification study is the ability to predict the abnormal behavior of civil infrastructures to avoid structural deterioration and loss of property (Kim et al. 2013). However, the major disadvantage of using such models is in analyzing constructed structures as these prediction models do not account for uncertainties that happen in the

real world. Mathematically modeling such uncertainties can lead to errors and improper decision-making (Gokce et al. 2013).

Structural engineers started using modeling and simulation framework studies to automatically assess a structure and predict its health. However, such system identification and parameter estimation studies lack quantification of the amount of uncertainty in predicted simulation results (Aghagholizadeh and Catbas 2015). Another disadvantage of using such techniques is the amount of computational complexity involved in simulating models of large-scale civil infrastructures. Simplified system identification methods have lower accuracy when compared to the actual behavior of the structure (Gokce et al. 2013). Hence, there is a need for the development of a computationally efficient tool that relies on the data collected onsite and accurately updates the simulated model. The following section presents the review of shape representation technique that can reduce the computational complexity in representing complicated shapes of structures.

Qualitative and Quantitative Shape Representation

Figure 34 shows an example of a quantitative and qualitative representation of a circular object. Engineers need to have a proper understanding of which representation to use for representing a change. For instance, deformation of a girder is a quantitative representation of a change, whereas the change in the direction of deformation is a qualitative representation of a change. Several researchers developed both qualitative and quantitative shape representations for performing structural analysis and deformation modeling (Fruchter et al. 1993; Museros et al. 2004; Tessler et al. 1993). Few examples of qualitative shape representations include structural mapping, reference point-based

representation, and topology-based representation and similarly few examples of quantitative shape representations include mental transformation, boundary shape representation, and pixel resolution-based shape representation (Liter 1998; Lovett and Forbus 2010).

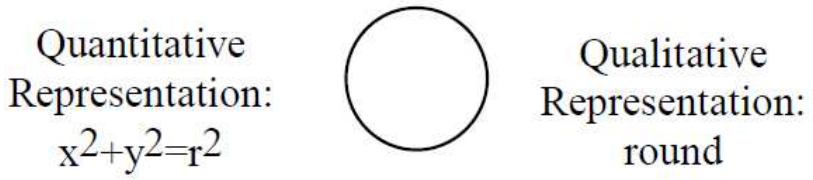

Figure 34. Quantitative Shape Representation vs. Qualitative Shape Representation

However, the major challenge lies in the computational complexity in automating the use of qualitative and quantitative shape representation technique in change analysis of large-scale civil infrastructure facilities such as bridges, water tanks, etc. Handling huge amounts of imagery data for automating the change analysis process requires large amount of manual segmentation, computational capacity, and continuous human intervention. Qualitative shape representation techniques have challenges in using relatively less information while representing a shape of a structure. For example, orientation-invariant shape representation does not take into account the direction of rotation and hence cannot be reliable in conducting accurate spatial change analysis. Similarly, quantitative analysis provides excess information, which causes problems in computational capabilities. Hence, accurately determining reliable shape representation techniques (qualitative or quantitative) for conducting efficient and effective spatial change analysis is an important task nowadays. Previous studied utilized detailed geometric data to perform modeling of the deformed elements of a structure (Cabaleiro et

al. 2014, 2015). The following section reviews few previous studies that implemented different types of deformed shape modeling techniques using 3D laser scanning data.

Deformation Modeling from LiDAR Data

Structural engineers collect geometric data of the deformed structure that helps in modeling the Finite Element (FE) model of the structure. Due to the advancements in the imaging technologies, several researchers developed automatic modeling tools to extract deformation models identified in the imagery data and calculate the amount of deformation (Armesto et al. 2010; Riveiro et al. 2013). The automatic modeling techniques help structural inspectors perform detailed structural analysis of deformed geometries of a structure with mm-level accuracy (Riveiro et al. 2013). Riveiro et al. presented a novel method for measuring the vertical under clearance of a bridge under structural inspection. The measurement results are validated by comparing the values obtained using a Total Station survey.

Recent advancements in sensor technologies enabled collecting detailed geometric data of the actual constructed structures (Luhmann et al. 2013). The author discussed several research studies in chapter 1 that started using the geometric data collected using such sensor technologies to analyze structural behaviors (José and Fernández-Martin 2007; Lindenbergh and Pfeifer 2005). The primary goal of all these previous research studies is to identify the deformation of an element and detect damages on the structure (Vezočnik et al. 2009).

Aghagholizadeh and Catbas, 2015 stated that simplification assumptions on the quantified uncertainty factors could lead to inaccurate finite element model updating (Aghagholizadeh and Catbas 2015). Creating and analyzing numerical models that are far

from the real behavior of the structure may cause poor condition assessment and structural failure. Therefore, there is a need for the development of a computationally efficient and reliable modeling approach that accurately resembles the actual behavior of the structure eventually aiding in precise finite element model updating and load prediction. In addition, the major disadvantage of using the modeling techniques is the amount of quantitative data generated after the automatic deformation shape modeling (Cabaleiro et al. 2014; Riveiro et al. 2011a). Such large amount of quantitative data creates computational complexities in performing accelerated structural behavior simulation and real-time condition assessment of structures. To achieve better computationally efficiency and reliability in load prediction analysis, the author adopted a qualitative deformation shape representation technique. The following section provides details about the qualitative shape representation technique that represents the deformed shape of a structure for performing reliable structural behavior simulation.

Qualitative Shape Representation Technique

Chapter 3 developed a spatial change classification study that recognizes local spatial changes (local deformations) by comparing two sets of 3D laser scanning data of a structure collected at different times. In this chapter, the author developed a unique qualitative shape representation to represent deformed elements of a structure. The developed shape representation first identifies the quantitative changes of an element and represents such quantitative change using a qualitative matrix representation. Such qualitative shape representation is computationally efficient that using the quantitative value of the observed change for determining the correlated local spatial changes between the connected structure elements. Figure 35 shows an example of the developed

qualitative shape representation technique for a beam element. To represent tension and compression of the beam, the technique first identifies the change in the length between the original and the deformed shape. This process will generate details about the type of deformation undergone by the beam element, which is either compression (decrease in length), or tension (increase in length) using the quantitative change of the beam element. After identifying the state of the beam element, the technique now uses a qualitative value (+1 or -1) to represent the direction of the load applied based on the displacement of the end points (joints) of the beam element.

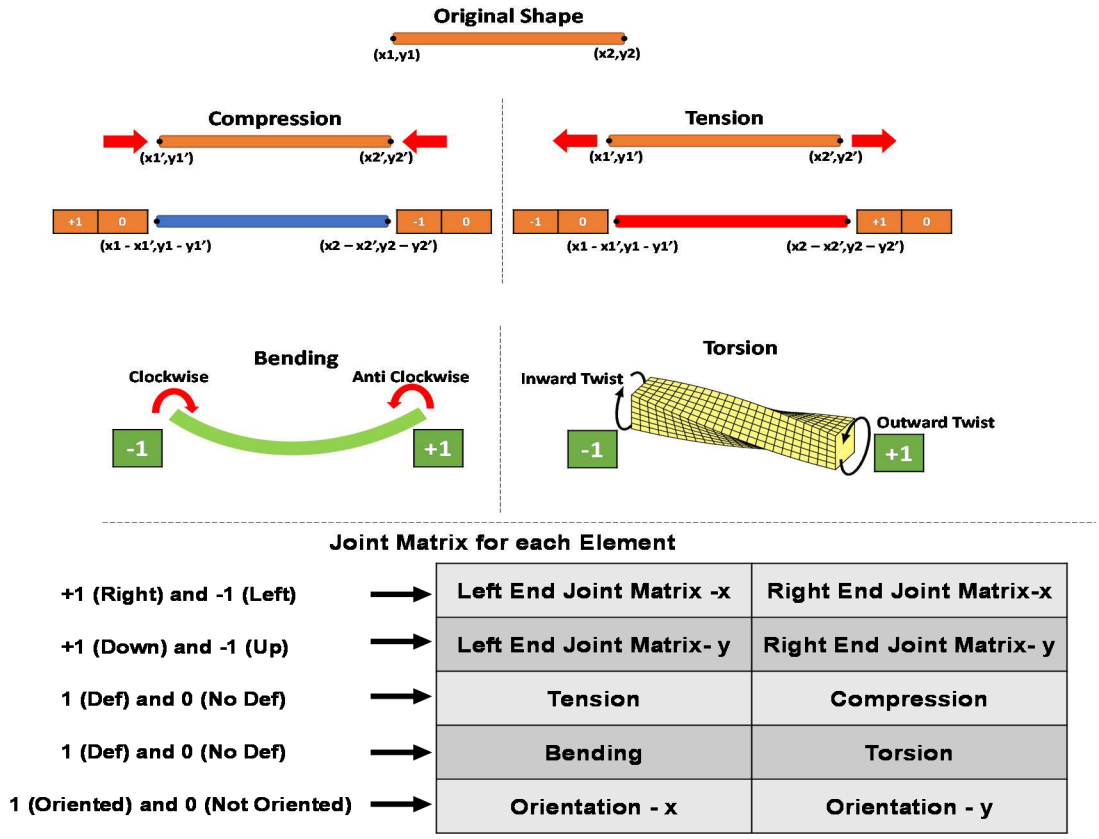

Figure 35. Developed Qualitative Shape Representation

Figure 35 shows that deformation due to compression loading can be represented using the +1 direction of loading at the left end and -1 direction of loading at the right end

of the beam element if the beam undergoes the shown displacement (left end move right and right end moves left). Similarly, this technique utilizes +1 for a clockwise rotation and -1 for an anti-clockwise rotation to represent downward bending at each end of the beam element. Therefore, the qualitative shape representation technique uses a matrix representation at each end of the beam element to represent the direction of the applied load along both the x & y direction, the local deformation that comprises of tension, compression, bending and torsion, and the orientation of the beam element. Such qualitative shape representation technique represents the most common local deformation of a beam element such as compression, tension, bending, and torsion as shown in Figure 35.

Spatial Change Correlation using Qualitative Shape Representation

The proposed qualitative shape representation technique assists in representing the observed local spatial changes (local deformations) of a structure and identifies probable loading condition applied on the structure. First, the author detects the local spatial changes of each individual element in a structure by comparing a structure's design model with its 3D laser scanning data or by comparing two sets of 3D laser scanning data collected at different time. The process of detecting the local deformation is systematically detailed in chapters 1 and 2. In this chapter, the author focuses on certain local spatial changes such as tension, compression, bending, or torsion of the elements of a structure caused due to external loading. Then the author utilizes the developed qualitative shape representation technique to qualitatively represent all the detected local spatial changes. This qualitative representation will help in simulating the most probable external loading causing the detected local spatial changes. To develop the

qualitative shape-based reasoning approach, the author studied the loading behavior of two statically determinate trusses and one statically indeterminate truss. Then the author applied the developed qualitative shape-based reasoning approach on a single span simply supported bridge under load testing. The following section provides a systematic explanation of the developed qualitative shape-based structural behavior reasoning approach.

Qualitative Shape-based Reasoning of 2D Trusses under Loading

The author designed three 2D trusses in Abaqus finite element analysis software (Dassault Systemes 2002) and analyzed them using the qualitative shape-based reasoning approach to identify the actual loading. The first 2D truss is a statically determinate truss under single point load, the second 2D truss is a statically indeterminate truss under single point load, and the third 2D truss is a statically determinate truss under multiple point loads. Here, the author first identifies the local spatial change of every element in a truss structure and apply the joint equilibrium (method of joints) at all the joints of the structure (Morgan 2015). The major principle behind the joint equilibrium condition is that it if a truss is in equilibrium, all its joints must be in equilibrium by satisfying the equilibrium equations for forces acting on the joint that are applied by the elements connected at that joint.

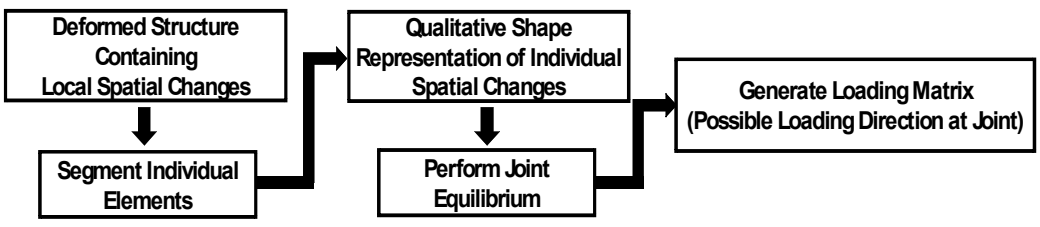

Figure 36. Qualitative shape-based reasoning of 2D trusses

Figure 36 shows the detailed systematic illustration of the process of using qualitative shape representation to identify the possible loading direction at each joint of a 2D truss. The local spatial change of an element can aid in deriving the applied forces at a joint and the qualitative shape representation can achieve joint equilibrium condition by satisfying all the applied forces. Therefore, the developed approach treats the unbalanced force on a joint as the applied external force, therefore, identifying the actual loading from the deformed truss structure. The major advantage of using the qualitative shape-based reasoning approach is that it is automatic and only utilizes the deformed shape of a truss structure to identify the most probable loading condition. In addition, if the applied loading is complicated in nature, this approach will eliminate all the improbable loading scenarios and provide a result that is closest to the actual loading condition. Hence, the developed qualitative shape-based reasoning approach acts as a reverse engineering tools to identify the most probable loading condition that caused spatial changes. This approach utilizes the deformed shape of the trusses caused due to the applied loading. These three case studies also act as a validation of the developed approach as the actual loading condition is known. The following subsections illustrate the three 2D truss case studies in detail. The author uses the statically determinate 2D truss to illustrate the methodology and discuss the results of the other two 2D trusses.

Statically Determinate Truss 1

The author designed a 2D statically determinate truss in Abaqus finite element analysis software and applied a single load on joint number 2 as shown in Figure 37. Figure 37 also shows the actual 2D truss and its deformed shape after loading. The author now utilizes the deformed shape of the 2D truss and segment into individual truss elements. The qualitative

shape representation technique now compares the shape of deformed truss elements to the undeformed truss elements to identify and qualitatively represent the local spatial changes. Figure 36 shows the qualitative shape representation of the truss elements using the joint matrices. These joint matrices help in representing the type of the local spatial change such as tension or compression. Since, a truss element is only subjected to either tension or compression, which makes all the element matrices that represent the bending/torsion of the 2D truss zero. Using all the derived joint matrices the author represented the local spatial changes using a colored truss, wherein a red color represents tension and a blue color represents compression.

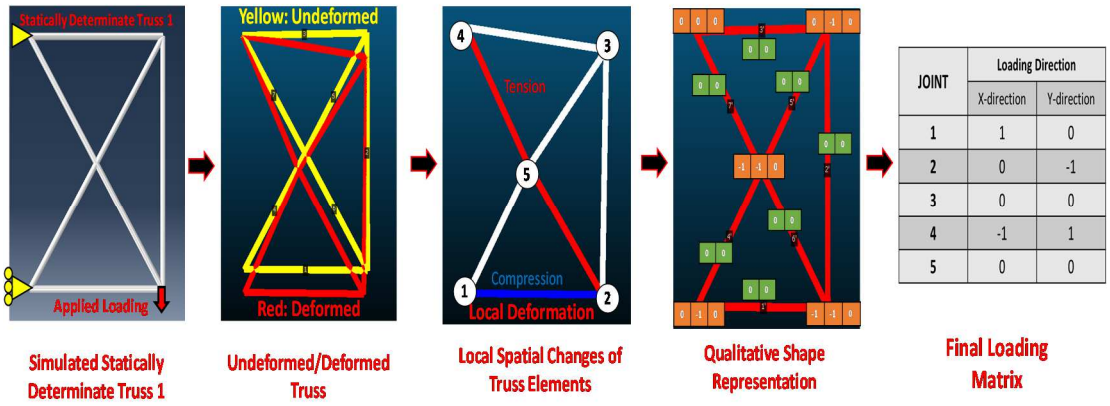

Figure 37. Determining final loading matrix of statically determinate truss 1

The developed qualitative shape-based reasoning approach uses the derived joint matrices to perform the method of joints (joint equilibrium) analysis at every joint of the 2D truss. Figure 38 shows the systematic flowchart of the developed method of joints analysis using the derived joint matrices. The main steps of the approach include; 1) generate joint matrices of all the elements; 2) identify joints having no displacement; 3) perform joint equilibrium by generating internal forces from the generated joint matrices; 4) obtain the unbalanced loading at each joint.

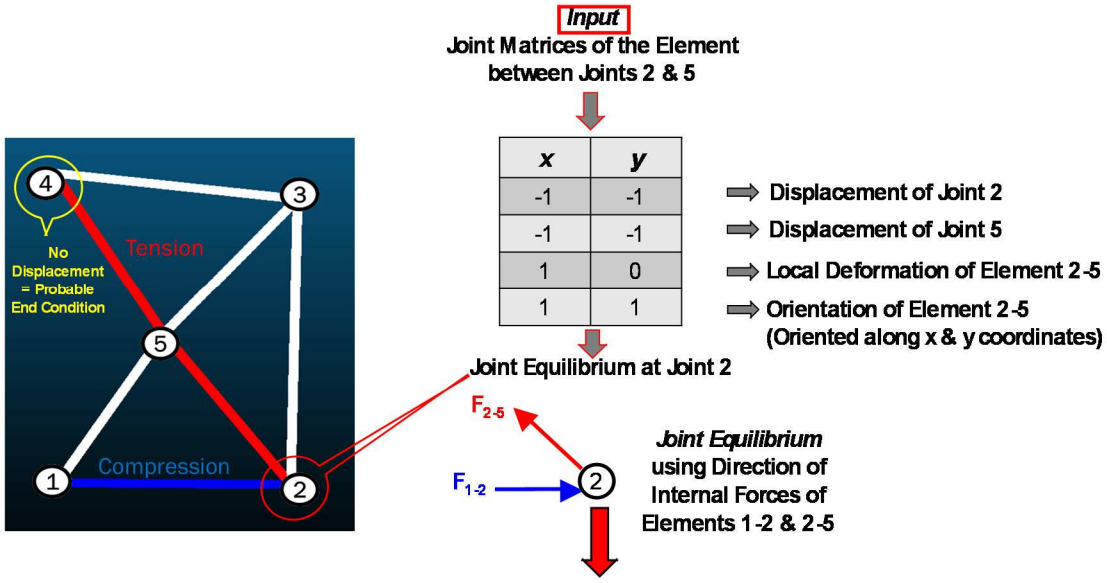

Figure 38. Joint equilibrium approach to determine unbalanced load at joint 2

The developed algorithm works using a systematic elimination process by first applying all possible loading at every joint of the 2D truss. Therefore, the algorithm applies four types of loading at every joint, namely loading along +ve x, -ve x, +ve y, and –ve y directions respectively. Initially, the inputs to the algorithm are the joint matrices of each individual element as shown in Figure 38. These joint matrices contain the information about the displacement of the ends of an element, local spatial change of an element, and the orientation of an element as shown in Figure 38. The first step in the algorithm is to identify the joints that do not have any displacement from its original place (joint 1). Next, the algorithm performs the joint equilibrium on all the joints and determines the unbalanced load. Figure 38 shows the joint equilibrium process applied at joint 2 to determine the probable loading condition (unbalanced load). Using this systematic process the algorithm identifies all unbalanced load at every joint of the 2D truss and generates a final joint loading matrix shown in Figure 37. Such joint loading matrix shows all unbalanced loads

at every joint along both x and y directions, wherein +1 represents loading along right or upward and -1 represents loading along the left or downward direction.

The final joint loading matrix (Figure 37) shows that joint 1 has an unbalanced load along –ve x direction and joint 4 has two unbalanced loads along +ve x and –ve y direction respectively. Now, the author utilizes the design information of the 2D truss to identify that these two joints are actually the supports of the truss and the obtained unbalanced loads are directions of the reaction forces. The remaining unbalanced load on joint 2 is the actual applied load along –ve y direction. Therefore, this reverse engineering approach using qualitative shape representation has accurately eliminated improbable loading combinations and reliably identified the actual loading condition of a statically determinate 2D truss. However, several real-world structures are statically indeterminate and analyzing an indeterminate structure to identify loading conditions is more complicated. The following section details the qualitative shape-based reasoning for identifying the actual loading condition of a statically indeterminate 2D truss.

Statically Indeterminate Truss 1

Figure 39 shows a statically indeterminate 2D truss structure subjected to single point load, which is derived from the previously designed determinate truss by adding an indeterminacy. The author repeats the steps performed in the previous section to extract individual joint matrices, perform joint equilibrium, and generate the final loading matrix. Figure 39 shows the detailed process involved in generating the final loading matrix of the statically indeterminate 2D truss structure. The generated final loading matrix shows that the developed approach can accurately eliminate improbable loading combinations to identify the applied point load at joint 2. Therefore, this study indicates that the

developed qualitative shape-based reasoning approach can handle analyzing indeterminate structures and aid in identifying the most probable loading that caused the local deformations of individual elements of the structure.

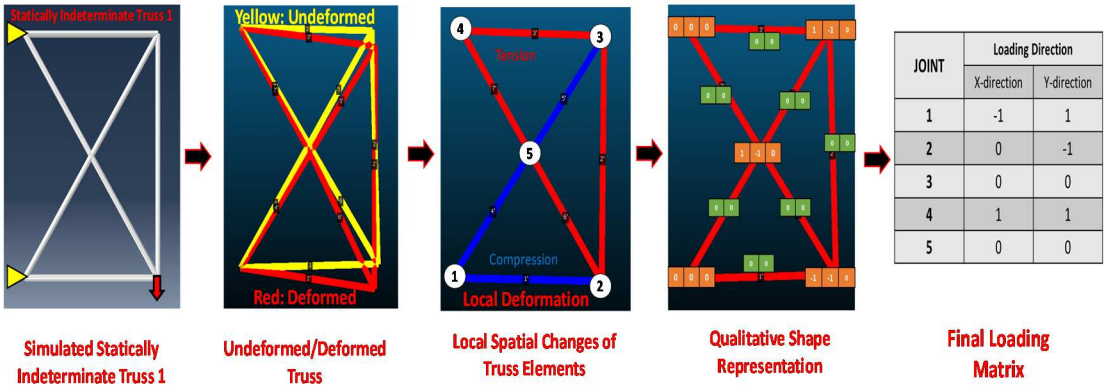

JOINT	Loading Direction	
	X-direction	Y-direction
1	-1	1
2	0	-1
3	0	0
4	1	1
5	0	0

Figure 39. Determining the final loading matrix of statically indeterminate truss 1

The author has validated that the developed qualitative shape representation technique can aid in predicting the most probable loading condition using a statistically determinate and indeterminate 2D truss structure. However, in both the case studies the trusses are under single point load. The following section validates the potential of the developed approach in determining the possible loading condition of a 2D truss subjected to multiple point loading.

Statically Determinate Truss 2

The author now implements the developed qualitative shape-based reasoning approach on a statically determinate 2D truss subjected to multiple point load as shown in Figure 40. Such implementation performed the joint equilibrium analysis using the deformed truss elements and generated a final loading matrix. However, such loading matrix shows abnormal loading detection at joints 6 and 8 respectively. This abnormality is due to the

unknown amount of the quantitative value of compression and tension forces acting at joint 6 and 7. A deformed shape of a structure cannot provide the quantitative information about the applied compression and tensile forces on the element. Therefore, the developed approach only utilizes the qualitative value of a compression or a tension force and does not take into account the quantitative value of the force, which cannot be determined using a deformed shape of the truss structure. Therefore, such qualitative analysis produces additional unbalanced loads at joints, which can be balanced using the quantitative value of the forces from the truss elements. Figure 40 highlights the abnormally detected loads at joint 6 and 8 which are unbalanced after the joint equilibrium analysis.

The major advantage of using a qualitative shape-based reasoning approach to determine loading is to remove all the improbable loading that caused the deformation in a truss structure. For instance, every joint in the 2D truss (Figure 39) has 4 possible loading directions (along +ve & -ve x direction and along +ve & -ve y direction), and this truss structure contains a total of 8 joints that makes a total 4^8 loading combinations. Manually checking every possible loading combination is tedious and becomes impossible for complex truss structures having more number of joints. However, the developed qualitative shape-based reasoning approach accurately identified the actual loading condition at joints 2,3 and 4 and generated a simplified loading combination at joint 6 and 8 that reduces the possible loading cases to 4^2. This generated loading combination is significantly smaller when compared to all the possible loading combinations on every joint (i.e. 4^2<<< 4^8).

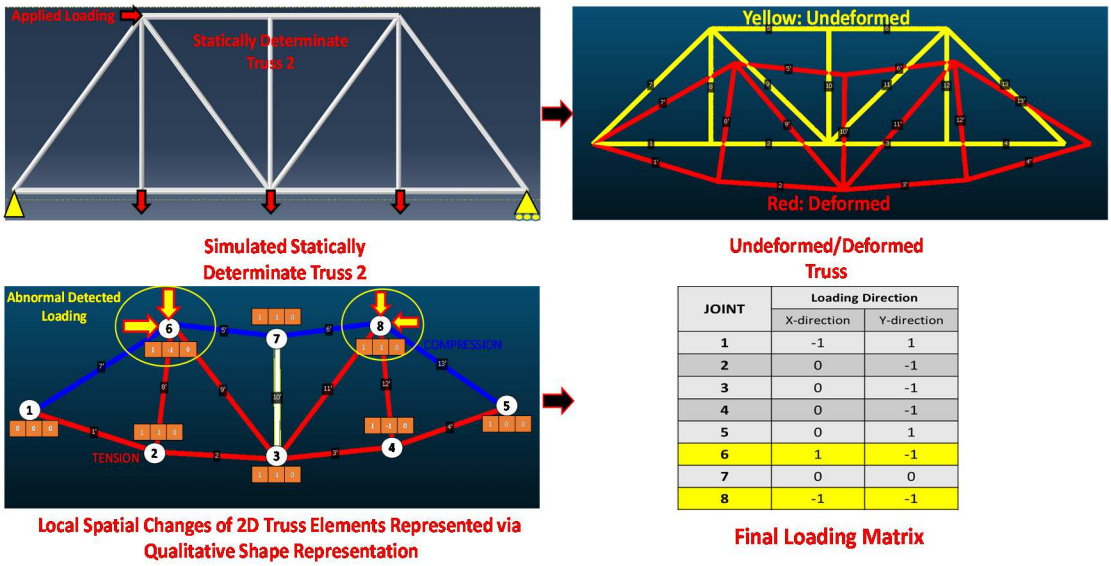

JOINT	Loading Direction	
	X-direction	Y-direction
1	-1	1
2	0	-1
3	0	-1
4	0	-1
5	0	1
6	1	-1
7	0	0
8	-1	-1

Figure 40. Determining the final loading matrix of statically determinate truss 2 (Abnormal detected load highlighted in yellow)

The developed qualitative shape-based reasoning approach accurately identified the applied load for 2D trusses subjected to single point load and generated a simplified load combination for a 2D truss subjected to multiple point loads by systematically eliminating improbable loading combinations. These three case studies validate the potential of the developed approach for use in generating the actual behavior of a structure under loading condition and significantly reducing all the probable loading combinations. Next, the author applies the developed qualitative shape-based reasoning approach on a simply supported bridge under load testing using the data collected by 3D laser scanning. 3D laser scanning will provide detailed geometric information of the deformed shape of the structure and implementing the developed approach will prove its potential in handling real-world problems as well.

Qualitative Shape-based Reasoning for Simply Supported Bridge under Load Testing

The author collected the 3D laser scanning data of a simply supported skewed bridge (Figure 41) under load testing. Figure 42 shows the top view of 3D laser scanning data, and the three types of loading scenarios (S1, S2, S3, and S4) applied on the bridge structure wherein S1 is under no loading, S2 and S3 are under 2 truck loading, and S4 is a single truck loading respectively. The aim of the author is to use the deformed shape of the simply supported bridge to automatically predict the applied truck loading.

Figure 41. Tested simply supported skewed bridge

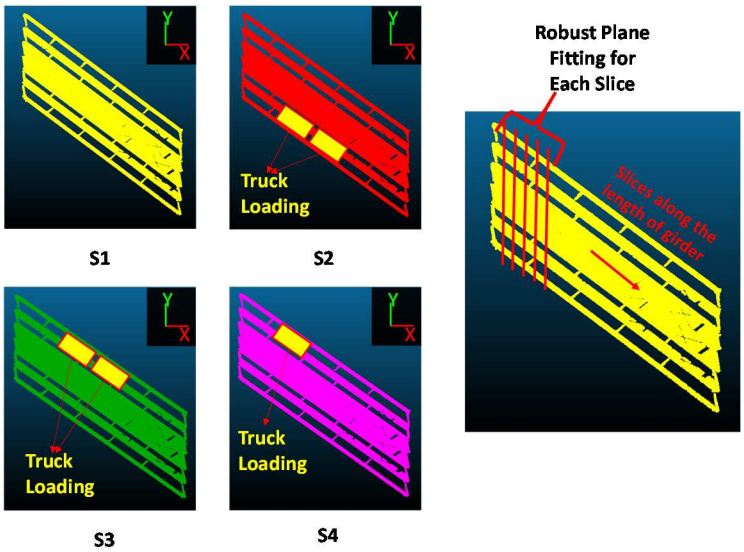

Figure 42. Load testing scenarios and plane fitting for qualitative shape representation of the bridge

The author uses the qualitative shape representation to represent the deformed shape of the bridge structure due to the applied loading. In general, the applied truck loading may cause a twist in the simply supported bridge structure, causing it to either twist inward or outward around the axis of the bridge. As shown in Figure 35, the author represents inward twist of a beam element using -1 and the outward twist of a beam element to be +1. To identify the direction of twisting of the bridge structure due to applied loading, the author first cut the 3D laser scanning data into smaller slices perpendicular to the direction of traffic as shown the Figure 42. Then the author uses a robust plane-fitting algorithm to fit a 3D plane for each of the extracted slices from the 3D laser scanning data. Such 3D planes for each of the slices will be very similar to each other in the case of loading scenario S1. However, for cases S2, S3, and S4 the robustly fitted planes will be oriented towards the deformation generating a relative angle between the planes of the generated slices. Now the author performs a one-to-one comparison between the extracted planes of S1 to the extracted planes of S2, S3, and S4 respectively to identify the change in the direction of deformation. The author now separates the planes that have a change in its direction with the planes that do not.

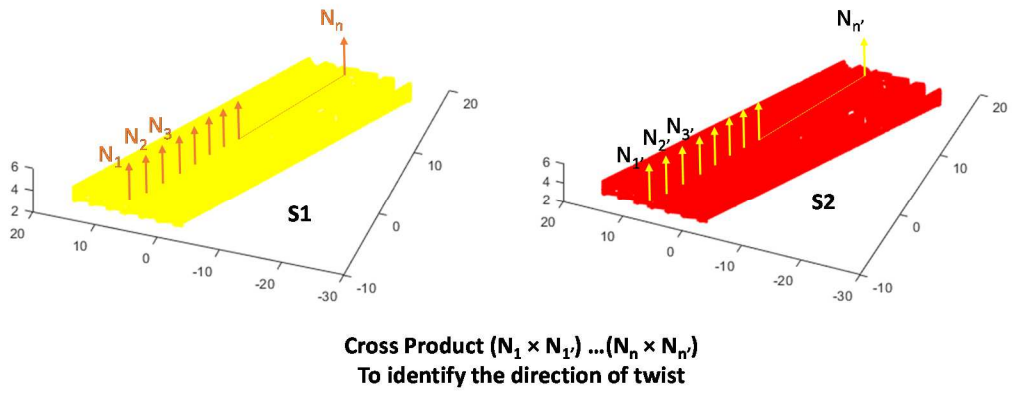

Figure 43. Normal vectors to identify the twist of bridge girder

The process of identifying the direction of deformation involves extracting the normal to all the planes that have a change in its direction from its original orientation. The author performs the cross product between undeformed planes with the planes representing the deformed shape of the bridge (Figure 43). Figure 43 shows the cross product between the extracted normal from data for S1 and S2 loading scenarios. Such cross-product analysis will provide the information about the direction of the twist of most of the planes from its original orientation to its deformed orientation. Using the developed approach the author automatically identified that the loading scenario S2 has an outward twist and the loading scenario S3, S4 has an inward twist as shown.

The qualitative shape-based representation that involves identifying the direction of the twist of the deformed shape of each loading scenario can aid in predicting the applied load on the simply supported bridge. Now, the author successfully distinguished the loading S2 with the loading scenario S3 and S4 respectively based on the direction of the twist of the bridge girder. However, using a qualitative representation cannot distinguish the loading scenarios S3 and S4 as both the loading conditions produce a similar direction of bending and twist. Therefore, the author identified the local maxima of the angles calculated between the normal of S1 versus S3 and S4 respectively. This analysis recognizes the maximum values of the calculated angles between its neighbors and identifies peaks as shown in Figure 44. As highlighted in Figure 44, the comparison identified an additional peak (for S3 loading scenario) near the area having larger angles calculated between the normal. This additional peak can actually distinguish the deformed shapes of S3 and S4 by identifying the number of peaks (local maxima) around a particular area of interest (an area having a large change in angles between the normal).

The adopted qualitative technique based on identifying the number of local maxima reliably distinguished the single truck loading in case S4 with the double truck loading in S3.

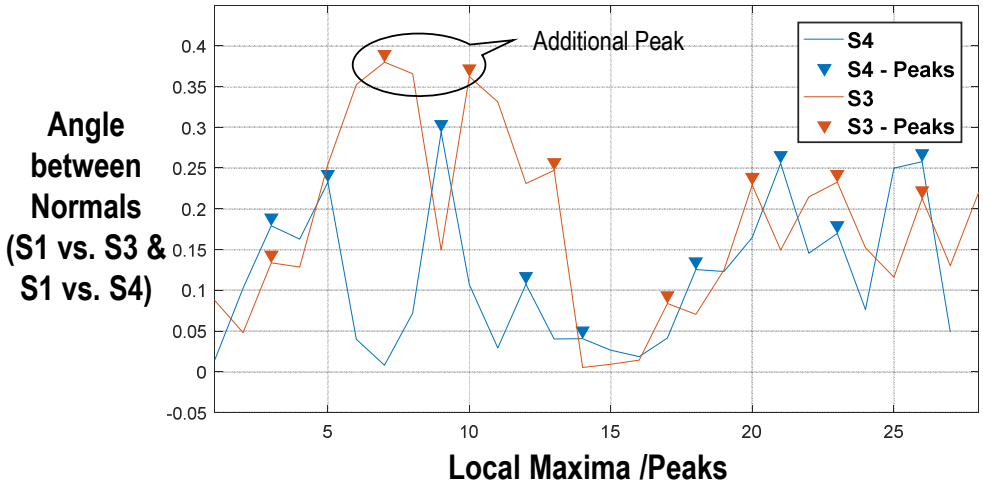

Figure 44. Local maxima comparison of angles between the normals of S1 vs. S3 and S1 vs. S4

Overall, the author accurately distinguished between all the available loading scenarios using the developed qualitative analysis technique. The major advantage of using such qualitative shape-based reasoning techniques is its computational advantage in comparing the quantitative amount of deformation under each loading scenario to identify the type of applied loading. However, the author would like to explore more types of qualitative shape-based techniques to distinguish elements of the structure under a similar type of loading and having similar shape. In future, the author plans to develop more reliable qualitative shape representation techniques that can be adopted to any complex shapes of civil infrastructures and accurately represent the applied loading causing spatial changes.

Discussion

The developed qualitative shape representation approach has several advantages over using large quantitative deformation data of an element. However, the author made few assumptions for developing this shape representation approach. Additionally, this approach also has few limitations in simulating the loading behavior of the structure, which are detailed in the following section.

Assumptions and Limitations

1. The author utilizes the deformed shape of the truss structure to identify improbable loading combinations leading to the observed spatial changes. However, in reality such deformations may not only be caused solely due to external loading but may be a result of the combination of different types of loading such as temperature changes, change in soil behavior around the structure, or change in the atmospheric humidity etc. The future work of the developed shape-based reasoning approach involves simulating different types of deformations resulting due to a function of different types of loading conditions. Such simulation models can help in recognizing the effect of the combined environmental factors and external loading on the deformation of the truss structure.
2. The author compared the as-designed shape of the truss structure with its deformed shape under loading condition. However, due to actual onsite conditions, the final as-built shape of the truss structure may not be similar to actual as-designed model of the truss before loading. The author assumes that the project manager may have built the truss structure similar to the design model and

hence the comparisons actually interpret the change due to loading rather a change that is already existed before the application of the loading.

3. The author does not consider the permanent change in the angle between the elements of the truss at every joint. The author assumes that an unloaded truss structure always maintains right angles between the elements and change its shape after the application of the load. Such assumption limits this approach to a large structure having longer elements wherein the change in the angles between the elements is generally minimum and can be ignored.
4. The major limitation of this approach is that it completely eliminates all the quantitative information available in the 3D laser scanning data. This limits the developed approach to only identify geometric shape changes and vulnerable to situations having localized defects that do not affect the shape of the structure but severely degrades the loading capacity of the element.

Directions for Future Research

Qualitative shape representation significantly reduces the amount of computational complexity, determines the geometric interactions between connected structure elements, helps to eliminate improbable loading combinations, and accelerates the simulation of structural behavior. The author proposes a relational network graph based approach that automatically updates the Finite Element model of the structure to accurately reflect the as-is loading behavior of the structure. Such relational network graph contains the qualitative representation of global deviation and local deformation of the elements of the structure to efficiently represent the as-built condition observed by comparing two sets of 3D laser scanning data of the structure collected at different times. Then the author plans

to generate the relational graph of the simulated FE model that closely represents the as-built relational graph. Such relational graph based approach will systematically eliminate improbable loading conditions causing the observed global and local deformations. The future work of the developed approach should consist of developing an automatic spatial change based structural behavior simulation framework that simulates and predicts the loading behavior of the structure. The inputs of the approach will be the as-designed model of the structure along with two sets of 3D laser scanning data of the structure collected at different times. The author proposes to develop an adaptive framework that automatically updates based on any additional 3D laser scanning data sets collected in future.

Conclusion

In general, the global deviations of the structure occur due to change in the boundary conditions of the entire structure or between the connected elements of the structure. Majority of the local deformations are caused due to change in loading condition on a structure. It is very crucial for structural engineers to identify the type of loading combination that leads to the observed local deformation of an element of the structure to simulate the actual structural behavior. Currently, structural engineers rely on qualitative information of the observed local deformations for updating the design model to reflect the as-is condition of a structure. Such methods have limitations in handling the computational complexity of large data sets and lack automation tools to identify the probable load causing the observed spatial change. In addition, manually checking every load combination that can lead to the observed change is tedious and error prone.

The author developed a qualitative shape representation technique that represents the deformed shape of each element of the structure for accelerating the simulation of

structure's loading behavior. The author implemented the developed approach on 3 simulated truss structures and eliminated improbable loading combinations for detecting the actual loading for two of the truss structures. Additionally, the developed approach significantly reduced the number of loading combinations and generated a loading matrix that can aid structural engineers to accelerate the process of structural behavior simulation.

References

Adeli, H., and Jiang, X. (2006). "Dynamic Fuzzy Wavelet Neural Network Model for Structural System Identification." Journal of Structural Engineering, 132(1), 102–111.

Aghagholizadeh, M., and Catbas, F. N. (2015). "A Review of Model Updating Methods for Civil Infrastructure Systems." Computational Techniques for Civil and Structural Engineering, (July 2016), 83–99.

Armesto, J., Roca-Pardiñas, J., Lorenzo, H., and Arias, P. (2010). "Modelling masonry arches shape using terrestrial laser scanning data and nonparametric methods." Engineering Structures, Elsevier Ltd, 32(2), 607–615.

Banan, M. R., and Hjelmstad, K. D. (1994). "Parameter Estimation of Structures from Static Response. I. Computational Aspects." Journal of Structural Engineering, 120(11), 3243–3258.

Cabaleiro, M., Riveiro, B., Arias, P., and Caamaño, J. C. (2015). "Algorithm for beam deformation modeling from LiDAR data." Measurement: Journal of the International Measurement Confederation, 76, 20–31.

Cabaleiro, M., Riveiro, B., Arias, P., Caamaño, J. C., and Vilán, J. A. (2014). "Automatic 3D modelling of metal frame connections from LiDAR data for structural engineering purposes." ISPRS Journal of Photogrammetry and Remote Sensing, International Society for Photogrammetry and Remote Sensing, Inc. (ISPRS), 96, 47–56.

Dassault Systemes. (n.d.). "Abaqus FEA." Dassault Systemes.

Fruchter, R., Law, K. H., and Iwasaki, Y. (1993). "QStruc: an approach for qualitative structural analysis." Computing Systems in Engineering, 4(2–3), 147–157.

Gokce, H. B., Catbas, F. N., Gul, M., and Frangopol, D. M. (2013). "Structural Identification for Performance Prediction Considering Uncertainties : Case Study of a Movable Bridge." Journal of Structural Engineering, 139(No. 10), 1703–1715.

José, J. S., and Fernández-Martin, J. (2007). "Evaluation of structural damages from 3D Laser Scans." XXI CIPA International …, (2002), 1–6.

Kim, C. W., Kawatani, M., and Hao, J. (2012). "Modal parameter identification of short span bridges under a moving vehicle by means of multivariate AR model." Structure and Infrastructure Engineering, 8(5), 459–472.

Kim, Y., Arsava, K. S., and El-korchi, T. (2013). "System Identification of High Impact Resistant Structures." 169–178.

Lindenbergh, R., and Pfeifer, N. (2005). "A statistical deformation analysis of two epochs of terrestrial laser data of a lock." Proc. Of Optical 3D Measurement Techniques, Vol II, Vienna, Austria, 61–70.

Liter, J. C. (1998). "The contribution of qualitative and quantitative shape features to object recognition across changes of view." Memory & cognition, 26(5), 1056–67.

Lovett, A., and Forbus, K. (2010). "Shape is like space: Modeling shape representation as a set of qualitative spatial relations." AAAI Spring Symposium Series: Cognitive Shape Processing, (Gentner 1983), 21–27.

Luhmann, T., Robson, S., Kyle, S., and Boehm, J. (n.d.). Close-range photogrammetry and 3D imaging.

Malek, A. M., Saadatmanesh, H., and Ehsani, M. R. (1998). "Prediction of failure load of R/C beams strengthened with FRP plate due to stress concentration at the plate end." ACI Structural Journal.

Morgan, G. (2015). "Analyzing a Simple Truss by the Method of Joints." <http://www.instructables.com/id/Analyzing-a-Simple-Truss-by-the-Method-of-Joints/> (Mar. 1, 2017).

Museros, L., Mar, A. Del, and Escrig, M. T. (2004). "A qualitative theory for shape representaion." Proceedings of the 18th International Workshop on Qualitative Reasoning (QR'04).

Riveiro, B., González-Jorge, H., Varela, M., and Jauregui, D. V. (2013). "Validation of terrestrial laser scanning and photogrammetry techniques for the measurement of vertical

underclearance and beam geometry in structural inspection of bridges." Measurement, Elsevier Ltd, 46(1), 784–794.

Solari, G. (1985). "Mathematical Model to Predict 3-D Wind Loading on Buildings." Journal of Engineering Mechanics, 111(2), 254–276.

Tessler, S., Iwasaki, Y., Law, K. H., and Shirley Tessler, Y. I. and K. L. (1993). "Qualitative Structural Analysis Using Diagrammatic Reasoning." The Seventh International Workshop on Qualitative Reasoning about Physical Systems, 885–891.

Vezočnik, R., Ambrožič, T., Sterle, O., Bilban, G., Pfeifer, N., and Stopar, B. (2009). "Use of terrestrial laser scanning technology for long term high precision deformation monitoring." Sensors, 9(12), 9873–9895.

CHAPTER 5

CONCLUSION AND FUTURE RESEARCH

Spatial changes originate very early in the construction process such as change between two design updates, clashes between two types of design models, changes between an updated as-designed model and the as-built data, and changes during the service period of the constructed structure. It is extremely important to periodically monitor spatial changes and understand their impact on the structural integrity of a civil infrastructure. The research conducted by the author in this dissertation focuses on identifying and understanding the impact of a spatial change by recognizing the spatial change path using spatiotemporal data collected using 3D laser scanning and as-designed models. The author first detects spatial changes between an as-designed model and an as-built data collected using 3D laser scanning. To reliably detect such spatial changes, the author developed an automatic change detection algorithm that compares the as-designed BIM and the 3D as-built laser scan model of a mechanical room of an educational building. This developed algorithm utilizes the previously developed nearest neighbor searching and integrate it with a relational graph based matching approach for achieving maximum precision and high computationally efficiency.

For validation, the author compared the developed change detection approach with the traditional nearest neighbor matching and previously developed spatial context approach. The findings reveal that the developed change detection approach is computationally efficient and maintains higher precision in cases having complex interconnected building elements packed in smaller areas. The computationally efficient change detection algorithm can accurately identify spatial changes between an as-

designed model and an as-built 3D laser scan data. Such analysis will aid in determining the quality of the construction activity and performing proactive project control.

After efficiently detecting changes between an as-designed model and an as-built 3D laser scan data, the author now understands the effect of a spatial change during the service life of the structure. The author now detects changes between two sets of 3D laser scanning data of a structure collected at different intervals and understand different types of spatial changes that originate during the service life of a structure. To identify different types of spatial changes, the author developed a spatial change classification approach that classifies the spatial changes detected between two 3D laser scanning data sets of a structure as global spatial changes (rigid body motion) and local spatial changes (element level deformation). The major advantage of classifying spatial changes is to resolve the problem of identifying mixed global and local spatial changes during the comparison process. This error in detecting the actual cause behaving a spatial change can lead to improper diagnosis of a structure and wastage of maintenance resources. The author developed a spatial change classification approach to reliably classify spatial changes of highway bridges using the data collected by 3D laser scanning.

First, the author developed a robust registration approach that utilizes unchanged features between the old and the new 3D laser scanning data sets to accurately register two sets of 3D laser scanning data collected at different intervals. The author validated the developed robust registration approach by comparing it with conventional registration approaches. After the robust registration process, the author detected the global rigid body motion (G1) of the entire bridge structure by comparing the robustly registered old and new 3D laser scanning collected in 2015 and 2016 respectively. Such process will

identify the rigid body motion of the entire bridge structure and helps in detecting the interaction between the bridge structures and its surrounding environment. Now, the author detects the global deviations of individual elements of the bridge structure (G2) to understand the relative displacement between the connected structural bridge elements. Such process will help in identifying the current state of the boundary conditions between the connected elements of the bridge structure. Finally, the author detect the local spatial changes of each individual bridge elements (L) to identify local deformations such as tension, compression, bending, and torsion of elements. Such systematic process of classifying the detected spatial changes aid in performing reliable condition assessment of the highway bridge structures and help structural engineers identify the root cause of the observed geometric deformations.

Classifying spatial changes can aid in understanding the actual cause of such change. For instance, a local deformation (L) of an individual element is primarily caused due to external loading on that element or may be due to the transfer of loading deformation from its connected element. Several previous studies developed theoretical models to predict the loading on an element of a structure. However, the major disadvantage of using such theoretical models is the fact that they account for actual changes that happen in the real world. It is extremely difficult for a structural engineering to manually check all possible loading combinations that might have caused such deformation. To significantly reduce the computational complexity and to approximately predict the most probable loading on an element, the author developed a qualitative shape-based reasoning approach for structural behavior simulation. Such shape-based reasoning approach utilizes the actual deformed shape of the structure to eliminate all

improbable loading conditions and output those that may have caused the deformation. This elimination process will significantly reduce the number of loading combinations and provide a feasible number of loading scenarios that are useful for structural engineers to perform the condition assessment of the structure. The author tested the developed approach using two statically determinate and one statically indeterminate structure subjected to single and multiple point loads and validated that the developed approach can significantly reduce the loading combinations to provide the most feasible number of loading scenarios. In addition, the author also tested the developed approach using real 3D laser scanning data of simply supported bridge under load testing. Such implementation revealed that the developed qualitative shape-based approach could aid in detecting the actual loading condition of the bridge structure, which is significantly beneficial for performing structural analysis and condition assessment.

Summary of Major Contributions

The detailed geometric information captured in the 3D laser scanning data is a huge advancement in field of civil/construction engineering to develop automation tools that significantly reduces human effort. The following section details several contributions and practical implications from the developed dissertation.

1. A computationally efficient spatial change detection approach of large-scale building systems

Project managers require intense manual effort to identify changes between the final updated as-designed model and the as-is condition of a building system. The most commonly used traditional method consists of using onsite RFI's to manually identify all the observed changes and update the design model. However, the amount of time

invested in such manual approach is significantly large and requires experienced professional to analyze all the observed changes. To automate the change detection process and significantly reduce the amount of time invested in manually detection each individual spatial change, the author developed an automatic spatial change algorithm that utilizes data captured using 3D laser scanning technology.

The inputs of the developed algorithm are an as-designed model and the 3D laser scanning data of the building system. The developed approach generates a relational network graph that provides the details about the element level deviations such as shape change, orientation change etc. Comparing the two relational graphs generated for the as-designed model and the 3D laser scanning data can systematically identify elements having spatial changes. The final output of the algorithm is a list of elements that have undergone spatial changes with respect to the as-designed model. In addition, the developed algorithm also highlights elements that are additionally included onsite that needs to be manually documented by the project manager. The major advantage of using the developed change detection algorithm is its computational efficiency in recognizing spatial changes of building system containing hundreds of elements packed in smaller spaces.

2. A robust registration algorithm for automatic and reliable geometric change detection of civil infrastructures using 3D laser scanning

Civil infrastructures undergo geometric spatial changes during their service period. Structural engineers perform periodic inspection of the structures to keep track of its changes and to accomplish structural health monitoring. Recent years saw an increase in the use of 3D laser scanning technology to collect geometric data of a structure to

understand its geometric changes. Several researchers collect 3D laser scan data of a structure at different times to detect the gradual geometric change between the data collection activities. However, the major disadvantage is that the observed geometric changes are significantly influenced by the accuracy of registering the two 3D laser scanning data sets. Improper registration may lead to detecting spatial changes that do not accurately reflect the as-is behavior of the structure.

To accurately perform the registration of two 3D laser scanning data sets collected at different times, the author developed a robust registration approach that relies on unchanged features between the two data sets. Such features can be either features on the surrounding environment of the structure (railings, road markings, banners etc.) or parts of the structure that did not have significant deviations. The robust registration approach automatically identifies unchanged features between the two 3D laser scanning data sets and performs the registration step. Such registration is robust in cases having spatial changes of objects found in the collected data sets, which significantly affect overall registration results and the results of change analysis. The inputs of this approach are two 3D laser scanning data sets of a structure collected at different times. The robust registration algorithm will automatically identify the transformation matrix required to reliably register the collected two sets of 3D laser scanning data.

3. Automated spatial change classification approach for classifying global rigid body motions, element level deviations, and element level local deformations

Spatial changes affect the structural behavior and load carrying capacity of a civil infrastructure. It is extremely important to understand the actual cause behind the observed spatial change and identify its impact on the entire structure. Currently,

structural engineers focus on localized defect detection and its impact on a particular element of the structure. In general, a spatial change of an element of a structure influences its other connected elements either causing local deformation or causing a change in the boundary condition between the connected elements. Therefore, there is need to identify and classify spatial changes based on the actual cause of such change and how such changes influence other connected elements.

The author developed a reliable spatial change classification approach that classifies all the detected spatial changes and resolves the mix of global deviations of the structure and the local deformation of the elements of the structure. The inputs of this approach are robustly registered two set of 3D laser scanning data of a structure collected at different times. The developed spatial change classification approach will identify all the spatial changes and classify them as global rigid body motion of the structure with respect to the surrounding environment, global deviations of connected elements of the structure, and local deformations of each individual elements of the structure.

4. A qualitative shape representation technique for representing complex deformed shapes of the civil infrastructure elements

Deformations of the elements of a structure are the most common type of spatial changes. These deformations include tension, compression, bending, and torsion of the elements of a structure. Structural engineers collect periodic geometric data of the element to identify its local deformation. Total Station sensors, 3D laser scanners have the capability to collect detailed geometric data of the deformed elements of the structure. The major limitation of utilizing the data collected using such technologies is the amount of computational complexity involved in analyzing the deformations of the structure and

updating the Finite Element model for reflecting the deformed shape of the element. Additionally, the amount of quantitative data generated after each investigation is large and requires intense computational capabilities for performing change analysis and FE model updating.

The author developed a novel qualitative shape representation technique that accurately represents the deformed shape of all the elements of a structure. The developed technique compares the actual shape of the element with its corresponding deformed shape to generate a qualitative representation that represents the probable type of loading that may have cause the observed deformation. Such qualitative shape representation significantly increase the efficiency of FE model updating based on as-is data collected using 3D laser scanning and helps in simulating the actual structural behavior. The major advantage of utilizing such qualitative shape representation is it significantly reduces the number of probable loading combinations causing the deformed shape of an element that a structural engineer has to check manually.

Recommended Future Research

In future, the author plans to develop a comprehensive spatial change analysis framework that analyzing complex civil infrastructures at different phases of construction and service period. The author plans to integrate geometric data extracted from BIM, 2D and 3D imagery data to perform construction progress monitoring, adaptive tolerance analysis, computationally efficient finite element updating, and systems identification of a civil infrastructure. Figure 45 shows the overall vision of the spatial change analysis framework that utilizes the developed change detection, classification, and interpretation principles from this dissertation.

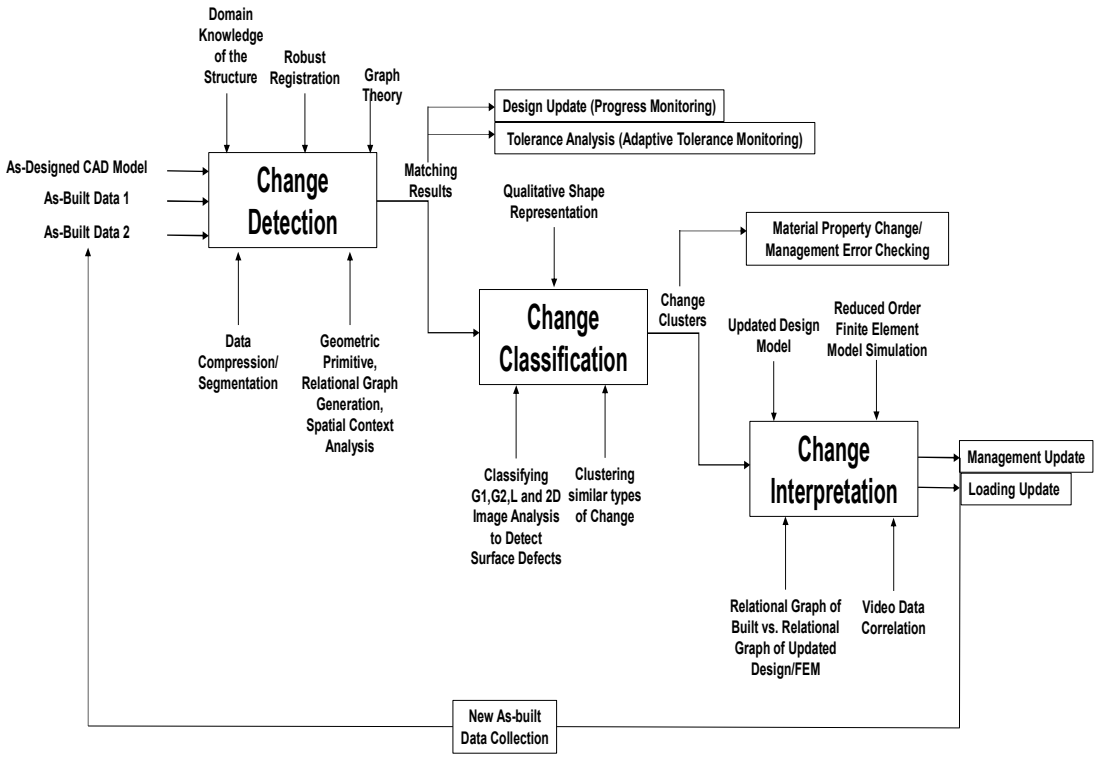

Figure 45. Vision for the automated spatial change analysis framework

Automatic Change Analysis Framework for Structural Health Monitoring of Highway Bridges

Large-scale civil infrastructures require periodic structural health monitoring that is reliable and accurately predicts the deterioration patterns of the structure. Structural engineers conduct periodic investigations of civil infrastructures and regularly update the Finite Element model to simulate and predict its structural behavior. Such periodic investigations include multiple experienced personal, several data collection activities, data exchanges, and significant manual work. The major limitation of such traditional structural health monitoring techniques is the large amount of time and resources invested to complete the analysis of a single structure. Additionally, such intense manual work and coordination between multiple personal will create several errors in decision-making and

wastage of resources. Structural health monitoring domain lack reliable automation tools that automatically detect, analyze, and predict defects on a structure. The future work of the dissertation involves developing a change analysis framework that automatically identifies spatial changes of a structure, classifies the detected spatial changes based on its actual cause, identifies the relationship between the spatial change and the structures loading condition, and accurately predicts the health of the structure based on its current condition assessment.

The author proposes a 3D imagery data driven change analysis framework (Figure 43) that first utilizes a scan planning based data collection activities to collect detailed laser scanning data of a structure at different time intervals. Then the framework uses an automatic change detection algorithm to identify all the spatial changes of the structure. The automatic change detection algorithm is computationally efficient and requires minimal human intervention. Next, the change analysis framework classifies the detected spatial changes as rigid body motion of the entire structure, element level global deviations, and element level local deformations. Such classification will significantly improve the change analysis study by identify the actual cause behind the observed spatial change. Finally, the proposed change analysis framework utilizes a qualitative shape representation technique to represent all the classified spatial changes and generate a relational network graph. Such relational network graph represents all the observed and classified spatial changes of a structure between the two data sets collected at different time intervals. In addition, the generated relational graph will act as an input to the Finite Element model of the structure to accurately simulate the as-is condition of the structure and predict its structural behavior. This automatic 3D data driven change-based framework can

significantly reduce human involvement, improve the accuracy of the assessment results, and reduce wastage of resources.

Automated Tolerance Analysis of Building Systems for Accelerated Construction using Adaptive 3D Imaging Technology

Accelerated constructions also bring challenges of "fit-up:" misalignments between components can occur due to less detailed tolerance assessments of components. Conventional tolerance checking approaches, such as manual mock-up, cannot provide detailed geometric assessments in a timely manner. The author proposes an the integration of an adaptive 3D imaging and spatial pattern analysis methods to achieve detailed and frequent "fit-up" analysis of prefabricated components. The adaptive 3D imaging methods progressively adjust imaging parameters of a laser scanner according to the geometric complexities of prefabricated components captured in data collected so far. The spatial pattern analysis methods automatically analyze deviations of prefabricated components from as-designed models to derive tolerance networks that capture relationships between tolerances of components and identify risks of misalignments.

After capturing detailed 3D geometric information, deriving tolerance information of the prefabricated components is tedious. It requires intense manual data processing to interpret the captured data. The author proposes an automated framework that identifies the deviations of the as-built geometries from as-designed conditions and generates a tolerance network to understand how prefabrication and installation errors of components influence each other. The generated tolerance network represents components as its nodes and the connections (joints) between components as edges joining those nodes. Every node (vertex) contains the "local attributes" about prefabrication errors of the object such

as deviations in lengths; radii etc., while the edge joining the vertices contain the "global attributes" about installation errors around joints. More specifically, the global attributes associated to edges include the relative orientation between the adjacent vertices (components) and the position of the edge (Joint) with respect to the origin. Tolerance networks have the potential to aid engineers to identify critical components that has higher impacts on error propagation and misalignments in field assemblies. These critical components act as the centers of a network and their prefabrication/installation errors will cascade throughout the interconnected network. Hence, identifying such regions prior to the construction process helps in maintaining the stability of the construction workflow and significantly reduces reworks and wastes.

Rapid Video-Driven Remote Assessment of Civil Infrastructures

The free vibration of bridge and patterns in bridge-vehicle dynamic interactions can help signify decaying components of bridges and predict structural risks. Traditional methods, including contact sensors, Laser vibrometers, and videogrammetric algorithms, often require a time-consuming process of manual interpretation to identify anomalous vibration modes that imply underlying defects. Engineers can hardly examine all possible correlations between vibration modes and various decay possibilities, because the number of combinations of vibration modes and possible deterioration conditions is exponentially large. The author proposes an assessment approach that can automatically correlate the vibrations of bridge components captured in videos through an algorithm that automatically update a numerical simulation model of the bridge based on video analyses. An algorithm then simulates various scenarios using the Finite Element

Analysis Model of the bridge, thereby determines the most likely as-is condition as those that produce similar vibrations extracted from videos.

To develop the video-driven remote assessment technique, the author proposes a constrained experiments study on a simple frame. The author plans to build a simple frame structure, apply known loading, collected short video data, and extract the displacement of the frame from the video data under the applied loading. Using the video magnification technique developed in (Chen et al. 2015), the author derive the minute displacements of the bridge piers. A Finite Element Analysis (FEA) model of the frame provides several vibration modes of the structure along with the information about the correlations between the vibrations of the frame's connected components. The author use the correlation between the natural frequency modes of the frame extracted from both the FE analysis and motion magnified video data to automatically predict the actual applied loading. Such video data driven frequency correlated analysis can aid in performing rapid remote assessment large structures such as bridge to identify anomalous loading conditions.

A Structural Model Simplification and Imagery Reduction Framework for Real-time Condition Diagnosis

Recent increase in the use of imaging sensors brings opportunities of detailed condition assessment of bridges. Compared with existing diagnosis techniques, imagery-data based structural health monitoring can achieve detailed measurements of the deformations of bridges without installing large number of contact sensors. Unfortunately, processing terabytes of imageries collected in field often involves hours of computation, making real-time condition diagnosis unrealistic. The author proposes a

structural model simplification and imagery reduction framework to enable real-time data-driven condition diagnosis of large-scale civil infrastructures. The structural model simplification technique simplifies a detailed Finite Element (FE) Model of the structure for reducing the computational complexity without losing critical information necessary for identifying structural defects. Such simplification involves reducing the degree of freedoms or changing certain parameters of a specific component that significantly reduces the computational time of the FE analysis while producing results that are still acceptable for supporting reliable diagnosis of structure. Comparing as-designed model with LiDAR imagery data can identify critical parts having large deviations that need denser imageries. Using the comparison results, the author plan to develop a 3D laser scanning data compression technique that focuses and increase the data density on the identified critical parts and compresses parts of the 3D laser scanning data are does not require higher data density for computation. Such process can potentially achieve real-time data-driven simulation. Therefore, such real-time simulation based on simplified FE model can guide a data reduction process that plans the imagery data collection to focus on those critical components of a structure that tend to undergo geometric deviations or changes.

REFERENCES

Abu-Yosef, A. E. (2013). "Development of Non-Contact Passive Wireless Sensors for Detection of Corrosion in Reinforced Concrete Bridge Decks."

ACSE. (2013). "Report Card for America's Infrastructure." *American Society fo Civil Engineers*, (March), 1–74.

Adeli, H., and Jiang, X. (2006). "Dynamic Fuzzy Wavelet Neural Network Model for Structural System Identification." *Journal of Structural Engineering*, 132(1), 102–111.

Agdas, D., Rice, J. A., Martinez, J. R., and Lasa, I. R. (2012). "Comparison of Visual Inspection and Structural-Health Monitoring As Bridge Condition Assessment Methods." *Journal of Performance of Constructed Facilities*, 26(4), 371–376.

Aghagholizadeh, M., and Catbas, F. N. (2015). "A Review of Model Updating Methods for Civil Infrastructure Systems." *Computational Techniques for Civil and Structural Engineering*, (July 2016), 83–99.

"AIA Homepage - The American Institute of Architects." (1857). <http://www.aia.org/> (Nov. 4, 2014).

Akinci, B., and Boukamp, F. (2003). "Representation and Integration of As-Built Information to IFC Based Product and Process Models for Automated Assessment of As-Built Conditions." *Proceedings of 19th International Symposium on Automation and Robotics in Construction*, IAARC, Washington, D.C., 543–550.

Akinci, B., Boukamp, F., Gordon, C., Huber, D., Lyons, C., and Park, K. (2006). "A formalism for utilization of sensor systems and integrated project models for active construction quality control." *Automation in Construction*, 15(2), 124–138.

Antova, G. (2015). "Registration Process of Laser Scan Data in the Field of Deformation Monitoring." *Procedia Earth and Planetary Science*, 15, 549–552.

Armesto, J., Roca-Pardiñas, J., Lorenzo, H., and Arias, P. (2010). "Modelling masonry arches shape using terrestrial laser scanning data and nonparametric methods." *Engineering Structures*, Elsevier Ltd, 32(2), 607–615.

ASCE. (2012). "Failure to act: the economic impact of current investment trends in water and wastewater treatment infrastructure." 61.

Azhar, S., Nadeem, A., Mok, Y. N. J., and Leung, H. Y. B. (2008). "Building Information Modeling (BIM): A New Paradigm for Visual Interactive Modeling and Simulation for Construction Projects." *First International Conference on Construction in Developing Countries (ICCIDC–I)*, 435.

Banan, M. R., and Hjelmstad, K. D. (1994). "Parameter Estimation of Structures from Static Response. I. Computational Aspects." *Journal of Structural Engineering*, 120(11), 3243–3258.

Barnea, S., and Filin, S. (2008). "Keypoint based autonomous registration of terrestrial laser point-clouds." *ISPRS Journal of Photogrammetry and Remote Sensing*, 63(1), 19–35.

Basharat, A., Catbas, N., and Mubarak Shah. (2005). "A Framework for Intelligent Sensor Network with Video Camera for Structural Health Monitoring of Bridges." *Third IEEE International Conference on Pervasive Computing and Communications Workshops*, IEEE, 385–389.

Beskhyroun, S., Wegner, L. D., and Sparling, B. F. (2011). "New methodology for the application of vibration-based damage detection techniques." *Structural Control and Health Monitoring*, (May 2011), n/a-n/a.

Bosché, F. (2010). "Automated recognition of 3D CAD model objects in laser scans and calculation of as-built dimensions for dimensional compliance control in construction." *Advanced Engineering Informatics*, 24(1), 107–118.

Bosché, F., Ahmed, M., Turkan, Y., Haas, C. T., and Haas, R. (2015). "The value of integrating Scan-to-BIM and Scan-vs-BIM techniques for construction monitoring using laser scanning and BIM: The case of cylindrical MEP components." *Automation in Construction*, Elsevier B.V., 49, 201–213.

Bosché, F., Guillemet, A., Turkan, Y., Haas, C. T., and Haas, R. (2014). "Tracking the Built Status of MEP Works: Assessing the Value of a Scan-vs-BIM System." *Journal of Computing in Civil Engineering*, American Society of Civil Engineers, 28(4), 5014004.

Briaud, L., and Diederichs, R. (2007). "Bridge Testing." *Nondestructive Testing (NDT)*, 1–4.

Cabaleiro, M., Riveiro, B., Arias, P., and Caamaño, J. C. (2015). "Algorithm for beam deformation modeling from LiDAR data." *Measurement: Journal of the International Measurement Confederation*, 76, 20–31.

Cabaleiro, M., Riveiro, B., Arias, P., Caamaño, J. C., and Vilán, J. A. (2014). "Automatic 3D modelling of metal frame connections from LiDAR data for structural engineering purposes." *ISPRS Journal of Photogrammetry and Remote Sensing*, International Society for Photogrammetry and Remote Sensing, Inc. (ISPRS), 96, 47–56.

Caetano, E., and Cunha, A. (2003). "Ambient Vibration Test and Finite Element Correlation of the New Hintze Ribeiro Bridge." *21st IMAC Conference & Exposition 2003*, 0–6.

Cai, H., and Rasdorf, W. (2008). "Modeling Road Centerlines and Predicting Lengths in 3-D Using LIDAR Point Cloud and Planimetric Road Centerline Data." *Computer-Aided Civil and Infrastructure Engineering*, 23(3), 157–173.

Chang, P. C., Flatau, A., and Liu, S. C. (2003). "Review Paper: Health Monitoring of Civil Infrastructure." *Structural Health Monitoring*, 2(3), 257–267.

Chen, J. G., Wadhwa, N., Cha, Y., Durand, F., Freeman, W. T., and Buyukozturk, O. (2015). "Modal identification of simple structures with high-speed video using motion magnification." *Journal of Sound and Vibration*, Elsevier, 345, 58–71.

Chen, L., Lin, L., Cheng, H., and Lee, S. (2010). "Change Detection of Building Models." *Symposium A Quarterly Journal In Modern Foreign Literatures*, XXXVIII, 121–126.

Clarkson, K. L. (2006). "Nearest-neighbor searching and metric space dimensions." *Nearest-Neighbor Methods for Learning and Vision: Theory and Practice*, (April), 15–59.

ClearEdge 3D. (2011). "EdgeWise Plant Suite | ClearEdge 3D."

Committee, I. B. M. (2012). "Report--Overview of Existing Bridge Management Systems." *Available at IABMAS website*.

Cosser, E., Roberts, G. W., Meng, X., and Dodson, A. H. (2003). "Measuring the dynamic deformation of bridges using a total station." *Proceedings, 11th FIG Symposium on Deformation Measurements*, (Meng 2002), 605–612.

Cross, E. J., Koo, K. Y., Brownjohn, J. M. W., and Worden, K. (2012). "Long-term monitoring and data analysis of the Tamar Bridge." *Mechanical Systems and Signal Processing*, 35, 16–34.

Dassault Systemes. (2002). "Abaqus FEA." *Dassault Systemes*.

Deruyter, G. (2013). “Risk Assessment: A Comparison between the Use of Laser Scanners and Total Stations in a Situation Where Time Is the Critical Factor.” *13th SGEM GeoConference on Informatics, Geoinformatics And Remote Sensing*, 687–694 pp.

Elliot, N. (2015). “Using Principal Components Analysis to determine the best fitting plane from locations in a #PointCloud | Garrett Asset Management.” *New York Tech Journal*, <https://elliotnoma.wordpress.com/2015/09/29/using-principal-components-analysis-to-determine-the-best-fitting-plane-from-locations-in-a-point-cloud/> (Mar. 7, 2017).

Erickson, M. S., Bauer, J. J., and Hayes, W. C. (2013). “The Accuracy of Photo-Based Three-Dimensional Scanning for Collision Reconstruction Using 123D Catch.” *System*.

“FARO Laser Scanner Software - SCENE - Overview.” (2010). <http://www.faro.com/en-us/products/faro-software/scene/overview> (Mar. 12, 2015).

Fröhlich, C., and Mettenleiter, M. (2004). “Terrestrial laser scanning–new perspectives in 3D surveying.” *Laser-Scanners for Forest and Landscape Assessment ISPRS*, 7–13.

Fruchter, R., Law, K. H., and Iwasaki, Y. (1993). “QStruc: an approach for qualitative structural analysis.” *Computing Systems in Engineering*, 4(2–3), 147–157.

Gentle, J. E. (2007). *Matrix Algebra: theory, computations, and applications in statistics*. *Books.Google.Com*.

Geosystems, L. (2006). “‘Leica Cyclone 5.4 Technical Specifications.’ product literature.”

Girardeau-Montaut, D. (2011). “CloudCompare-Open Source project.” *OpenSource Project*.

Girardeau-Montaut, D., and Roux, M. (2005). “Change detection on points cloud data acquired with a ground laser scanner.” *International Archives of Photogrammetry, Remote Sensing and Spatial Information Sciences*, 36, W19.

Gokce, H. B., Catbas, F. N., Gul, M., and Frangopol, D. M. (2013). “Structural Identification for Performance Prediction Considering Uncertainties : Case Study of a Movable Bridge.” *Journal of Structural Engineering*, 139(No. 10), 1703–1715.

Goor, B. Van. (2011). “Change detection and deformation analysis using Terrestrial Laser Scanning.” *Master Thesis*.

Green, M. F., and Cebon, D. (1994). "Dynamic Response of Highway Bridges to Heavy Vehicle Loads: Theory and Experimental Validation." *Journal of Sound and Vibration*, 170(1), 51–78.

Guo, H., Xiao, G., Mrad, N., and Yao, J. (2011). "Fiber optic sensors for structural health monitoring of air platforms." *Sensors*, 11(4), 3687–3705.

Gvili, R. (2010). "Iterative Closest Point." *Insight*.

Han, S., Lee, S., and Peña-Mora, F. (2012). "Identification and Quantification of Non-Value-Adding Effort from Errors and Changes in Design and Construction Projects." *Journal of Construction Engineering and Management*, 138(1), 98–109.

Hao, Q., Shen, W., Neelamkavil, J., and Thomas, R. (2008). "Change Management in Construction Projects." *CIB W78 International Conference on Information Technology in Construction*, 1–11.

Hindmarch, H., Gale, A., and Harrison, R. (2010). "A Proposed Construction Design Change Management Tool To Aid in Making Informed Design Decisions." *26th Annual Association of Researchers in Construction Management Conference*, (September), 21–29.

Hobbs, B., and Tchoketch Kebir, M. (2007). "Non-destructive testing techniques for the forensic engineering investigation of reinforced concrete buildings." *Forensic Science International*, 167(2–3), 167–172.

Hsiao, K., Liu, J., Yu, M., and Tseng, Y. (2004). "Change detection of landslide terrains using ground-based LiDAR data." *XXth ISPRS Congress, Istanbul, Turkey, Comission VII*, VII, 1–5.

Innovmetric Software. (2016). "PolyWorks | InnovMetric Software." <http://www.innovmetric.com/en/about/about-innovmetric>.

José, J. S., and Fernández-Martin, J. (2007). "Evaluation of structural damages from 3D Laser Scans." *XXI CIPA International ...*, (2002), 1–6.

Kalasapudi, V. S., and Tang, P. (2015a). "Condition Diagnostics of Steel Water Tanks Using Correlated Visual Pattern." *5th Internaltional COnstruction Specialtiy Conference*, ICSC15 – The Canadian Society for Civil Engineering's 5th International/11th Construction Specialty Conference.

Kalasapudi, V. S., and Tang, P. (2015b). "Automated Tolerance Analysis of Curvilinear

Components Using 3D Point Clouds for Adaptive Construction Quality Control." *Computing in Civil Engineering 2015*, American Society of Civil Engineers, Reston, VA, 57–65.

Kalasapudi, V. S., Tang, P., and Turkan, Y. (2014a). "Toward Automated Spatial Change Analysis of MEP Components Using 3D Point Clouds and As-Designed BIM Models." *2014 2nd International Conference on 3D Vision*, IEEE, 145–152.

Kalasapudi, V. S., Tang, P., Zhang, C., Diosdado, J., and Ganapathy, R. (2014b). "Adaptive 3D Imaging and Tolerance Analysis of Prefabricated Components for Accelerated Construction." *Proceeding of the 3rd International Conference on Sustainable, Design, Engineering and Construction (ICSDEC 2014)*.

Kim, C. W., Kawatani, M., and Hao, J. (2012). "Modal parameter identification of short span bridges under a moving vehicle by means of multivariate AR model." *Structure and Infrastructure Engineering*, 8(5), 459–472.

Kim, M.-K., Sohn, H., and Chang, C.-C. (2014). "Automated dimensional quality assessment of precast concrete panels using terrestrial laser scanning." *Automation in Construction*, Elsevier B.V., 45, 163–177.

Kim, Y., Arsava, K. S., and El-korchi, T. (2013). "System Identification of High Impact Resistant Structures." 169–178.

Koh, B. H., and Dyke, S. J. (2007). "Structural health monitoring for flexible bridge structures using correlation and sensitivity of modal data." *Computers and Structures*, 85(3–4), 117–130.

Kovačič, B., Kamnik, R., Štrukelj, A., and Vatin, N. (2015). "Processing of signals produced by strain gauges in testing measurements of the bridges." *Procedia Engineering*, 800–806.

Langroodi, B. P., and Staub-French, S. (2012). "Change Management with Building Information Models: A Case Study." *Construction Research Congress 2012*, American Society of Civil Engineers, Reston, VA, 1182–1191.

Lattanzi, D., and Miller, G. R. (2012). "Robust Automated Concrete Damage Detection Algorithms for Field Applications." *Journal of Computing in Civil Engineering*, (April), 120917010504009.

Lee, H. M., and Hyo, S. P. (2013). "Stress Estimation of Beam Structures Based on 3D Coordinate Information from Terrestrial Laser Scanning." *Proceedings of the Third*

International Conference on Control, Automation and Systems Engineering, Atlantis Press, Paris, France, (Case), 81–83.

Lee, J., Son, H., Kim, C., and Kim, C. (2013). "Skeleton-based 3D reconstruction of as-built pipelines from laser-scan data." *Automation in Construction*, Elsevier B.V., 35, 199–207.

Liang-Chien, C. (2010). "Change detection of building models from aerial images and lidar data." *International Society for Photogrammetry and Remote Sensing TC VII Symposium*, 121–126.

Lindenbergh, R., and Pfeifer, N. (2005). "A statistical deformation analysis of two epochs of terrestrial laser data of a lock." *Proc. Of Optical 3D Measurement Techniques, Vol II, Vienna, Austria*, 61–70.

Liter, J. C. (1998). "The contribution of qualitative and quantitative shape features to object recognition across changes of view." *Memory & cognition*, 26(5), 1056–67.

Lovett, A., and Forbus, K. (2010). "Shape is like space: Modeling shape representation as a set of qualitative spatial relations." *AAAI Spring Symposium Series: Cognitive Shape Processing*, (Gentner 1983), 21–27.

Luhmann, T., Robson, S., Kyle, S., and Boehm, J. (2013). *Close-Range Photogrammetry and 3D Imaging*. *Close-Range Photogrammetry and 3D Imaging*.

Mabsout, M. E., Tarhini, K. M., Frederick, G. R., and Tayar, C. (1997). "Finite-Element Analysis of Steel Girder Highway Bridges." *Journal of Bridge Engineering*, 2(3), 83–87.

Malek, A. M., Saadatmanesh, H., and Ehsani, M. R. (1998). "Prediction of failure load of R/C beams strengthened with FRP plate due to stress concentration at the plate end." *ACI Structural Journal*.

Maragakis, E. A., and Jennings, P. C. (1989). "Analytical models for the rigid body motions of skew bridges." *Mathematical and Computer Modelling*, 12(3), 377.

Monserrat, O., and Crosetto, M. (2008a). "Deformation measurement using terrestrial laser scanning data and least squares 3D surface matching." *ISPRS Journal of Photogrammetry and Remote Sensing*, 63(1), 142–154.

Monserrat, O., and Crosetto, M. (2008b). "Deformation measurement using terrestrial laser scanning data and least squares 3D surface matching." *ISPRS Journal of*

Photogrammetry and Remote Sensing, 63(1), 142–154.

Moore, M., Phares, B., Graybeal, B., Rolander, D., and Washer, G. (2001). "Reliability of Visual Inspection for Highway Bridges." *Journal of Engineering Mechanics*, II(FHWA-RD-01-020), 486.

Morgan, G. (2015). "Analyzing a Simple Truss by the Method of Joints." <http://www.instructables.com/id/Analyzing-a-Simple-Truss-by-the-Method-of-Joints/> (Mar. 1, 2017).

Mosalam, K. M., Takhirov, S. M., and Park, S. (2014). "Applications of laser scanning to structures in laboratory tests and field surveys." *Structural Control & Health Monitoring*, 21(1), 115–134.

Moschas, F., and Stiros, S. (2011). "Measurement of the dynamic displacements and of the modal frequencies of a short-span pedestrian bridge using GPS and an accelerometer." *Engineering Structures*, 33(1), 10–17.

Museros, L., Mar, A. Del, and Escrig, M. T. (2004). "A qualitative theory for shape representaion." *Proceedings of the 18th International Workshop on Qualitative Reasoning (QR'04)*.

Nahangi, M., and Haas, C. T. (2014). "Automated 3D compliance checking in pipe spool fabrication." *Advanced Engineering Informatics*, 360–369.

Olsen, M. J., Kuester, F., Chang, B. J., and Hutchinson, T. C. (2009). "Terrestrial Laser Scanning-Based Structural Damage Assessment." *Journal of Computing in Civil Engineering*, 24(3), 264–272.

Park, H. S., Lee, H. M., Adeli, H., and Lee, I. (2007). "A New Approach for Health Monitoring of Structures: Terrestrial Laser Scanning." *Computer-Aided Civil and Infrastructure Engineering*, 22(1), 19–30.

Park, J. H., Kim, J. T., Hong, D. S., Mascarenas, D., and Peter Lynch, J. (2010). "Autonomous smart sensor nodes for global and local damage detection of prestressed concrete bridges based on accelerations and impedance measurements." *Smart Structures and Systems*, 6(5–6), 711–730.

Park, M., and Pena-Mora, F. (2003). "Dynamic change management for construction: Introducing the change cycle into model-based project management." *System Dynamics Review*, 19(3), 213–242.

Parvan, K., Rahmandad, H., and Haghani, A. (2012). "Estimating the impact factor of undiscovered design errors on construction quality." *Proceedings of the 30th International Conference of the System Dynamics Society*, 1–16.

Patil, N. R., and Patil, J. R. (2008). "Non destructive testing (ndt) advantages and limitations." *SRES College of Engineering*, 71–78.

Patjawit, A., and Kanok-Nukulchai, W. (2005). "Health monitoring of highway bridges based on a Global Flexibility Index." *Engineering Structures*, 27(9), 1385–1391.

Poreba, M., and Goulette, F. (2015). "A robust linear feature-based procedure for automated registration of point clouds." *Sensors (Switzerland)*, 15(1), 1435–1457.

"Project Review Software | Navisworks Family | Autodesk." (2007). .

Rabbani, T., van den Heuvel, F. a, and Vosselman, G. (2006). "Segmentation of point clouds using smoothness constraint." *International Archives of Photogrammetry, Remote Sensing and Spatial Information Sciences - Commission V Symposium "Image Engineering and Vision Metrology,"* 36(5).

Raghavendrachar, M., and Aktan, A. E. (1992). "Flexibility by Multireference Impact Testing for Bridge Diagnostics." *Journal of Structural Engineering*, 118(8), 2186–2203.

Riveiro, B., González-Jorge, H., Varela, M., and Jauregui, D. V. (2013). "Validation of terrestrial laser scanning and photogrammetry techniques for the measurement of vertical underclearance and beam geometry in structural inspection of bridges." *Measurement*, Elsevier Ltd, 46(1), 784–794.

Riveiro, B., Morer, P., Arias, P., and de Arteaga, I. (2011a). "Terrestrial laser scanning and limit analysis of masonry arch bridges." *Construction and Building Materials*, Elsevier Ltd, 25(4), 1726–1735.

Riveiro, B., Morer, P., Arias, P., and De Arteaga, I. (2011b). "Terrestrial laser scanning and limit analysis of masonry arch bridges." *Construction and Building Materials*, Elsevier Ltd, 25(4), 1726–1735.

Seppo, T. (2013). "Change detection in BIM models – Computing diffs between versions." *Built Environment Innovations*.

Solari, G. (1985). "Mathematical Model to Predict 3-D Wind Loading on Buildings." *Journal of Engineering Mechanics*, 111(2), 254–276.

Son, H., Kim, C., Asce, A. M., Cho, Y. K., and Asce, M. (2017). "Automated Schedule Updates Using As-Built Data and a 4D Building Information Model." *Journal of Management in Engineering*, 1–13.

Son, H., Kim, C., and Kim, C. (2015). "3D reconstruction of as-built industrial instrumentation models from laser-scan data and a 3D CAD database based on prior knowledge." *Automation in Construction*, Elsevier B.V., 49, 193–200.

Stephen, G. a., Brownjohn, J. M. W., and Taylor, C. a. (1993). "Measurements of static and dynamic displacement from visual monitoring of the Humber Bridge." *Engineering Structures*, 15(3), 197–208.

Su, Y. Y., Hashash, Y. M. A., and Liu, L. Y. (2006). "Integration of Construction As-Built Data via Laser Scanning with Geotechnical Monitoring of Urban Excavation." *Journal of Construction Engineering and Management*, ASCE, 132(12), 1234–1241.

Swart, A., Broere, J., Veltkamp, R., and Tan, R. (2011). "Refined Non-rigid Registration of a Panoramic Image Sequence to a LiDAR Point Cloud." *Lecture Notes in Computer Science*, 73–84.

Tang, P., Chen, G., Shen, Z., and Ganapathy, R. (2015). "A Spatial-Context-Based Approach for Automated Spatial Change Analysis of Piece-Wise Linear Building Elements." *Computer-Aided Civil and Infrastructure Engineering*, 31, 65–80.

Tang, P., Huber, D., Akinci, B., Lipman, R., and Lytle, A. (2010). "Automatic reconstruction of as-built building information models from laser-scanned point clouds: A review of related techniques." *Automation in Construction*, Elsevier B.V., 19(7), 829–843.

Tang, P., and Rasheed, S. H. (2013). "Simulation for characterizing a progressive registration algorithm aligning as-built 3D point clouds against as-designed models." *2013 Winter Simulations Conference (WSC)*, IEEE, 3169–3180.

Tang, P., Shen, Z., and Ganapathy, R. (2013). "Automated Spatial Change Analysis of Building Systems Using 3D Imagery Data." *30th CIB W78 International Conference - October 9-12, Beijing, China*, Proceedings of the 30th CIB W78 International Conference, 252–261.

Technodigit. (2009). "3DReshaper (Home) |About Technodigit | Contact."

Tessler, S., Iwasaki, Y., Law, K. H., and Shirley Tessler, Y. I. and K. L. (1993). "Qualitative Structural Analysis Using Diagrammatic Reasoning." *The Seventh*

International Workshop on Qualitative Reasoning about Physical Systems, 885–891.

Turkan, Y., Bosche, F., Haas, C. T., and Haas, R. (2012). "Automated progress tracking using 4D schedule and 3D sensing technologies." *Automation in Construction*, Elsevier B.V., 22, 414–421.

Vezočnik, R., Ambrožič, T., Sterle, O., Bilban, G., Pfeifer, N., and Stopar, B. (2009). "Use of terrestrial laser scanning technology for long term high precision deformation monitoring." *Sensors*, 9(12), 9873–9895.

Wahbeh, a M., Caffrey, J. P., and Masri, S. F. (2003). "A vision-based approach for the direct measurement of displacements in vibrating systems." *Smart Materials and Structures*, 12(5), 785–794.

Wakefield, R. R., Nazmy, A. S., and Billington, D. P. (1991). "Analysis of Seismic Failure In Skew Rc Bridge." *Journal of Structural Engineering*, 117(3), 972–986.

Wang, J., Sun, W., Shou, W., Wang, X., Wu, C., Chong, H.-Y., Liu, Y., and Sun, C. (2015). "Integrating BIM and LiDAR for Real-Time Construction Quality Control." *Journal of Intelligent & Robotic Systems*, 79(3–4), 417–432.

Xiong, X., Adan, A., Akinci, B., and Huber, D. (2013). "Automatic creation of semantically rich 3D building models from laser scanner data." *Automation in Construction*, Elsevier B.V., 31, 325–337.

Xiong, X., and Huber, D. (2010). "Using Context to Create Semantic 3D Models of Indoor Environments." *Proceedings of the British Machine Vision Conference 2010*, British Machine Vision Association, 1–11.

Yang, S., Wang, C., and Chang, C. (2010). "RANSAC Matching : Simultaneous Registration and Segmentation." *Robotics and Automation (ICRA), 2010 IEEE International Conference on*, 1905–1912.

Yi, T. H., Li, H. N., and Gu, M. (2013). "Experimental assessment of high-rate GPS receivers for deformation monitoring of bridge." *Measurement: Journal of the International Measurement Confederation*, 46(1), 420–432.

Zanyar, M., Bryan, T. A., Leo, K., and Jung, S. K. (2012). *The IABMAS Bridge Management Committee Overview of the Existing Bridge Management Systems*.

Zeibak, R., and Filin, S. (2007). "Change detection via terrestrial laser scanning." *Proceedings of the ISPRS Workshop*, 430–435.

Zhao, X., Liu, H., Yu, Y., Xu, X., Hu, W., Li, M., and Ou, J. (2015). "Bridge displacement monitoring method based on laser projection-sensing technology." *Sensors (Switzerland)*, 15(4), 8444–8643.

Zogg, H.-M., and Ingensand, H. (2008). "Terrestrial Laser Scanning for Deformation Monitoring--Load Tests on the Felsenau Viaduct (CH)." *International Archives of Photogrammetry and Remote Sensing*, 37, 555–562.

APPENDIX A

DESIGN MODEL AND 3D LASER SCANNING DATA OF THE MECHANICAL ROOM OF A BUILDING

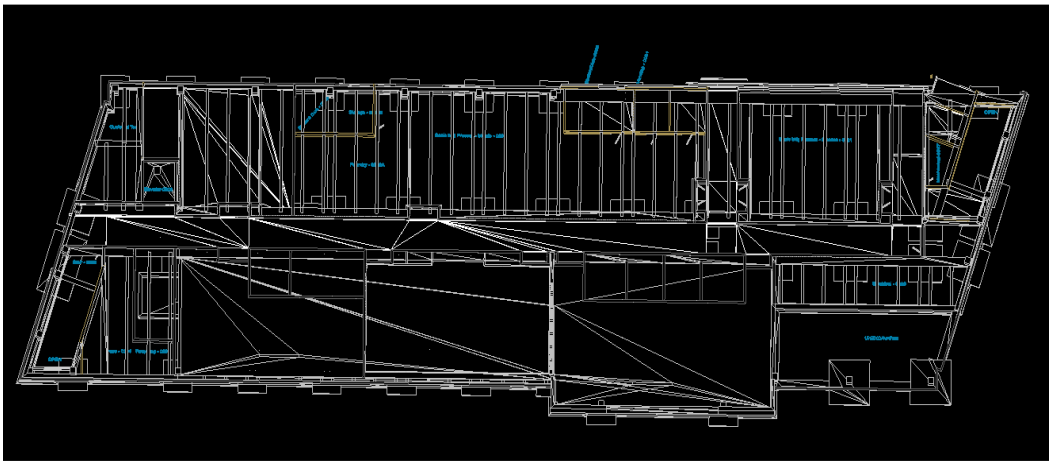

Top View of the Design Model of the Educational Building Located in Iowa State University

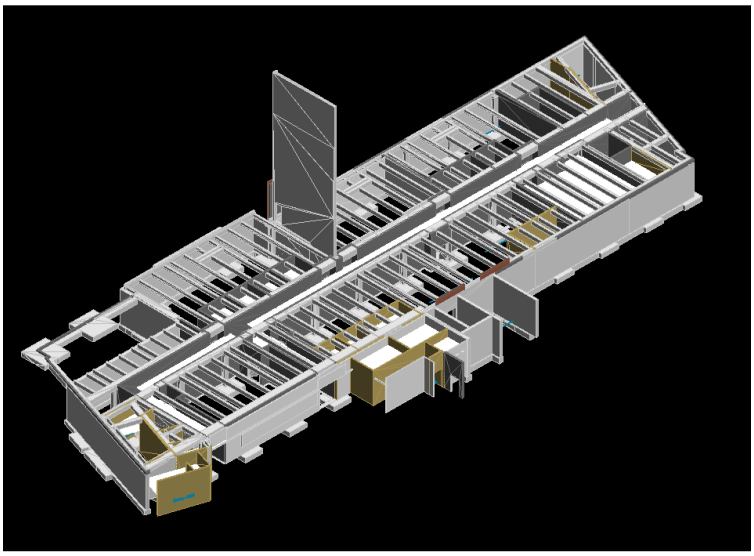

Extruded View of the Building Information Model (BIM) of the Educational Building Located in Iowa State University

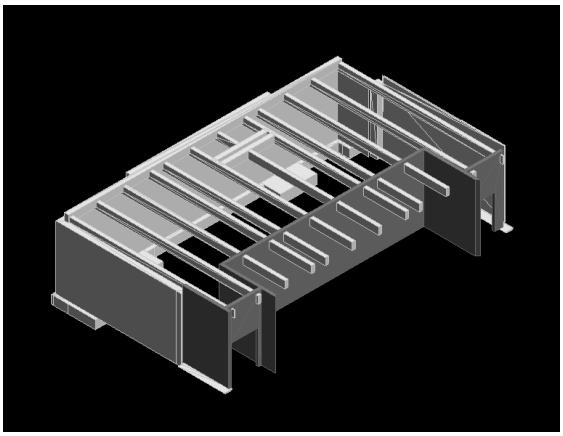

Building Information Model (BIM) of the Mechanical Room

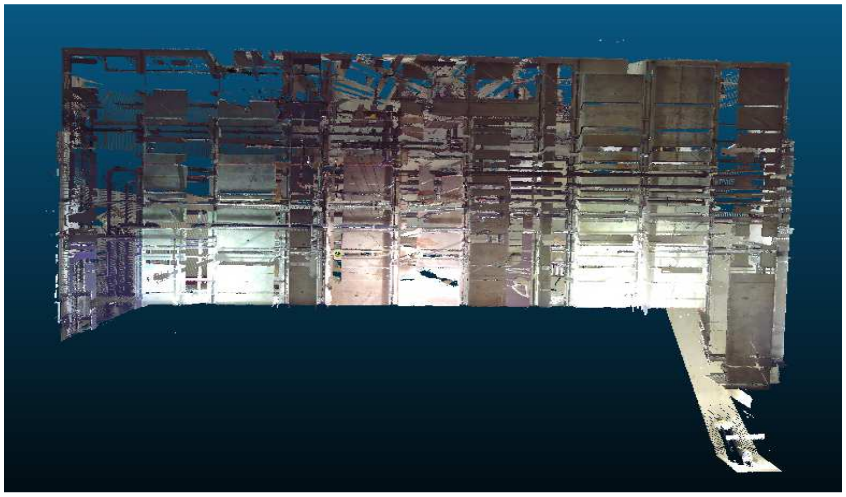

Top View of the Collected 3D Laser Scanning Data of the Mechanical Room

Inside View of the 3D Laser Scanning Data of the Mechanical Room

APPENDIX B

AUTOMATIC SPATIAL CHANGE CLASSIFICATION OF A HIGHWAY SINGLE-PIER BRIDGE 3

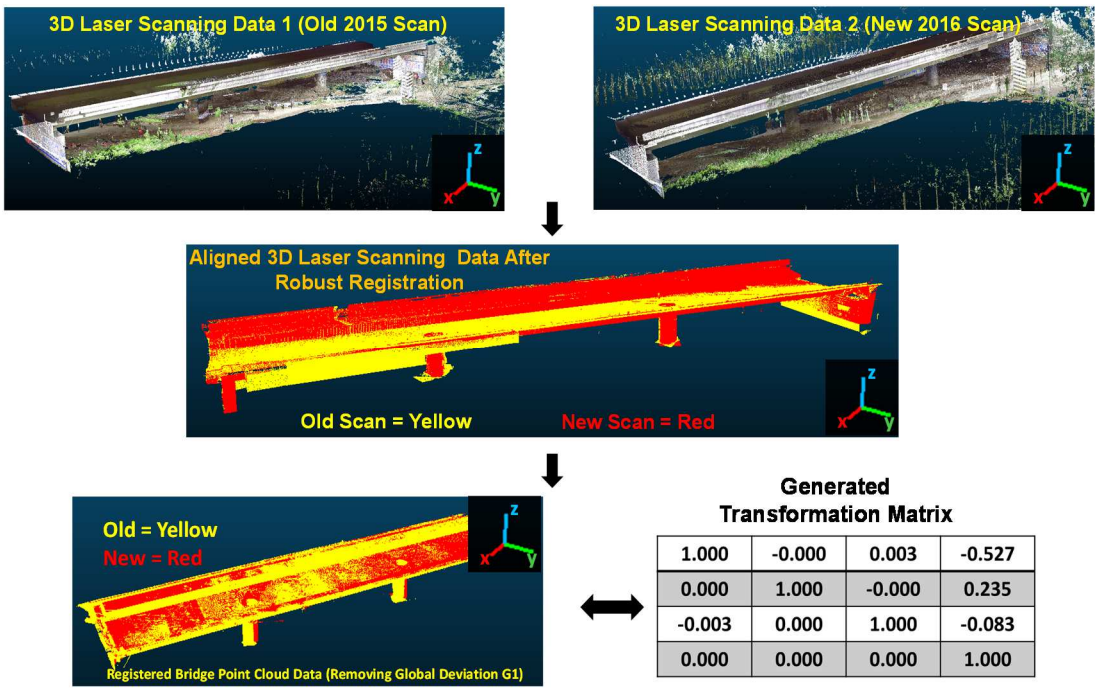

Robust Registration and Global Deviation (G1) for Highway Bridge 3

ELEMENT	TRANSLATION (meters)			ROTATION (degrees)		
	x	y	z	α	β	γ
GIRDER	-0.342	0.012	-0.012	0	-0.0030	0.001
COLUMN 1	-0.001	-0.042	0.001	1.00e-3	0	0.0020
COLUMN 2	0.232	0.110	0.005	0	0	-0.0120

Global Deviation (G2) between the Girder and the Column of the Highway Bridge 3

ELEMENT	COMPRESSION	TENSION	BENDING	TORSION
GIRDER	No	Yes (Increase in Length)	No	No
COLUMN 1	No	No	No	No
COLUMN 2	Yes (Decrease in height)	No	No	No

Local Deformation (L) of the Girder of the Highway Bridge 3